

博士論文

**Synthesis, liquid crystalline properties, gelation abilities and applications of
perfluoroalkyl derivatives without protic groups**

(プロトン性グループを含まないペルフルオロアルキル基誘導体の合成、
液晶性、ゲル化能及び応用)

平成 29 年 3 月
又は (西暦 2017 年 3 月)

Cao Banpeng

山口大学大学院理工学研究科

Abstract

In the past several decades, liquid crystals and supramolecular gels have been widely applied to liquid crystal display, gelling cryogenic fuels *etc.* Multifunctional materials containing liquid crystalline property and gelation ability as liquid crystalline physical gels have been prepared. The liquid crystalline physical gels usually compose two major components, liquid crystals and gelators. In this study, multifunctional materials showing liquid crystalline property and gelation ability are explored in 4-alkoxy-4'-semifluoroalkoxybiphenyl and 4-[4-(perfluorohexyl)butoxy]phenyl 4-alkoxybenzoates derivatives. As supramolecular phase selective gelators, 4-alkoxy-4'-semifluoroalkoxybiphenyl derivatives have been investigated in environmental recovery. 4-[2-(Perfluorohexyl)ethylthio]-3'-fluoro-4'-alkoxybiphenyl derivatives, as a kind of low molecular weight gelators, have been investigated in quasi-solid-state electrolytes. The research backgrounds for soft matter and research purposes in this work were introduced in Chapter 1.

In Chapter 2, in order to explore the driving force for the formation of liquid crystalline physical gels in the subsequent study, different kinds of compounds such as 4-semifluoroalkoxybiphenyl derivatives and 4-[4-(perfluorohexyl)butoxy]phenyl 4-alkoxybenzoates derivatives were synthesized. In order to investigate effect of semifluoroalkyl group, compounds with alkyl groups were also synthesized. And in order to investigate π - π interactions, the number of benzene in core groups were explored. 4-[2-(Perfluorohexyl)ethylthio]-3'-fluoro-4'-alkoxybiphenyl derivatives were also synthesized and applied to quasi-solid-state dye-sensitized electrolytes.

In Chapter 3, liquid crystalline properties of 4-alkoxy-4'-semifluoroalkoxybiphenyl derivatives were explored. The terminal groups of 4-alkoxy-4'-[4-(perfluorohexyl)butoxy]-1,1'-biphenyl derivatives were explored from butoxyl group to decyloxyl group. The types of textures mesophases such as smectic C, smectic A mesophase were observed. Compounds with a single benzene group do not show liquid crystalline property, while with a biphenyl group show liquid crystalline properties. Liquid crystalline properties of 4-alkoxy-4'-[4-(perfluorohexyl)butoxy]-1,1'-biphenyl derivatives depending on terminal groups, the core groups and semifluoroalkoxy groups which were proved.

In Chapter 4, gelation ability of 4-alkoxy-4'-semifluoroalkoxybiphenyl derivatives were investigated. 4-Pentyloxy-4'-[4-(perfluorohexyl)butoxy]-1,1'-biphenyl and 4-hexyloxy-4'-[4-(perfluorohexyl)-butoxy]-1,1'-biphenyl can gelatinize γ -butyrolactone (GBL) even at critical gelation concentration of 0.5 wt%. 4-Octyloxy-4'-[4-(perfluorohexyl)butoxy]-1,1'-biphenyl and 4-decyloxy-4'-[4-(perfluorohexyl)butoxy]-1,1'-biphenyl also gelatinize propylene carbonate at the similar critical gelation concentration. The aggregation state was explored using scanning electron microscope, infrared spectra and ^1H NMR spectra. In propylene carbonate xerogel system formed by 4-pentyloxy-4'-[4-(perfluorohexyl)-butoxy]-1,1'-biphenyl, the molecules form three dimensional fiber networks without hydrogen bonding. Thermal and rheological properties of supramolecular gels were also investigated. Supramolecular gels formed by 4-octyloxy-4'-[4-(perfluorohexyl)butoxy]-1,1'-biphenyl and 4-decyloxy-4'-[4-(perfluorohexyl)-butoxy]-1,1'-biphenyl in

propylene carbonate are more thermally stable than other solvents such as γ -butyrolactone and DMSO, and show rigidity and elastic characters.

In Chapter 5, 4-decyloxy-4'-[4-(perfluorohexyl)butoxy]-1,1'-biphenyl were studied as a phase selective gelator. The gelators show effective gelation abilities in different solvents, especially in oil and amine. 4-Decyloxy-4'-[4-(perfluorohexyl)-butoxy]-1,1'-biphenyl can gelatinize oil and amine at low concentration even of 0.2 wt% in heating-cooling cycle. In order to suit for environmental applications, the gelation abilities of 4-decyloxy-4'-[4-(perfluorohexyl)-butoxy]-1,1'-biphenyl solutions in THF and toluene were investigated with the mixture of sea water and oil/amine at room temperature. The results show that selective gelation abilities of solution in THF are better than that in toluene. The reason of low effective gelation ability of 4-decyloxy-4'-[4-(perfluorohexyl)butoxy]-1,1'-biphenyl solution in toluene was investigated by scanning electron microscope.

In Chapter 6, 4-[4-(perfluorohexyl)butoxy]phenyl 4-alkoxybenzoates as a new types of molecular structure were explored in liquid crystalline property and gelation ability. As the carbon number of terminal alkoxy group slightly increases, the gelation abilities are increased. The ester derivatives with biphenyl carboxylates show wider thermal range of mesophase than that with fewer aromatic cores. At the same time, the gel to sol transition temperature of ester derivatives with biphenyl carboxylates in *n*-octane and γ -butyrolactone are higher than that with benzoates. The benzene groups and terminal substitution groups play important roles in liquid crystalline property and gelation ability, which were proved again.

In Chapter 7, 4-[2-(perfluorohexyl)ethylthio]-3'-fluoro-4'-alkoxybiphenyl derivatives as low molecular weight gelators were explored in quasi-solid-state dye-sensitized electrolytes. The gel electrolyte with 4-[2-(perfluorohexyl)ethylthio]-3'-fluoro-4'-dodecyloxy-1,1'-biphenyl shows similar effective ionic conductivity to electrolyte solution.

In Chapter 8, the conclusions of this dissertation and prospects for future study were described.

要旨

過去数十年の間に、液晶化合物と超分子ゲルは液晶ディスプレイや低温用の燃料などに応用されてきた。液晶性とゲル化能をもつ液晶物理ゲルも開発されてきたが、これらは、液晶材料とゲル化剤の二成分から成り立っている。本研究では、液晶性とゲル化能を持つ機能性材料として 4-アルコキシ-4'-セミフルオロアルコキシビフェニル誘導体と 4-アルコキシ安息香酸 4-[4-(ペルフルオロヘキシル)ブトキシフェニルエステル誘導体について研究した。4-アルコキシ-4'-セミフルオロアルコキシビフェニル誘導体については、環境改善物質として検討した。4-[2-ペルフルオロヘキシル]エチルチオ-3'-フルオロ-4'-アルコキシビフェニル誘導体は擬ゲル電解質としての性能を検討した。

第一章においては、ソフトマターと研究目的に関する研究の背景について記載した。

第二章においては、液晶物理ゲルの形成の駆動力を解明するために、二種類の化合物、すなわち 4-アルコキシ-4'-セミフルオロアルコキシビフェニル誘導体と 4-アルコキシ安息香酸 4-[4-(ペルフルオロヘキシル)ブトキシフェニルエステル誘導体を合成した。さらに、フルオロアルキル基の効果を検討するために、アルキル基を持つ化合物を合成した。 π - π 相互作用を検討するために、ベンゼンの数について検討した。さらに、4-[2-ペルフルオロヘキシル]エチルチオ-3'-フルオロ-4'-アルコキシビフェニル誘導体を合成した。

第三章においては、4-アルコキシ-4'-セミフルオロアルコキシビフェニル誘導体の液晶性について検討した。4-アルコキシ-4'-セミフルオロアルコキシビフェニル誘導体の末端置換基についてブチル基からデシル基まで検討

した。その結果、これらの化合物ではスメクチック A 相とスメクチック C 相が発現し、ベンゼン環が一つの化合物では、液晶性は見られなかった。

第四章においては、4-アルコキシ-4'-セミフルオロアルコキシビフェニル誘導体のゲル化能について検討した。末端アルコキシ基がペンチル基およびヘキシル基の化合物では、 γ -ブチロラクトン (GBL) を 0.5wt%程度の添加量でゲル化した。末端アルコキシ基がオクチル基およびデシル基を持つ化合物に関しても同様にプロピレンカーボネートをゲル化した。集合状態は走査型電子顕微鏡、赤外吸収スペクトルおよび ^1H NMR スペクトルによって検討した。プロピレンカーボネートゲルから形成したキセロゲルにおいては、分子は水素結合することなく、三次元のネットワークファイバーを形成している。超分子ゲルの熱的性質とレオロジー的性質も検討した。超分子ゲルオクチル基とデシル基を持つ化合物ではプロピレンカーボネートゲルの熱安定性が GBL ゲルや DMSO ゲルよりも高く、固くて弾性的性質もある。

第五章では、4-デシルオキシ-4'-ペルフルオロヘキシルブトキシ-1,1'-ビフェニルの相選択的なゲル化剤としての機能を検討した。この化合物では、異なる溶媒系、特にアミンと油において効果的なゲル化能を示した。加熱冷却することで、0.2wt%程度の低濃度で油とアミンをゲル化できた。環境改善材料への応用を考慮し、THF 溶液とトルエン溶液を用いたゲル化能を検討したところ、海水との混合溶媒においては THF 溶液がトルエン溶液よりも優れていることが分かった。トルエン溶液では、効果的ではなかった原因を走査型電子顕微鏡観察から検討した。

第六章では、4-アルコキシ安息香酸 4-[4-(ペルフルオロヘキシル)ブトキ

シフェニルエステル誘導体の液晶性とゲル化能を検討した。その結果、末端炭素鎖が伸長するとゲル化能が上昇した。ビフェニルカルボン酸にすることで、ゲル化能も上昇し、液晶性を示す温度幅も拡大した。

第七章においては、4-[2-ペルフルオヘキシル]エチルチオ-3'-フルオロ-4'-アルコキシビフェニル誘導体を用いた擬ゲル状態の色素増感電解質を検討した。4-[2-ペルフルオヘキシル]エチルチオ-3'-フルオロ-4'-アルコキシビフェニル誘導体を含むゲル電解質では、電解液と同等のイオン伝導度を示すことが分かった。

第8章では、本学位論文の結論と今後の展望について記した。

Contents

Chapter 1 General introduction.....	1
1.1 Introduction to soft matter	1
1.2 Introduction to liquid crystals	2
1.3 Introduction to gels	10
1.4 Research purpose	20
1.5 References.....	21
Chapter 2 Synthesis of perfluoroalkyl derivatives without protic groups	24
2.1 General materials and methods.....	24
2.2 Synthesis of 4-alkoxy-4'-[4-(perfluorohexyl)butoxy]-1,1'-biphenyl	25
2.3 Synthesis of 4-alkoxy-4'-[4-(perfluorohexyl)butoxy]benzene.....	34
2.4 Synthesis of 4-alkoxy-4'-alkoxy-1,1'-biphenyl	37
2.5 Synthesis of 4-(butoxy)-4'-[4-(perfluorohexyl)allyloxy]-1,1'-biphenyl	38
2.6 Synthesis of 1-(decyloxy)-4-(pentyloxy)benzene.....	40
2.7 Synthesis of 4-[4-(perfluorohexyl)butoxy]phenyl 4-alkoxybenzoates	42
2.8 Synthesis of compounds 4-[4-(perfluorohexyl)butoxy]phenyl 4-phenylbenzoate derivatives.....	50
2.9 Synthesis of 4-alkoxyphenyl 4-alkoxybenzoates.....	51
2.10 Synthesis of 4-[2-(perfluorohexyl)ethylthio]-3'-fluoro-4'-alkoxy-1,1'-biphenyl	53
2.11 References.....	59
Chapter 3 Liquid crystals based on 4-alkoxy-4'-[4-(perfluorohexyl)butoxy]-1,1'-biphenyl derivatives	60
3.1 Introduction.....	60
3.2 Liquid crystalline properties	62
3.3 Conclusions.....	73
3.4 References.....	75
Chapter 4 Gelation abilities of 4-alkoxy-4'-[4-(perfluorohexyl)butoxy]-1,1'- biphenyl derivatives	76
4.1 Introduction.....	76
4.2 General gelation abilities	78
4.3 Particular gelation abilities	80
4.4 The driving force for self-assemble	83
4.5 Rheological property of gels	89
4.6 Conclusions.....	91
4.7 References.....	93
Chapter 5 Supramolecular phase-selective gelation abilities by 4-alkoxy-4'-[4-(perfluorohexyl)butoxy]-1,1'-biphenyl derivatives.....	95
5.1 Introduction.....	95
5.2 Phase selective gelation abilities.....	97
5.3 The effect of phase selective properties	108
5.4 Conclusions.....	110
5.5 References.....	112

Chapter 6 Liquid crystalline property and gelation ability of 4-[4-(perfluorohexyl)butoxy]phenyl 4-alkoxybenzoates.....	114
6.1 Introduction.....	114
6.2 Liquid crystalline properties	115
6.3 Gelation abilities	123
6.4 Conclusions.....	128
6.5 Reference	130
Chapter 7 4-[2-(Perfluorohexyl)ethylthio]-3'-fluoro-4'-alkoxy-1,1'-biphenyl derivatives as low molecular weight gelators applied in quasi-solid-state dye-sensitized electrolytes	131
7.1 Introduction.....	131
7.2 Gelation properties.....	133
7.3 Electrochemical properties.....	138
7.4 Conclusions.....	142
7.5 References.....	143
Chapter 8 General conclusions	145
Acknowledgments.....	147

Chapter 1 General introduction

1.1 Introduction to soft matter

In our life, we can find several different states of matter defined as solid, liquid, gas and plasma (**Figure 1-1**).¹ A state of matter is always characterized by phase transitions and latent heat changes. A phase transition indicates a change in molecular arrangement. For example, H₂O can show both of solid and liquid states at 0 °C. The density of ice is 0.9167 g/mL, and water has a density of 0.9998 g/mL at the same temperature (0 °C). That means at the same temperature but in different states molecular numbers and molecular arrangements are different in the same volume.

In chemistry, when we refine compounds from saturated solutions, we may come across supersaturated solution where solute does not precipitate. Likewise, when a material is changing from one state to another state, intermediate state may show two phases with thermodynamic and kinetic properties beyond imagination. The material which can show two phases properties is called soft matter.

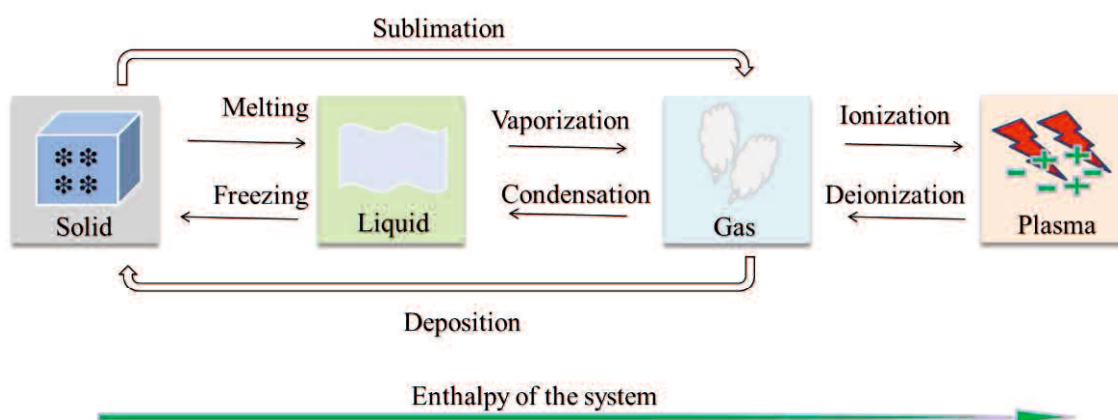


Figure 1-1. Different states of matter

Soft matter is easily deformed by thermal fluctuations, or whose total energy and the corresponding energy minima are of order of kT .² The amazing feature of soft matter is capricious without being predicted. That's because soft matter molecules quickly adjust themselves by an energetic minimum in a thermodynamically driven self-assembly process. Soft matter is quite sensitive to respond to environment changes such as magnetic, electric, chemical or mechanical. These special properties make soft matter essential for living life and unique for technical applications.³

Soft matter includes liquids, colloids, polymers, foams, gels, granular materials, liquid crystals and a number of biological materials. Over the past decades, gels and liquid crystals fields have evolved into a research hotspot, not least in chemistry.⁴

1.2 Introduction to liquid crystals

Liquid crystal is a kind of soft matter which is partially ordered, anisotropic fluids and thermodynamically located between solid phase and isotropic liquid. In 1888, Friedrich Reinitzer observed the typical light scattering of a liquid crystal and published it in *Journal of Monatshefte für Chemie*.⁵

Liquid crystals can be divided into two categories which named lyotropic liquid crystals and thermotropic liquid crystals (**Figure 1-2**).⁶ Lyotropic liquid crystals form in the presence of an isotropic solvent, while thermotropic liquid crystals are observed by changing temperature. Amphotropic liquid crystal is a kind of matter which shows both of lyotropic liquid crystalline properties and thermotropic liquid crystalline properties.

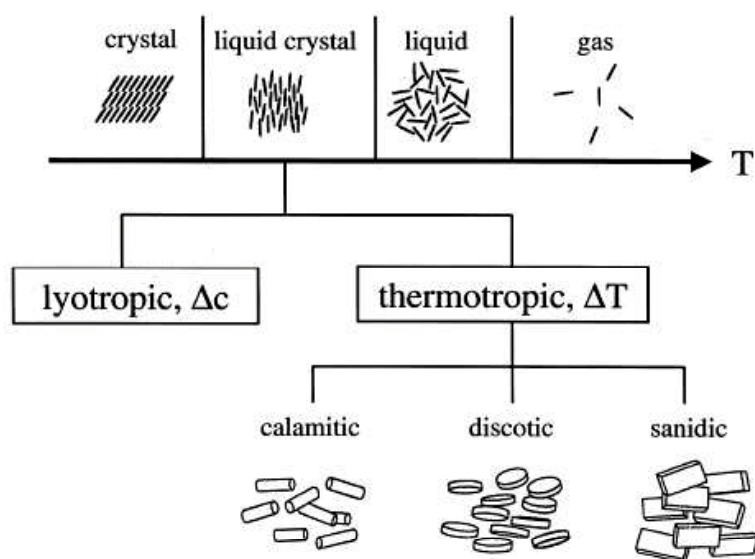
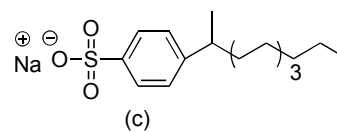
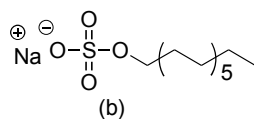
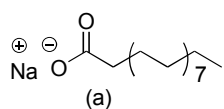


Figure 1-2. Placement of the liquid crystal within the general scheme of the common states of matter⁶

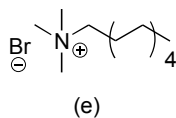
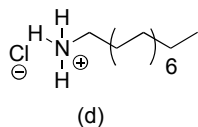
1.2.1 Lyotropic liquid crystals

Lyotropic liquid crystals are abundant in our daily life, for example, soap and other surfactants dissolving in water and forming lyotropic liquid crystals. In boiling process for soap manufacture, lyotropic liquid crystals are also used.⁷ Lyotropic liquid crystals also play a key role in human body, such as organelles of cells, noncellular forms and blood.⁸ The molecular structures which generate lyotropic liquid crystals are amphiphilic. Two distinct parts of amphiphilic structures (hydrophilic head and lipophilic tail) show different actions in self-assemble process. The hydrophilic head plunges into water, while the lipophilic tail keeps far from water. Three typical examples of amphiphilic molecules are given in **Figure 1-3.**⁹

Anionic surfactants



Cationic surfactants



Nonionic surfactants

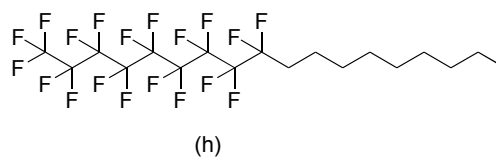
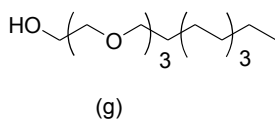
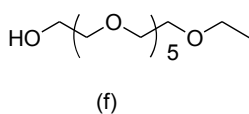


Figure 1-3. Three typical examples of amphiphilic molecules

1.2.1.1 Classification by amphiphilic molecules

Anionic surfactants have a polar head group with a long hydrocarbon fragment, while cationic surfactants have an amine with a long terminal chain. Amphiphilic molecules also can be formed by nonionic structures. Compound (h) (**Figure 1-3**) is a special example of amphiphilic molecule which contains a long perfluoroalkyl chain connected directly to a long hydrocarbon chain.

1.2.1.2 Classification by lyotropic liquid crystalline mesophases

Based on the types of low-angle X-ray diffraction patterns, lyotropic liquid crystalline mesophase can be divided into three categories: the lamellar mesophase, the hexagonal mesophase and the cubic mesophase (**Figure 1-4**).¹⁰ In lamellar mesophase, the amphiphilic molecules are arranged in bilayers separated which extend over large distances by water layers. The thickness of water layers between bilayer units is about 10 Å to more than 100 Å. The thickness of bilayer is usually about 70-90% of twice

the length of lipophilic tail group. As the surfactant concentration below 50 wt%, the lamellar mesophase may change into hexagonal mesophase or an isotropic micellar solution.¹¹ However, the lamellar mesophase in extremely dilute solutions also has been reported.

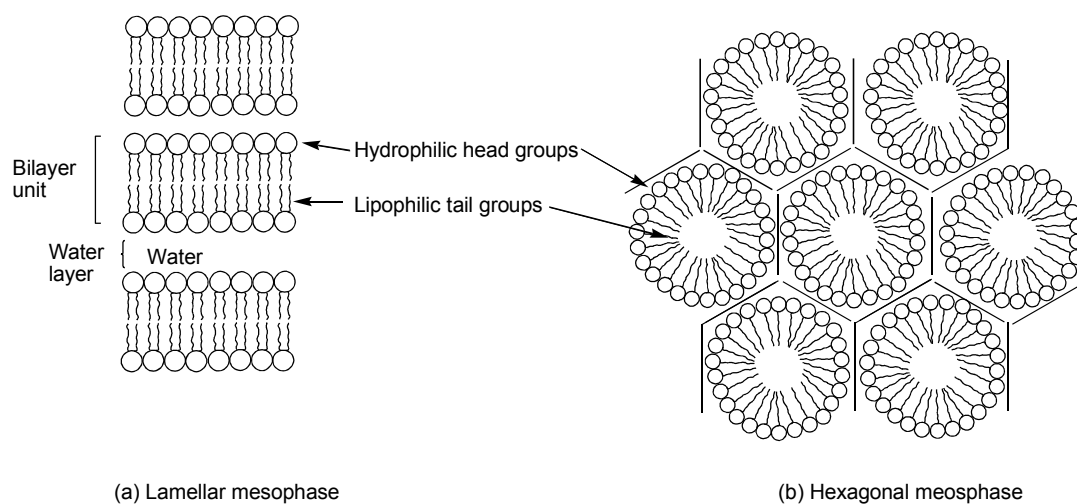


Figure 1-4. Structure of lyotropic liquid crystalline mesophases: (a) lamellar mesophase, (b) hexagonal mesophase

Hexagonal mesophase typically aggregate to micellar cylinders (**Figure 1-4 (b)**), and the diameter of the micellar cylinders is about 70-90% of twice the length of lipophilic tail group. The space between cylinders is about 10 Å to more than 50 Å. The surfactant concentrations typically range from 40 wt% to 70 wt% in hexagonal mesophase.

The cubic mesophase is called by the cubic arrangement of molecular aggregate characters. Except that, the cubic lyotropic mesophase has no special structural characteristics of molecular aggregation. Because the cubic mesophase is viscous and optically isotropic, the cubic mesophase also is named the viscous isotropic

mesophase.

1.2.2 Thermotropic liquid crystals

Since the first time cholesteryl benzoate derivatives have been published as liquid crystals,⁵ thermotropic liquid crystals have created new avenues in our daily life, such as display devices, pressure sensors, light valves sensors, pH sensors, and biosensors.¹² Without doubt, there is a significant interest in design and development of novel liquid crystals with multifunctional properties.

1.2.2.1 Classification by molecular structures of thermotropic liquid crystals

To generate liquid crystals, one must use anisotropic units. According to the shapes of anisotropic units, thermotropic liquid crystals can be divided into four types, where are called rod-like (calamitic) liquid crystals, disk-like (discotic) liquid crystals, board-like (sanidic) liquid crystals and banana-shaped (bent-core) liquid crystals (**Figure 1-5**).¹³ As typical thermotropic liquid crystals, rod-like liquid crystals and disk-like liquid crystals are well investigated and extremely useful for the practical applications.

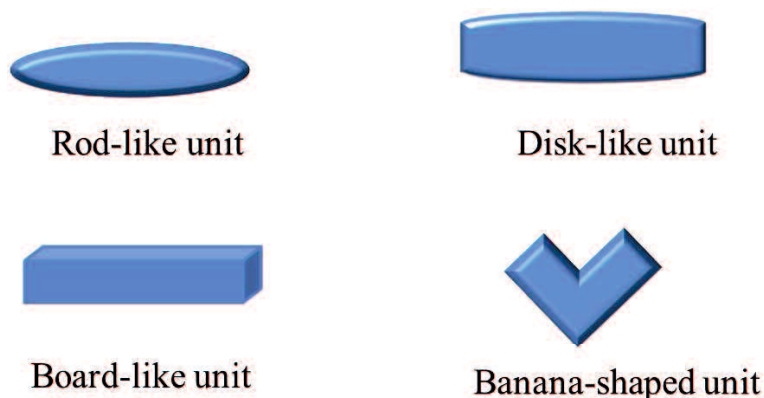
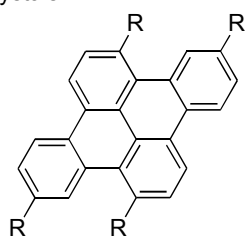


Figure 1-5. Core shapes for molecular structures of thermotropic liquid crystals

Molecular structures of rod-like liquid crystals can be divided into rigid, semiflexible and flexible groups based on the difference in the rotational energy barrier of different configurational isomers or conformers of calamitic liquid crystals.¹⁴ Benzene and biphenyl groups are often introduced to the rigid groups. Molecular structures of disk-like liquid crystals are commonly containing six flexible endgroups attached to rigid, and disk-like units. Board-like liquid crystals and banana-shaped liquid crystals are so complicated that the structural characteristics are still not very clear. In **Figure 1-6**, example for some typical board-like liquid crystals^{13(b)} and banana-shaped liquid crystals^{13(c)} are shown.

(a) Board-like liquid crystals:

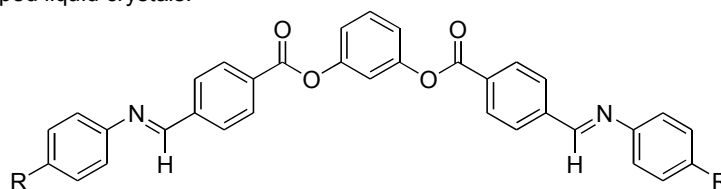


DBN(C_n): R = C_nH_{2n+1}

DBN(C₅) Cryst 91 SmA 106 Iso

DBN(C₇) Cryst 90 SmA 105 Iso

(b) Banana-shaped liquid crystals:



R = OC₅H₁₁ Cryst 176 B₁ 181 Iso

R = C₅H₁₁ Cryst 106 B₃ 143 B₂ 150 Iso

Figure 1-6. Some typical examples of board-like liquid crystals and banana-shaped liquid crystals (Cryst., SmA, Iso., B₁ and B₃ indicated crystalline solid, smectic A mesophase, isotropic liquid, banana mesophase 1 and banana mesophase 3, respectively)

1.2.2.2 Classification by thermotropic liquid crystalline mesophases

Thermotropic liquid crystalline mesophases as well as lyotropic liquid crystalline mesophases, exist in several different types (Figure 1-7).¹⁵ On the basis of the symmetry of molecules, the classification of mesophase can be largely divided into two categories: non-chiral mesophase and chiral mesophase.

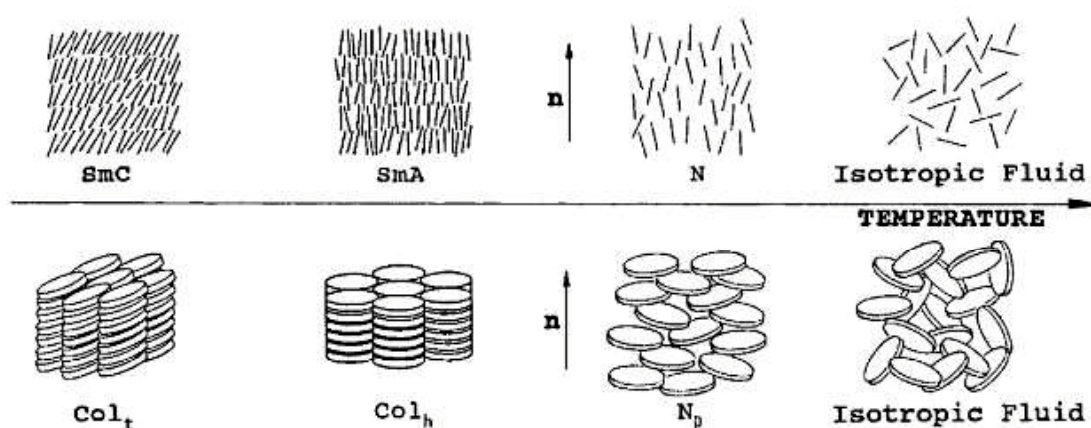


Figure 1-7. Typical mesophases sequence in thermotropic liquid crystals. Top: rod-like liquid crystals, Bottom: disk-like liquid crystals¹⁵ (SmC, SmA, N, Col_t, Col_h and N_D indicated smectic C mesophase, smectic A mesophase, columnar tetragonal mesophase, hexagonal disordered mesophase and discotic nematic mesophase, respectively)

Rod-like liquid crystals always show nematic (N) mesophase and smectic (Sm) mesophase. According to chirality, nematic mesophase (N mesophase) and chiral nematic mesophase (N* mesophase) are defined. SmA, SmC and SmC* mesophases are generally observed in liquid crystals.

Although the total number of smectic mesophases cannot be specified, the

following types have been defined: SmA, SmC and SmF. As a crude rule of thumb we may deduce a hypothetical mesophase sequence on cooling from the isotropic melt (still disregarding various chiral mesophases): Iso_N_SmA_SmC_SmF_Cryst.

Disk-like liquid crystals are primarily of four types: nematic, smectic, columnar and cubic mesophases. Columnar and cubic mesophases are often observed in disk-like liquid crystals. Most of the disk-like liquid crystals only exhibit one of the four types.

Thermotropic liquid crystals show different mesophase behaviors and the molecular alignment in accordance with temperature changing. The phase transition behavior is illustrated in **Figure 1-8**.^{12(b)}

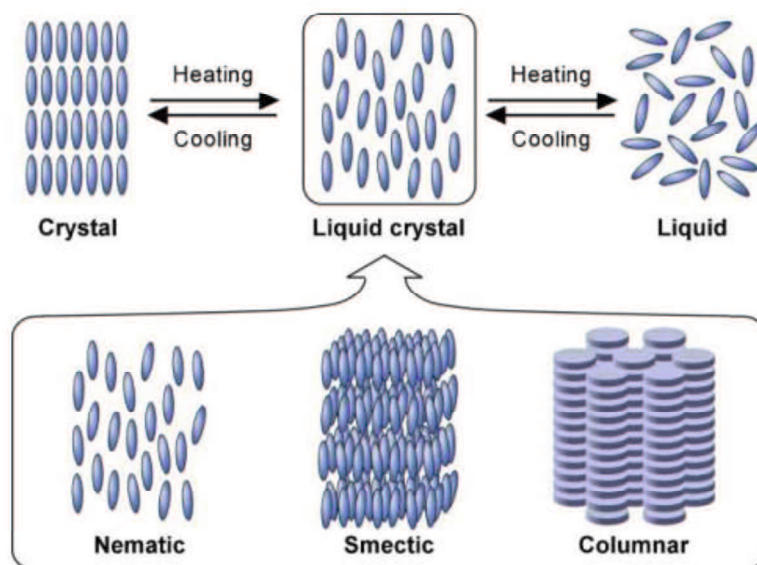


Figure 1-8. Schematic illustration of mesophase transition behavior and the molecular alignment of liquid crystals

Obviously, no single compound exhibits the whole range of mesophases, but

investigations on numerous liquid crystals have shown that their individual mesophase sequences mostly follow this hypothetical sequence with the omission of those mesophases that do not appear.

1.3 Introduction to gels

Gels are not unique materials which can be traced back to at least Neolithic times. They play an important role in current life, especially in medicine, art and technology. Although gels have been widely applied, gels are so complex systems that the mechanisms of gels are not very clear.¹⁶

1.3.1 Classification of gels

Gels are fascinating materials. Gels as a kind of soft matters are difficult to be classified because gels show special states. Until now, the classification of gels has no a unified standard. Gels can be divided into different categories by different ways depending upon the type of cross-linking interactions, their mechanical properties and their components. According to the nature of the interactions, rheology, nature of solvents and nature of solids, gels can be classified into four basic types.

1.3.1.1 Nature of the interactions

Based on the nature of interactions between molecules of the components, gels can be divided into two types: physical gel and chemical gel (**Figure 1-9**). Physical gels mean that using non-covalent intermolecular interactions, such as hydrogen bonding, halogen bonding, π - π interactions, van der Waals and solvophobic forces in solvents, to self-assemble into nano- or micro-scale network structures. The

interaction is so weak that slight environmental change can lead gels tempestuously respond. Chemical gels mean that nano- or micro-scale network structures are formed via covalent bonds between molecules of components. Chemical gels are more stable than physical gels. So in some cases, for example sol-gel process, chemical and physical processes work together to form network structures.

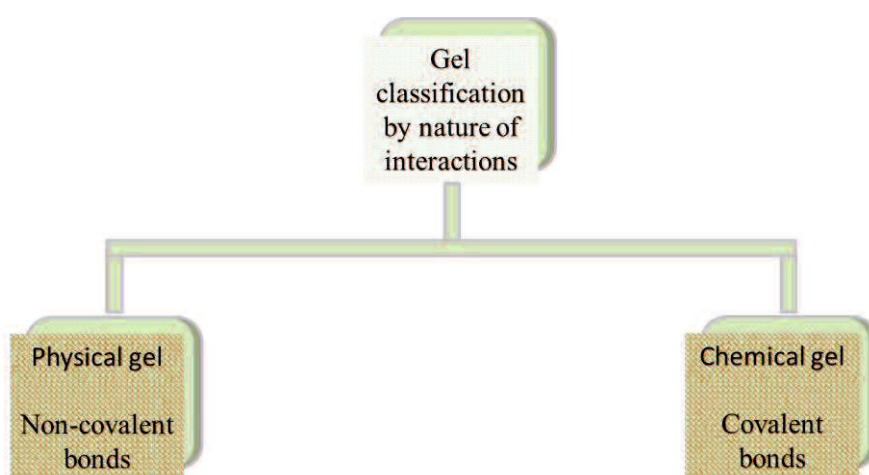


Figure 1-9. Gel classification by the nature of interactions

1.3.1.2 Rheology

Gels characterization is principally related with rheological properties, even defined.¹⁷ Gel state is between solid state and liquid state. Rheological properties of gels also show solid-like and liquid-like rheological behaviors. The rigidity and flow behaviors show in rheological measurement by storage modulus (G') and loss modulus (G''), respectively. G' of gels should be held the line with frequency up to a particular yield point and should be stronger than G'' .

1.3.1.3 Nature of solvents

Gels always contain two parts: solid and solvent. The solid component of gel is,

in most of cases, organogelator. Solvents are so important to gels that the same organogelator shows varying gelation abilities in different solvents. Gels can be classified by the nature of the solvent showed in **Figure 1-10**.

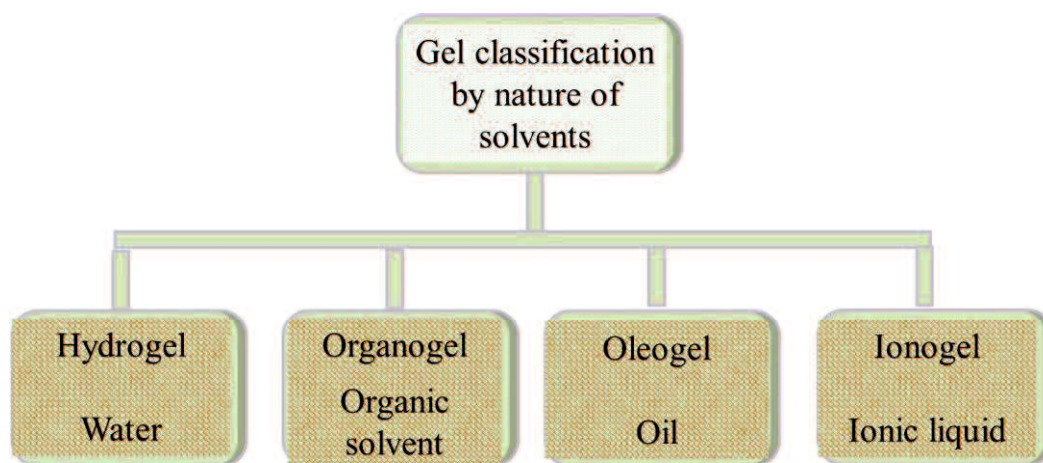


Figure 1-10. Gel classification by the nature of solvents

Hydrogel has high absorbent ability which even can contain water over 90%. Hydrogel which is similar with animal tissue has become a research hotspot since it has been found. Since now, hydrogel can be applied into drug delivery systems, glue, cell culture, repair tissue, contact lenses and so on. So hydrogel is an important discovery to our life.

Organogel is a kind of gels which traps organic solvent molecules by three dimensional nanofiber networks. Rheological properties are important characteristics for organogel. Usually, organogel is based on self-assembly of organogelator molecules. In order to make organic solvent convenient in transport and more ecofriendly, different kinds of organogelator are published for studying their gelation abilities every year.

Organogel formed by organogelator and oil is so important that it is defined as oleogel. Oil and fats are daily life materials which make up of variety of triacylglycerol molecules.¹⁸ Most oil structuring strategies in oleogel formation rely on organogelator by self-assemble to form a solid-like fat structure at room temperature. More and more researchers focus on exploring functionality for potential applications. Some notable examples are as follows: (a) ethyl cellulose oleogels as a part of source to replace food, (b) wax-based oleogels for margarine and cooky production, (c) colours oleogels for oil painting.

Ionic liquid (IL) is a kind of green solvent. IL has all special physicochemical properties including non-flammability, high thermal and chemical stability, high conductivity, negligible vapor pressure. Hence, IL has been widely used in field of chemical research and chemical engineering. In order to enlarge the application and decrease the risk of leak, lots of organogelator for ionic liquid gels (IL gels or ionogels) have been published and explored in different fields, especially in electrochemistry.¹⁹

Materials formed by polymers sustain our modern life. As the study of gels, polymers are also introduced into gels field. The gel which contains a polymer is named polymer gel.²⁰ Polymer gel is found in many applications ranging from foods, drug delivery, consumer, super absorber and so on.

1.3.1.4 Nature of solids

Gel can be categorized not only according to the nature of solvents, but also by

the nature of solids.²¹ Generally speaking, gel can be divided into macromolecular gel, colloidal gel and supramolecular gel (**Figure 1-11**).

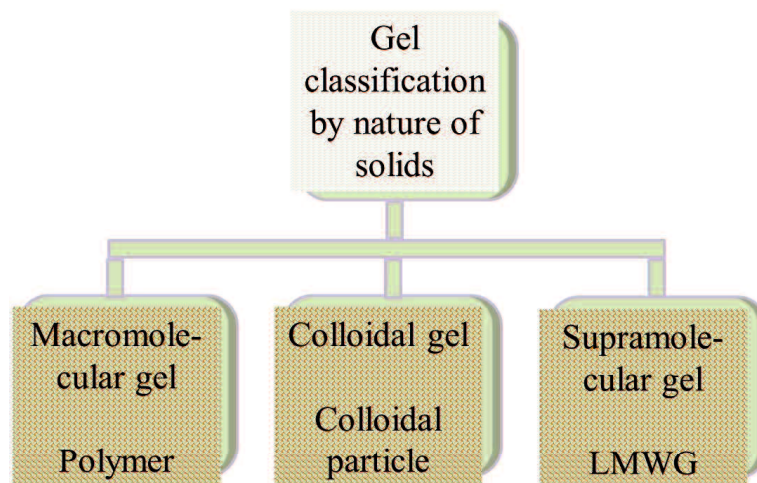


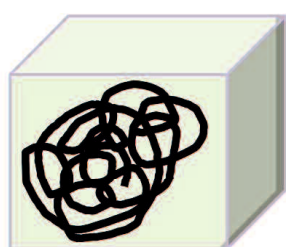
Figure 1-11. Gel classification of the nature of solids

Macromolecular gel also is named as polymer gel because the solid of macromolecular gel usually is a polymer. Huge polymer molecules can assemble themselves by non-covalent and/or covalent interactions to trap liquid molecules forming gel (**Figure 1-12 (a)**). Of course, solid of macromolecular gel sometimes except polymer such as crosslinkers cause the liquid phase to become trapped within the crosslinked matrix.²²

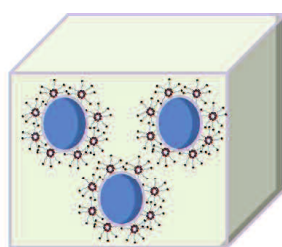
Colloidal gel is formed by colloidal particles. As the concentration of colloidal particles increases, the overlapping aggregates formed by colloidal particles produce a continuous network to trap liquid molecules.²³ Colloidal particles are larger than molecules and smaller than macromolecules. Typical size of colloidal particles is about 1-1000 nm. Although colloidal particle is large, it does not quickly settle down under gravity. That's because colloidal gel is a two-phase heterogeneous system

consisting of the dispersed phase and dispersion medium. Colloidal particles can reach a balance in liquid phase through dispersion or growth of discrete colloidal particles (**Figure 1-12 (b)**).²⁴

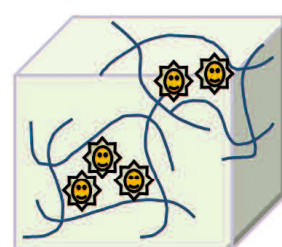
Supramolecular gel which depends upon non-covalent intermolecular interaction to self-assemble into three dimensional nanofiber networks also is described as molecular gel (**Figure 1-12 (c)**). The organic solid which can gelatinize solvents to supramolecular gel is named as organogelator. When the molecular weight of organogelator is ranged from 300-1000 Dalton, the organogelator can be named as low molecular weight gelator (LMWG), low molecular weight organic gelator (LMWOG) and low molecular mass gelator (LMMG). In this thesis, organogelator and LMWG are chosen to name the organic solid of supramolecular gel. These aggregation processes rely on a delicate balance between the LMWG's solubility and insolubility in a given physical and chemical environment, for example temperature, solvent characteristics and so on. The stability of supramolecular gel is not very good, even can easily be disassembled when the environment changed such as temperature and shear. Different kinds of supramolecular gels which can respond to environment changes have been published.



(a) Macromolecular gel



(b) Colloidal gel



(c) Supramolecular gel

Figure 1-12. Schematic representation of microparticles of macromolecular gel, colloidal gel and supramolecular gel

1.3.2 Gelation mechanism of supramolecular gel

Although a lot of supramolecular gels have been reported by chance, it is still a terrible work to design and synthesize a new kind of organogelator until now.²⁵ At the same time, many aspects of supramolecular gel are poorly understood. Supramolecular gel with three dimensional nanofiber networks formed by LMWGs has been certificated using scanning electron microscope (SEM). The liquid molecules are effectively immobilized and entrapped by three dimensional nanofiber networks. The self-assembly process of one dimensional particles to three dimensional nanofiber networks is more well-known than molecule (zero dimensional structure) to form one dimensional particles (**Figure 1-13**).²⁶

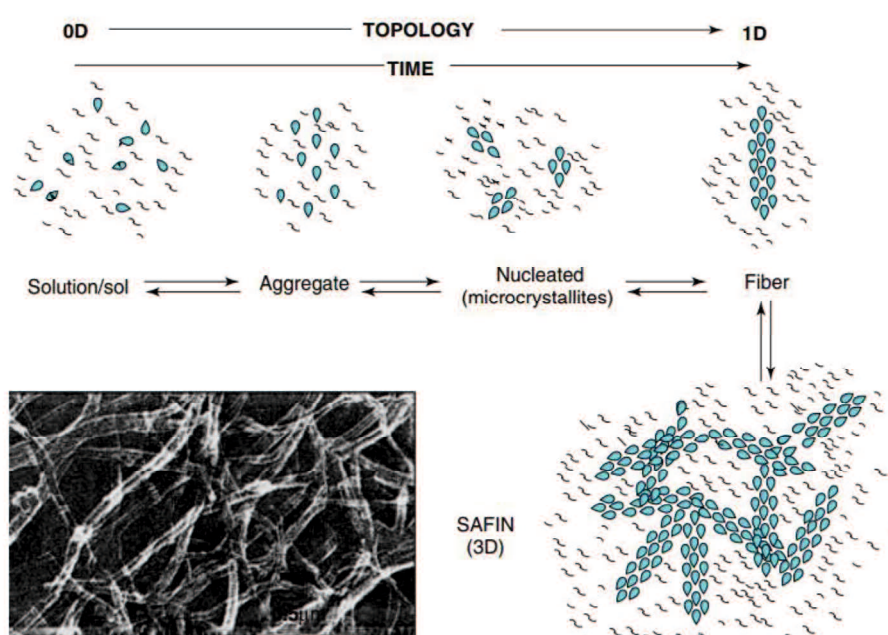


Figure 1-13. Illustrate the steps of three dimensional nanofiber networks from

molecules²⁶ (SAFIN indicated self-assembled fibrillar networks)

For the three dimensional nanofiber network structures precipitated from liquid, crystallization is the most magical process that molecules arranging from random to ordered arrangement. The driving force for the magical process is $\Delta\mu$, which is defined as the difference between the chemical potential of mother solution (μ_{mother}) and the chemical potential of crystalline solution (μ_{crystal}).

$$\Delta\mu = \mu_{\text{mother}} - \mu_{\text{crystal}}$$

When $\Delta\mu > 0$, it means that the solution system is supersaturated. This is the thermodynamic precondition for nucleation and growth of the crystalline solution.²⁷

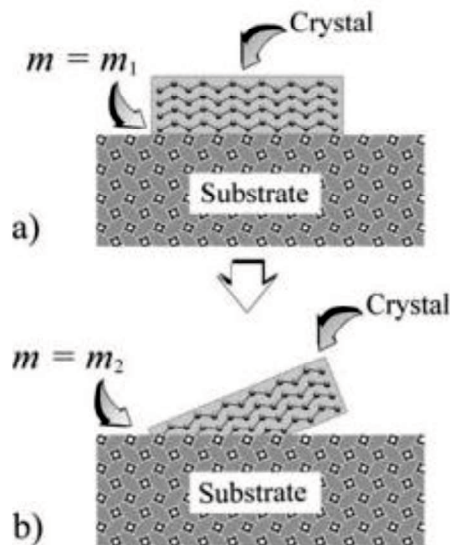


Figure 1-14. The structural match between a nucleus and the substrate and the corresponding m . (a) Good interfacial structural match between the nucleus and the substrate. m_1 . (b) Poor interfacial structural match between the nucleus and the substrate. m_2 . $m_1 > m_2$, and $f(m_1) < f(m_2)$ ²⁷

In kinetics, the substrates will affect nucleation barrier and surface integration.

The function of m ($-1 \leq m \leq 1$) which describes the structural match between the nuclei and the substrate is described by $f(m) = 1/4(2-3m+m^3)$. At low supersaturations, if $f(m) \rightarrow 0$, the nucleating phase and the substrate will show a strong interaction and an optimal structural match, which is kinetically favored called heterogeneous nucleation (**Figure 1-14 (a)**). Otherwise when $f(m) \rightarrow 1$, the nucleating phase and the substrate are rarely correlated with each other (**Figure 1-14 (b)**). In this case, nuclei completely disordered are called homogeneous nucleation.

It should be noted that the heterogeneous nucleation is the main way to form the primary nucleation of fibers. A fiber network of *N*-lauroyl-L-glutamic acid di-*n*-butylamide from a nucleation center can exactly show the process gelation of supramolecular gels (**Figure 1-15**).²⁷

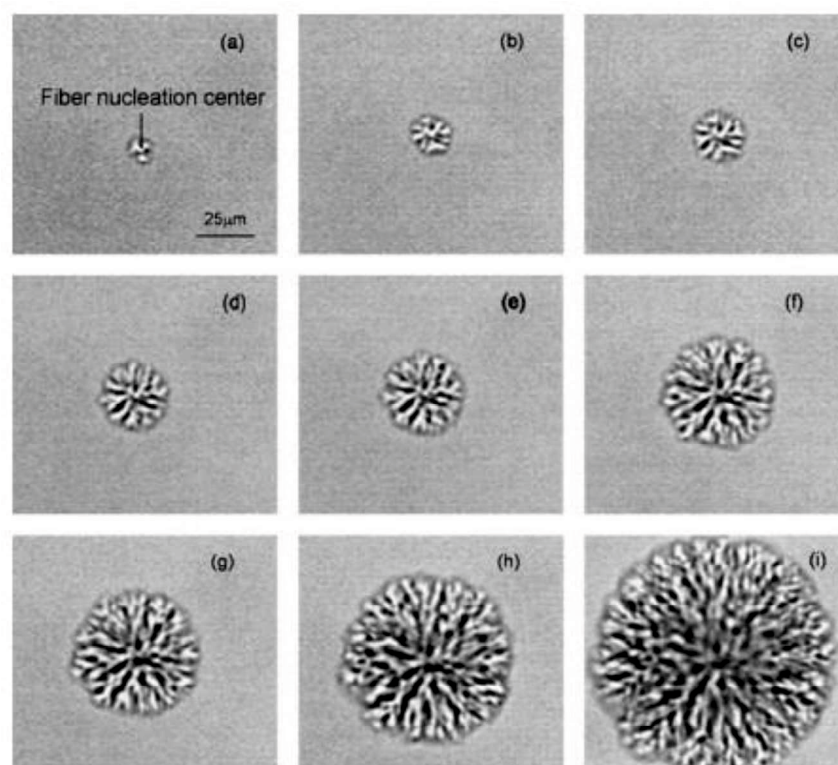


Figure 1-15. In situ observation on the formation of an *N*-lauroyl-L-glutamic acid

di-*n*-butylamide (GP-*I*) fiber network. (a) The formation of primary fibers initiates from a nucleation center. The formation of GP-*I* fibers and the branching process is shown by (a)-(h), in which the time interval between neighboring photographs is of 0.2 s. Solvent 1,2-propanediol; $\sigma = 6.92$; $T = 330\text{k}^{27}$

1.3.3 The application of supramolecular gels

Supramolecular gels formed by non-covalent interactions exhibit a reversible gel to sol phase transition in response to the stimulating environment enlarging their application fields. For example, some supramolecular gels are sensitive to temperature, pH, metal ion, photoinduction, or electric induction. Generally speaking, those applications of gels can be divided into six categories as follows:

- 1). Reacts to physical and chemical stimuli as a responder;
- 2). Reacts to biomaterials as an enzyme-responder;
- 3). Applied to biomedical materials as extracellular matrix mimics and drug delivery;
- 4). Applied to nanostructured materials as templates;
- 5). Applied to environment recovery;
- 6). Applied to optic and electronic materials.

The liquid crystalline physical gel is of current interest in advanced functional materials because of the unique and favourable properties. Liquid crystalline physical gel contains two components, liquid crystal and organogelator, respectively. LMWGs

applied in quasi-solid-state electrolytes have also attracted much attention for their good performance and stability.

1.4 Research purpose

Advanced functional materials which have unique and favourable properties are being focused on a wide range of applications with a rapid popularity. Herein, the major work in order to evaluate the possibility of applications for perfluoroalkyl derivatives in different fields will be studied as follows.

- 1). Functional materials showing liquid crystalline properties and gelation abilities are explored.
- 2). As phase-selective organogelators, 4-alkoxy-4'-[4-(perfluorohexyl)butoxy]-1,1'-biphenyl derivatives are researched in environmental recovery.
- 3). As a kind of LMWG, 4-[2-(perfluorohexyl)ethylthio]-4'-alkoxy-1,1'-biphenyl derivatives have been investigated in quasi-solid-state electrolytes.

1.5 References

1. Bergaya, F.; Lagaly, G. *Developments in clay science* **2006**, *1*, 1.
2. Ubbink, J.; Burbidge, A.; Mezzenga, R. *Soft matter* **2008**, *4* (8), 1569.
3. Tschierske, C. *Annual Reports Section C (Physical Chemistry)* **2001**, *97*, 191.
4. (a) Peters, G. M.; Davis, J. T. *Chemical Society Reviews* **2016**, *45*, 3188; (b) Luisier, N.; Scopelliti, R.; Severin, K. *Soft Matter* **2016**, *12* (2), 588; (c) Shalaev, E.; Wu, K.; Shamblin, S.; Krzyzaniak, J. F.; Descamps, M. *Advanced Drug Delivery Reviews* **2016**, *100*, 194.
5. Reinitze, F. *Monatshefte für Chemie* **1888**, *9*, 421.
6. Dierking, I. *Textures of Liquid Crystals*, John Wiley & Son **2006**, p 1-3.
7. Fairhurst, C. E.; Fuller, S.; Gray, J.; Holmes, M. C.; Tiddy, G. J.; Demus, D.; Goodby, J.; Gray, G.; Spiess, H. W.; Vill, V. *Handbook of Liquid Crystals*, John Wiley & Son **1998**, p 341.
8. Small, D. M. *Jouranl of Colloid and Interface Science* **1977**, *58*(3), 581
9. Singh, S.; Dunmur, D. A. *Liquid Crystals: Fundamentals*, World Scientific **2002**, p 453-455.
10. Blunk, D.; Bierganns, P.; Bongartz, N.; Tessendorf, R.; Stubenrauch, C. *New Journal of Chemistry* **2006**, *30* (12), 1705.
11. Collings, P. J.; Hird, M. *Introduction to liquid crystals: chemistry and physics*,

CRC Press **1997**, p 139.

12. (a) Geelhaar, T.; Griesar, K.; Reckmann, B. *Angewandte Chemie International Edition* **2013**, *52* (34), 8798; (b) Kato, T.; Hirai, Y.; Nakaso, S.; Moriyama, M. *Chemical Society Reviews* **2007**, *36*(12), 1857.
13. (a) Demus, D.; Goodby, J.; Gray, G.; Spiess, H. W.; Vill, V. *Handbook of Liquid Crystals* John Wiley & Son, **1998**, p 133-187; (b) Repasky, P. J.; Agra-Kooijman, D. M.; Kumar, S.; Hartlry, C. S. *Journal of Physical Chemistry B* **2016**, *120*(10), 2829; (c) Pelzl, G.; Diele, S.; Weossflog, W. *Advanced Materials* **1999**, *11*(9), 707.
14. Jin, J. I.; Antoun, S.; Ober, C.; Lenz, R. *British Polymer Journal* **1980**, *12* (4), 132.
15. Bahr, C.; Kitzerow, H.-S. *Chirality in Liquid Crystals*, Springer **2001**, p 13.
16. Colombo, J.; Del Gado, E. *Soft Matter* **2014**, *10* (22), 4003.
17. Piepenbrock, M.-O. M.; Lloyd, G. O.; Clarke, N.; Steed, J. W. *Chemical Reviews* **2009**, *110* (4), 1960.
18. Davidovich-Pinhas, M. *Therapeutic Delivery* **2016**, *7* (1), 1.
19. Hanabusa, K. *Electrochemical Aspects of Ionic Liquids* **2011**, 395.
20. Rogovina, L.; Vasil'ev, V.; Braudo, E. *Polymer Science Series C* **2008**, *50* (1), 85.
21. Flory, P. *Faraday Discussions* **1975**, *57*, 7.
22. Jagur - Grodzinski, J. *Polymers for Advanced Technologies* **2010**, *21* (1), 27.

23. Shih, W. Y.; Shih, W.-H.; Aksay, I. A. In *Mechanical Properties of Colloidal gels subject to particle rearrangement*, MRS Proceedings, Cambridge Univ Press **1990**, p 477.
24. Triantafillidis, C.; Elsaesser, M. S.; Hüsing, N. *Chemical Society Reviews* **2013**, 42 (9), 3833.
25. Yadav, P.; Ballabh, A. *Colloids and Surfaces A: Physicochemical and Engineering Aspects* **2012**, 414, 333.
26. (a) Dastidar, P. *Chemical Society Reviews* **2008**, 37 (12), 2699; (b) Lin, Y. C.; Kachar, B.; Weiss, R. G. *Journal of the American Chemical Society* **1989**, 111 (15), 5542.
27. Frederic, F. *Low Molecular Mass Gelators Design, Self-assemble, Function*, Springer: **2005**, p 1-37.

Chapter 2 Synthesis of perfluoroalkyl derivatives without protic groups

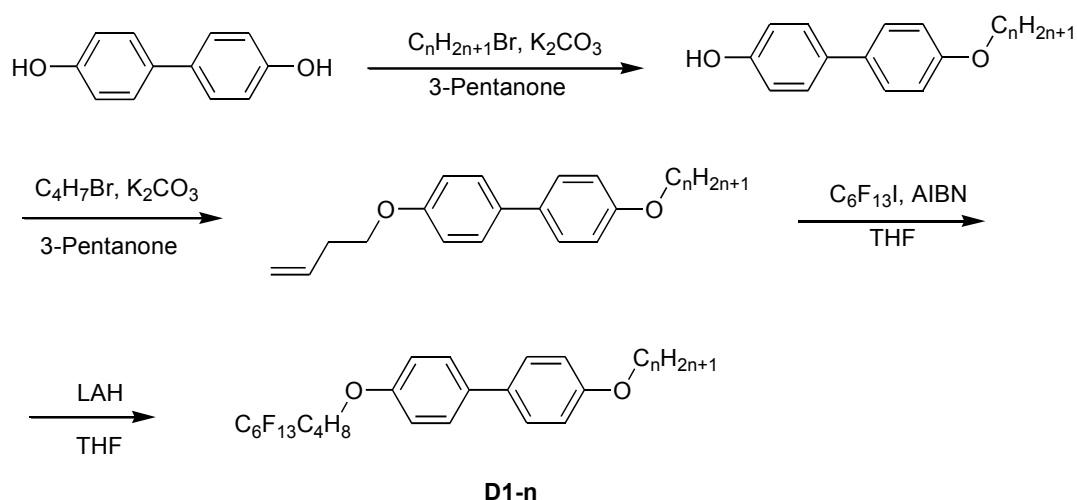
2.1 General materials and methods

4,4'-Biphenol was purchased from Wako Industries, Ltd.; 1-iodoperfluorohexane was purchased from Daikin Industries, Ltd.; 2,2'-azobis(isobutyronitrile) (AIBN), 4-(benzyloxy)phenol, *N,N'*-dicyclohexylcarbodiimide (DCC) and 4-dimethylaminopyridine were purchased from Tokyo Chemical Industry Co., Ltd.. AIBN was recrystallized from cold ethanol before being used. Rape oil was purchased from Nisshin oil group Ltd.. Other reagents and solvents were obtained from general commercial sources. Synthetic lubricant and mineral oil provided by Cosmo oil lubricants co. Ltd. and formalin provided by Meiwa Plastic Industries Ltd. Marine water ($\rho = 1.0198 \text{ g mL}^{-1}$, $\text{pH} \approx 8$) which was picked up from Tokiwa beaches in Yamaguchi prefecture of Japan was used.

Melting point was obtained with a Yanaco MP-J3 micro melting point apparatus. Infrared spectra were recorded on a Shimadzu IR Prestige-21 spectrometer using KBr disc. ^1H NMR, ^{13}C NMR and ^{19}F NMR spectra were recorded with JMN-LA500 (500 MHz) spectrometer, where tetramethylsilane was used as an internal standard. High resolution mass spectra (HRMS) were recorded with a Waters LCT Premier™ XE. The transition temperatures and latent heats were determined using a Seiko SSC-5200 DSC, where indium (99.9%) was used as a calibration standard ($\text{mp}=156.6^\circ\text{C}$, 28.4 J/g). The DSC thermogram was operated at a heating or cooling rate of $5 \text{ }^\circ\text{C min}^{-1}$. The mesophases were characterized using a Nikon POH polarizing microscope fitted

with a Mettler thermo-control system (FP-900). Scanning electron microscope (SEM) images were observed with a JEOL JSM-6510LA. The rheological properties of sample with high viscosity were measured using a Dynamic Viscoelasticity Measurement Apparatus (Reogel-G1000, UBM Co., Ltd.) equipped with cone and plate geometry of 40 mm diameter and 2° angle. The conductivities of ionogel electrolytes were measured by impedance spectroscopy using a Solartron 1280C frequency response analyzer with alternating current (AC) voltage amplitude of 50 mV. The ionic conductivities were evaluated by alternating current measurements from 5 Hz and 20 kHz at 0.5 V.

2.2 Synthesis of 4-alkoxy-4'-[4-(perfluorohexyl)butoxy]-1,1'-biphenyl



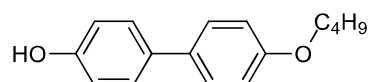
Scheme 2-1. Synthetic route of 4-alkoxy-4'-[4-(perfluorohexyl)butoxy]-1,1'-biphenyl

2.2.1 Synthetic procedure for preparation of 4-alkoxy-4'-hydroxy-1,1'-biphenyl

4,4'-Biphenol (1.86 g, 10 mmol) was dissolved in 3-pentanone (10 mL), potassium carbonate (2.07 g, 15 mmol) was added, and then 1-bromoalkane (10 mmol)

was dropped into the reaction mixture.¹ The reaction mixture was stirred at 80 °C for one day and separated by filtration. Filtrate was concentrated in *vacuo*, the residue was purified by silica gel column chromatography, and then recrystallized from CH₃OH to give pure product, as a colorless crystalline solid.

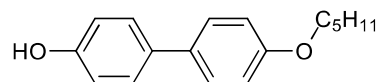
Physical data of 4-(butoxy)-4'-hydroxy-1,1'-biphenyl



Yield = 35%, mp = 167-168 °C, IR (KBr disc) ν = 3421.7, 2956.8, 2933.7, 1618.3, 1506.4, 1286.2, 817.8 cm⁻¹.

¹H NMR (500 MHz, *d*₆-DMSO) δ 7.46 (d, *J* = 8.7 Hz, 2H), 7.40 (d, *J* = 8.5 Hz, 2H), 6.94 (d, *J* = 8.6 Hz, 2H), 6.80 (d, *J* = 8.7 Hz, 2H), 3.96 (t, *J* = 6.5 Hz, 2H), 1.7-1.66 (m, 2H), 1.52-1.35 (m, 2H), 0.93 (t, *J* = 7.4 Hz, 3H) ppm.

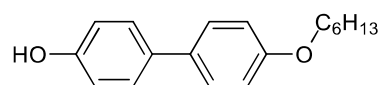
Physical data of 4-(pentyloxy)-4'-hydroxy-1,1'-biphenyl



Yield = 50%, colorless needles, mp = 166-167 °C, IR (KBr disc) ν = 3346.5, 2956.8, 2933.7, 2864.3, 1502.6, 1271.1, 1253.7, 823.6 cm⁻¹.

¹H NMR (500 MHz, CDCl₃) δ 7.53-7.37 (m, 4H), 7.02-6.92 (m, 2H), 6.92-6.83 (m, 2H), 4.78 (s, 1H), 3.99 (t, *J* = 6.6 Hz, 2H), 1.87-1.72 (m, 2H), 1.54-1.33 (m, 4H), 0.94 (t, *J* = 7.1 Hz, 3H) ppm.

Physical data of 4-(hexyloxy)-4'-hydroxy-1,1'-biphenyl

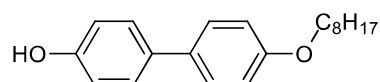


Yield = 45%, colorless needles, mp = 155-156 °C, IR (KBr disc) ν = 3346.5, 2955.0,

2933.7, 2870.1, 1608.6, 1502.6, 1230.0, 816.0 cm^{-1} .

^1H NMR (500 MHz, CDCl_3) δ 7.45-7.41 (m, 4H), 6.94 (d, $J = 8.6$ Hz, 2H), 6.87 (d, $J = 8.6$ Hz, 2H), 5.02 (s, 1H), 3.98 (t, $J = 6.6$ Hz, 2H), 1.82-1.78 (m, 2H), 1.48-1.45 (m, 2H), 1.38-1.32 (m, 4H), 0.91 (t, $J = 7.2$ Hz, 3H) ppm.

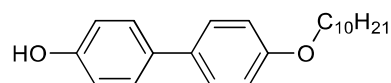
Physical data of 4-(octyloxy)-4'-hydroxy-1,1'-biphenyl



Yield = 40%, colorless needles, mp = 152-153 $^{\circ}\text{C}$, IR (KBr disc) $\nu = 3352.3, 2955.0, 2920.2, 1608.6, 1500.6, 1261.5, 814.0$ cm^{-1} .

^1H NMR (500 MHz, d_6 -DMSO) δ 9.44 (s, 1H), 7.47 (d, $J = 8.5$ Hz, 2H), 7.41 (d, $J = 8.5$ Hz, 2H), 6.94 (d, $J = 8.6$ Hz, 2H), 6.81 (d, $J = 8.5$ Hz, 2H), 3.96 (t, $J = 6.5$ Hz, 2H), 1.79-1.60 (m, 2H), 1.40 (dd, $J = 14.4, 6.8$ Hz, 2H), 1.36-1.16 (m, 8H), 0.86 (t, $J = 6.6$ Hz, 3H) ppm.

Physical data of 4-(decyloxy)-4'-hydroxy-1,1'-biphenyl



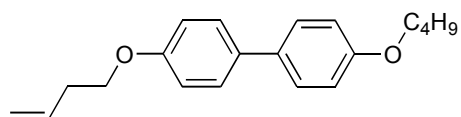
Yield = 44%, colorless needles, mp = 145-147 $^{\circ}\text{C}$, IR (KBr disc) $\nu = 3371.6, 2929.9, 2854.7, 1614.4, 1506.4, 1251.8, 817.8$ cm^{-1} .

^1H NMR (500 MHz, CDCl_3) δ 7.51-7.38 (m, 4H), 7.03-6.73 (m, 4H), 4.73 (s, 1H), 3.98 (t, $J = 6.6$ Hz, 2H), 1.90-1.70 (m, 2H), 1.46 (m, 2H), 1.40-1.23 (m, 12H), 0.88 (t, $J = 6.9$ Hz, 3H) ppm.

2.2.2 Synthetic procedure for preparation of 4-enyloxy-4'-alkoxy-1,1'-biphenyl

4-Alkoxy-4'-hydroxy-1,1'-biphenyl (10 mmol) was dissolved in 3-pentanone (10 mL), potassium carbonate (2.07 g, 15 mmol) was added, and then 1-bromoalkene (10 mmol) was dropped into the reaction mixture. The reaction mixture was stirred at 80 °C for one day and separated by filtration. Filtrate was concentrated in *vacuo*, the residue was refined by silica gel column chromatography, and then recrystallized from CH₃OH to give pure product, as a colorless crystalline solid.

Physical data of 4-(but-3-enyloxy)-4'-(butoxy)-1,1'-biphenyl

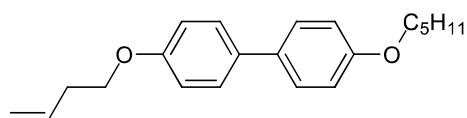


Yield = 50%, colorless needles, mp = 133-135 °C, IR (KBr disc) ν = 3456.4, 2949.2, 2883.6, 2357.0, 1604.8, 1500.6, 1273.0, 1246.0, 825.5 cm⁻¹.

¹H NMR (500 MHz, CDCl₃) δ 7.53-7.38 (m, 4H), 7.04-6.84 (m, 4H), 5.92 (ddt, J = 17.1, 10.3, 6.7 Hz, 1H), 5.19 (d, J = 17.1 Hz, 1H), 5.12 (d, J = 10.3 Hz, 1H), 4.05 (t, J = 6.7 Hz, 2H), 3.99 (t, J = 6.6 Hz, 2H), 2.59-2.54 (m, 2H), 1.81-1.76 (m, 2H), 1.55-1.46 (m, 2H), 0.99 (t, J = 7.4 Hz, 3H) ppm.

ESI-TOF-MS: m/z calculated for C₂₀H₂₄O₂, [M+H]⁺: 297.1855, found: 297.1853.

Physical data of 4-(but-3-enyloxy)-4'-(pentyloxy)-1,1'-biphenyl



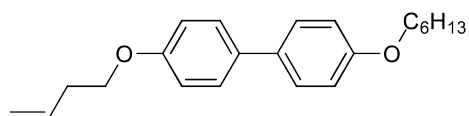
Yield = 30%, colorless needles, mp = 126-127 °C, IR (KBr disc) ν = 2958.8, 2933.7, 2873.9, 1606.7, 1500.6, 1275.0, 1248.0, 825.5 cm⁻¹.

¹H NMR (500 MHz, CDCl₃) δ 7.55- 7.38 (m, 4H), 7.02-6.87 (m, 4H), 5.93 (ddt, J =

17.2, 10.4, 6.7 Hz, 1H), 5.19 (d, $J = 17.2$ Hz, 1H), 5.12 (d, $J = 10.3$ Hz, 1H), 4.05 (t, $J = 6.7$ Hz, 2H), 3.98 (t, $J = 6.5$ Hz, 2H), 2.63-2.51 (m, 2H), 1.81 (dd, $J = 10.7, 4.0$ Hz, 2H), 1.54-1.34 (m, 4H), 0.94 (t, $J = 7.2$ Hz, 3H) ppm.

ESI-TOF-MS: m/z calcd for $C_{21}H_{26}O_2$, $[M+H]^+$: 311.2011, found: 311.2004.

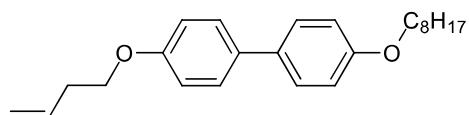
Physical data of 4-(but-3-enyloxy)-4'-(hexyloxy)-1,1'-biphenyl



Yield = 35%, colorless needles, mp = 117-128 °C, IR (KBr disc) $\nu = 2955.0, 2933.7, 1606.7, 1500.6, 1273.0, 1248.0, 825.5$ cm^{-1} .

1H NMR (500 MHz, $CDCl_3$) δ 7.45-7.33 (m, 4H), 6.94-6.84 (m, 4H), 5.85 (ddt, $J = 17.0, 10.3, 6.7$ Hz, 1H), 5.12 (d, $J = 17.0$ Hz, 1H), 5.06 (d, $J = 10.3$ Hz, 1H), 3.98 (t, $J = 6.7$ Hz, 2H), 3.91 (t, $J = 6.6$ Hz, 2H), 2.52-2.47 (m, 2H), 1.81-1.62 (m, 2H), 1.47-1.36 (m, 2H), 1.30-1.28 (m, 4H), 0.88 (t, $J = 7.2$ Hz, 3H) ppm.

Physical data of 4-(but-3-enyloxy)-4'-(octyloxy)-1,1'-biphenyl

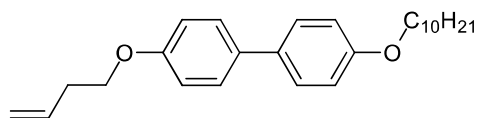


Yield = 46%, colorless needles, mp = 108-110 °C, IR (KBr disc) $\nu = 3456.4, 2933.7, 2922.2, 2864.3, 1608.6, 1500.6, 1176.6, 1043.5, 825.5$ cm^{-1} .

1H NMR (500 MHz, $CDCl_3$) δ 7.52-7.34 (m, 4H), 7.04-6.87 (m, 4H), 5.93 (ddt, $J = 17.0, 10.2, 6.7$ Hz, 1H), 5.19 (d, $J = 17.0$ Hz, 1H), 5.12 (d, $J = 10.2$ Hz, 1H), 4.05 (t, $J = 6.7$ Hz, 2H), 3.98 (t, $J = 6.6$ Hz, 2H), 2.57 (q, $J = 6.7$ Hz, 2H), 1.87-1.74 (m, 2H), 1.52-1.41 (m, 2H), 1.41-1.17 (m, 8H), 0.89 (t, $J = 6.9$ Hz, 3H) ppm.

ESI-TOF-MS: m/z calculated for $C_{24}H_{32}O_2$, $[M+H]^+$: 353.2481, found: 353.2481.

Physical data of 4-(but-3-enyloxy)-4'-(decyloxy)-1,1'-biphenyl



Yield = 45%, colorless needles, mp = 107-108 °C, IR (KBr disc) ν = 3437.2, 2955.0, 2931.8, 2850.8, 1820.8, 1510.3, 1275.0, 1246.0, 827.5 cm^{-1} .

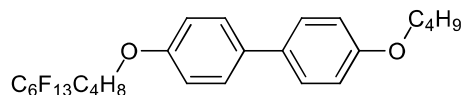
^1H NMR (500 MHz, CDCl_3) δ 7.56-7.33 (m, 4H), 7.02-6.85 (m, 4H), 5.92 (ddt, J = 17.0, 10.3, 6.7 Hz, 1H), 5.19 (d, J = 17.0 Hz, 1H), 5.12 (d, J = 10.3 Hz, 1H), 4.05 (t, J = 6.7 Hz, 2H), 3.98 (t, J = 6.5 Hz, 2H), 2.59-2.54 (m, 2H), 1.89-1.67 (m, 2H), 1.47 (dt, J = 15.2, 7.0 Hz, 3H), 1.41-1.13 (m, 13H), 0.88 (t, J = 6.9 Hz, 3H) ppm.

ESI-TOF-MS: m/z calculated for $\text{C}_{26}\text{H}_{36}\text{O}_2$, $[\text{M}+\text{H}]^+$: 381.2793, found: 381.2793.

2.2.3 Synthetic procedure for preparation of compounds D1-n

4-Alkenyloxy-4'-alkoxy-1,1'-biphenyl (3 mmol), 1-iodoperfluorohexane (1.35 g, 3 mmol), and AIBN (0.50 g, 3 mmol) were dissolved in THF and stirred at 70 °C under nitrogen atmosphere for one day. The reaction was quenched with Na_2CO_3 (aq.), diluted with ethyl acetate and rinsed with water and then with brine.² After the organic layer was dried using anhydrous magnesium sulphate, the solvent was evaporated in *vacuo*. The residue without any other refinement was dissolved in THF (anhydrous) to the next step. The mixture with LiAlH_4 (1 *eq.*) stirred at room temperature for one day. The reaction quenched with NH_4Cl (aq.). The mixture was filtered and the filtrate was concentrated in *vacuo*. The residue was purified by silica gel column chromatography, and then recrystallized from CH_3OH to give pure product, as a colorless solid.

Physical data of D1-4



Yield = 37%, colorless needles, mp = 93-95 °C, IR (KBr disc) ν = 3456.4, 2937.6, 2875.9, 1606.7, 1500.6, 1275.0, 1190.1, 1180.5, 1041.6, 825.5 cm^{-1} .

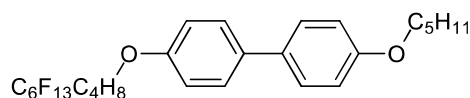
^1H NMR (500 MHz, CDCl_3) δ 7.44-7.30 (m, 4H), 6.9-6.82 (m, 4H), 3.95 (t, J = 5.9 Hz, 2H), 3.92 (t, J = 6.5 Hz, 2H), 2.15-2.05 (m, 2H), 1.85-1.68 (m, 6H), 1.51-1.25 (m, 2H), 0.91 (t, J = 7.4 Hz, 3H) ppm.

^{13}C NMR (126 MHz, CDCl_3) δ 158.13, 157.67, 133.51, 132.98, 127.51, 127.46, 114.53, 114.47, 67.50, 66.98, 31.06, 30.38 (t, J = 22.3 Hz), 28.43, 18.95, 17.00, 13.53 ppm.

^{19}F NMR (471 MHz, CDCl_3) δ -80.68, -114.35, -121.82, -122.78, -123.44, -126.04 ppm.

ESI-TOF-MS: m/z calculated for $\text{C}_{26}\text{H}_{25}\text{F}_{13}\text{O}_2$, $[\text{M}+\text{HCOO}]^-$: 661.1624, found: 661.1630.

Physical data of D1-5



Yield = 35%, colorless needles, mp = 86-88 °C, IR (KBr disc) ν = 2958.8, 2933.7, 2875.9, 1606.7, 1500.6, 1273.0, 1246.0, 1211.3, 1190.1, 1180.2, 1143.8, 1037.7, 823.6, 700.2 cm^{-1} .

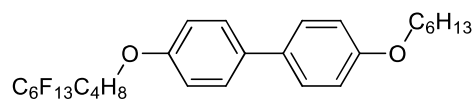
^1H NMR (500 MHz, CDCl_3) δ 7.59-7.38 (m, 4H), 7.01-6.86 (m, 4H), 4.03 (t, J = 5.8 Hz, 2H), 3.98 (t, J = 6.6 Hz, 2H), 2.17 (m, 2H), 1.84 (m, 6H), 1.51-1.31 (m, 4H), 0.94 (t, J = 7.1 Hz, 3H).

^{13}C NMR (126 MHz, CDCl_3) δ 158.37, 157.93, 133.77, 133.23, 127.76, 127.71, 114.78, 114.72, 68.07, 67.24, 30.63, 28.96 (t, $J = 22.4$ Hz), 28.68, 28.17, 22.42, 17.25, 13.95 ppm.

^{19}F NMR (471 MHz, CDCl_3) δ -80.68, -114.35, -121.82, -122.78, -123.44, -126.04 ppm.

ESI-TOF-MS: m/z calcd for $\text{C}_{27}\text{H}_{27}\text{F}_{13}\text{O}_2$, $[\text{M}+\text{HCOO}]^-$: 675.1780, found: 675.1789.

Physical data of D1-6



Yield = 40%, colorless needles, mp = 93-95 °C, IR (KBr disc) ν = 2931.8, 2875.9, 1606.7, 1500.6, 1273.0, 1247.9, 1190.1, 1143.8, 1041.6, 825.5, 700.2 cm^{-1} .

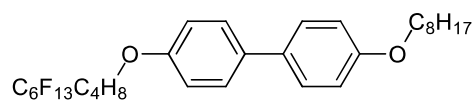
^1H NMR (500 MHz, CDCl_3) δ 7.48-4.73 (m, 4H), 7.02- 6.88 (m, 4H), 4.04 (t, $J = 5.9$ Hz, 2H), 3.99 (t, $J = 6.6$ Hz, 2H), 2.22-2.11 (m, 7.8 Hz, 2H), 1.91-1.70 (m, 6H), 1.54-1.43 (m, 2H), 1.42-1.29 (m, 4H), 1.04-0.81 (m, 3H).

^{13}C NMR (126 MHz, CDCl_3) δ 158.37, 157.92, 133.76, 133.23, 127.76, 127.71, 114.78, 114.71, 68.08, 67.23, 31.55, 30.64 (t, $J = 22.1$ Hz), 29.23, 28.68, 25.69, 22.56, 17.27, 13.96 ppm.

^{19}F NMR (471 MHz, CDCl_3) δ -80.69, -114.35, -121.82, -122.78, -123.44, -126.04 ppm.

ESI-TOF-MS: m/z calcd for $\text{C}_{28}\text{H}_{29}\text{F}_{13}\text{O}_2$, $[\text{M}+\text{HCOO}]^-$: 689.1937, found: 689.1940.

Physical data of D1-8



Yield = 35%, colorless needles, mp = 103-104 °C, IR (KBr disc) ν = 3456.4, 2958.8, 2875.9, 1606.7, 1500.6, 1275.0, 1190.1, 1178.5, 1041.6, 825.5 cm^{-1} .

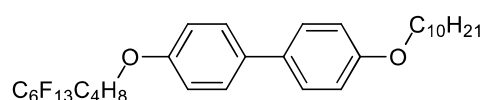
^1H NMR (500 MHz, CDCl_3) δ 7.49-7.31 (m, 4H), 6.95-6.71 (m, 4H), 3.95 (t, J = 5.8 Hz, 2H), 3.91 (t, J = 6.6 Hz, 2H), 2.15-2.05 (m, 2H), 1.91-1.62 (m, 6H), 1.45-1.33 (m, 2H), 1.33-1.14 (m, 8H), 0.82 (t, J = 6.8 Hz, 3H) ppm.

^{13}C NMR (126 MHz, CDCl_3) δ 158.37, 157.92, 133.76, 133.22, 127.76, 127.71, 114.77, 114.71, 68.08, 67.23, 31.78, 30.63 (t, J = 22.3 Hz), 29.33, 29.26, 29.21, 28.68, 26.02, 22.61, 17.25, 14.03 ppm.

^{19}F NMR (471 MHz, CDCl_3) δ -80.68, -114.35, -121.82, -122.78, -123.44, -126.04 ppm

ESI-TOF-MS: m/z calculated for $\text{C}_{30}\text{H}_{33}\text{F}_{13}\text{O}_2$, $[\text{M}+\text{HCOO}]^-$: 717.2250, found: 717.2269.

Physical data of D1-10



Yield = 38%, colorless needles, mp = 105-106 °C, IR (KBr disc) ν = 3446.8, 2922.2, 2852.7, 1608.6, 1500.6, 1275.0, 1190.1, 1179.5, 1143.8, 825.5 cm^{-1} .

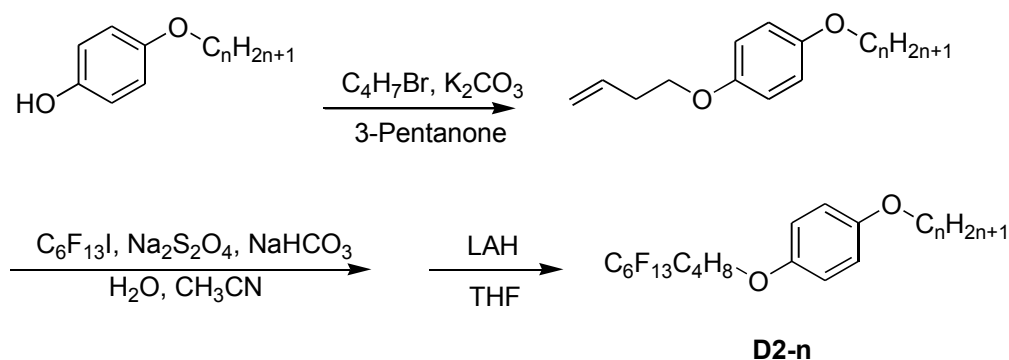
^1H NMR (500 MHz, CDCl_3) δ 7.55-7.36 (m, 4H), 7.03-6.83 (m, 4H), 4.03 (t, J = 5.8 Hz, 2H), 3.98 (t, J = 6.5 Hz, 2H), 2.23-2.13 (m, 2H), 1.98-1.71 (m, 6H), 1.51-1.41 (m, 2H), 1.41-1.20 (m, 12H), 0.88 (t, J = 6.9 Hz, 3H) ppm.

^{13}C NMR (126 MHz, CDCl_3) δ 158.37, 157.91, 133.76, 133.22, 127.76, 127.71, 114.77, 114.71, 68.08, 67.23, 31.86, 30.63 (t, J = 22.5 Hz), 29.54, 29.52, 29.37, 29.28, 28.68, 26.01, 22.63, 17.25, 14.05 ppm.

^{19}F NMR (471 MHz, CDCl_3) δ -80.68, -114.34, -121.82, -122.78, -123.44, -126.04 ppm

ESI-TOF-MS: m/z calculated for $\text{C}_{32}\text{H}_{37}\text{F}_{13}\text{O}_2$, $[\text{M}+\text{NH}_4]^+$: 718.2930, found: 718.2924.

2.3 Synthesis of 4-alkoxy-4'-[4-(perfluorohexyl)butoxy]benzene

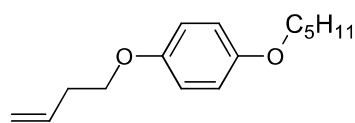


Scheme 2-2. Synthetic route of 4-alkoxy-4'-[4-(perfluorohexyl)butoxy]benzene

2.3.1 Synthetic procedure for preparation of 4-enoxy-4'-alkoxybenzene

4-Bromo-1-butene (5.40 g, 40 mmol) and potassium carbonate (5.52 g, 40 mmol) were added to 3-pentanone solution (40 mL) of 4-pentyloxyphenol (or 4-hexyloxyphenol) (40 mmol) and the reaction mixture was refluxed for 2 days. The precipitate of reaction mixture was removed by filtration, the filtrate was evaporated *in vacuo*, and the residue was purified by silica gel column chromatography, and then recrystallized from CH_3OH to give pure products.

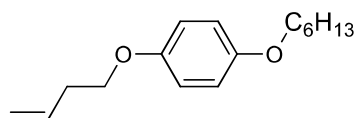
Physical data of 1-(but-3-enoxy)-4'-(pentyloxy)benzene



Yield = 40 %, a colorless oil.

^1H NMR (500 MHz, CDCl_3) δ = 6.82 (s, 4H), 5.90 (ddt, J = 17.1, 10.1, 6.6 Hz, 1H), 5.16 (d, J = 17.1 Hz, 1H), 5.10 (d, J = 10.1 Hz, 1H), 3.96 (t, J = 6.6 Hz, 2H), 3.89 (t, J = 6.4 Hz, 2H), 2.51 (m, 2H), 1.75 (m, 2H), 1.33-1.46 (m, 4H), 0.92 (t, J = 6.9 Hz, 3H) ppm.

Physical data of 1-(but-3-en-1-yloxy)-4-(hexyloxy)benzene



Yield = 43 %, a colorless oil.

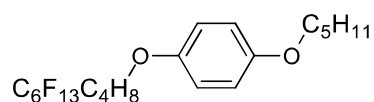
^1H NMR (500 MHz, CDCl_3) δ 7.07 (t, J = 5.6 Hz, 2H), 6.89-6.76 (m, 2H), 5.90 (ddt, J = 17.1, 10.1, 6.7 Hz, 1H), 5.16 (d, J = 17.1 Hz, 1H), 5.09 (d, J = 10.1 Hz, 1H), 3.99 (t, J = 6.7 Hz, 2H), 2.56-2.48 (m, 4H), 1.57 (t, J = 7.2 Hz, 2H), 1.33-1.27 (m, 6H), 0.87 (t, J = 7.2 Hz, 3H) ppm.

2.3.2 Synthetic procedure for preparation of D2-n

1-Iodoperfluorohexane (4.80 g, 8.79 mmol), sodium hydrogen carbonate (0.70 g, 8.69 mmol) and hydrosulfite sodium (1.50 g, 8.79 mmol) were added to an acetonitrile (8.5 ml) and water (5.5 ml) solution of 4-alkenyloxy-4'-alkoxybenzene derivatives (8.77 mmol) and stirred under shielded light for one night. The reaction solution was quenched with Na_2CO_3 (aq.), diluted with ethyl acetate and rinsed with water twice and then with brine. After the organic layer was dried using anhydrous magnesium sulphate, the solvent evaporated in *vacuo*. The residue without any other refinement was dissolved in THF (anhydrous) to the next step. The mixture with LiAlH_4 (1 *eq.*) was stirred at room temperature for one day. The reaction

quenched with NH_4Cl (aq.). The mixture was filtered and the filtrate was evaporated in *vacuo*. The residue was purified by silica gel column chromatography, and then recrystallized from CH_3OH to give pure product (**D2-n**).

Physical data of D2-5

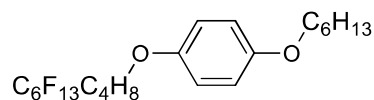


Yield = 25 %, colorless needles, mp = 42-43°C, IR (KBr disc) ν = 2952.5, 2913.9, 2873.4, 1508.1, 1238.1, 1209.1, 1149.4 cm^{-1} .

^1H NMR (270 MHz, CDCl_3) δ = 6.82 (s, 4H), 3.92 (t, J = 7.0 Hz, 2H), 3.90 (t, J = 7.0 Hz, 2H), 2.15 (m, 2H), 1.70-1.90 (m, 6H), 1.30-1.45 (m, 4H), 0.93 (t, J = 7.0 Hz, 3H) ppm.

ESI-TOF-MS: m/z calcd for $\text{C}_{21}\text{H}_{23}\text{F}_{13}\text{O}_2$, $[\text{M}-\text{H}]^-$: 553.1412, found: 553.1413.

Physical data of D2-6

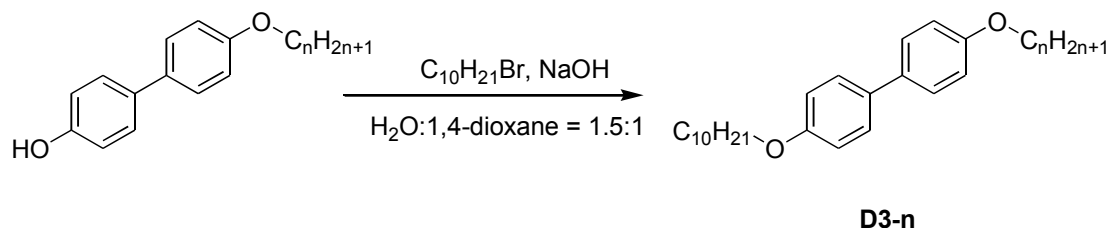


Yield = 20%, a colorless oil.

^1H NMR (500 MHz, CDCl_3) δ 7.13-7.11 (m, 2H), 6.85-6.83 (m, 2H), 3.99 (t, J = 5.6 Hz, 2H), 2.68-2.51 (m, 2H), 2.20-2.18 (m, 2H), 1.87 (t, J = 10.6 Hz, 4H), 1.62 (d, J = 6.4 Hz, 2H), 1.34 (s, 6H), 0.92 (t, J = 6.6 Hz, 3H) ppm.

ESI-TOF-MS: m/z calcd for $\text{C}_{22}\text{H}_{25}\text{F}_{13}\text{O}_2$, $[\text{M}-\text{H}]^-$: 567.1569, found: 567.1575.

2.4 Synthesis of 4-alkoxy-4'-alkoxy-1,1'-biphenyl



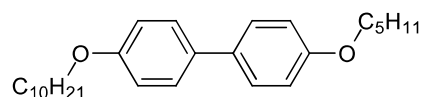
Scheme 2-3. Synthetic route of 4-alkoxy-4'-decyloxy-1,1'-biphenyl

2.4.1 Synthetic procedure for preparation of 4-alkoxy-4'-alkoxy-1,1'-biphenyl

(D3-n)

1,4-Dioxane of 4-alkoxy-4'-hydroxy-1,1'-biphenyl (20 mmol) was dissolved in solution of NaOH (1 mol/L, 20 mL), 40 mL water and 40 mL 1,4-dioxane, then 1-bromodecane (20 mmol) was added and stirred at 70 °C for one day. The mixture was poured into 200 mL ice water. The precipitate of reaction mixture was removed by filtration, the filtrate was evaporated in *vacuo*, and the residue was purified by silica gel column chromatography, and then recrystallized from CH₃OH to give pure product (**D3-n**).

Physical data of 4-(decyloxy)-4'-(pentyloxy)-1,1'-biphenyl (D3-5)



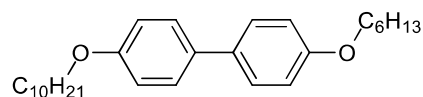
Yield = 65 %, colorless needles, mp = 107-108 °C, IR (KBr disc) ν = 2956.9, 2935.7, 2850.8, 1608.6, 1500.6, 1275.0, 1251.8, 1033.9, 825.5 cm⁻¹.

¹H NMR (500 MHz, CDCl₃) δ 7.45 (d, J = 8.6 Hz, 4H), 6.94 (d, J = 8.6 Hz, 4H), 3.98 (t, J = 6.6 Hz, 4H), 1.88-1.73 (m, 4H), 1.51-1.18 (m, 19H), 0.94 (t, J = 7.1 Hz, 3H),

0.88 (t, $J = 6.8$ Hz, 3H) ppm.

ESI-TOF-MS: m/z calcd for $C_{27}H_{40}O_2$, $[M+H]^+$: 397.3107, found: 397.3099.

Physical data of 4-(decyloxy)-4'-(hexyloxy)-1,1'-biphenyl (D3-6)

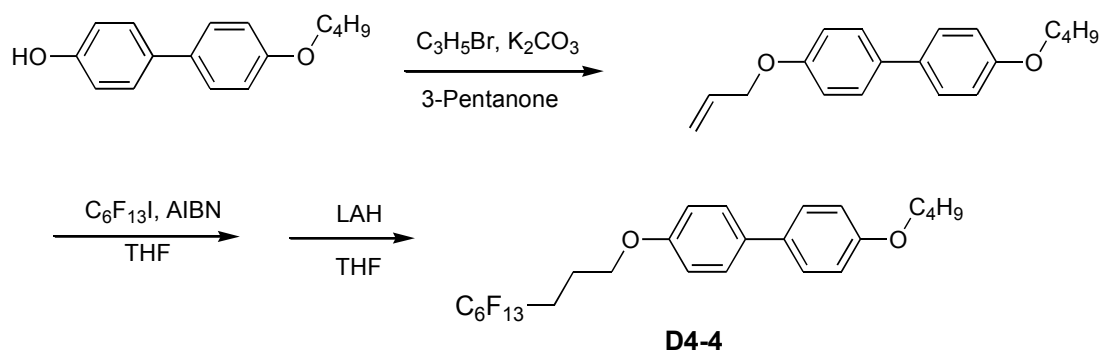


Yield = 70 %, colorless needles, IR (KBr disc) $\nu = 2955.0, 2933.7, 2872.0, 2362.8, 1606.7, 1500.6, 1273.0, 1251.8, 1039.7, 825.5$ cm^{-1} .

1H NMR (500 MHz, $CDCl_3$) δ 7.45 (d, $J = 8.6$ Hz, 4H), 6.94 (d, $J = 8.6$ Hz, 4H), 3.98 (t, $J = 6.6$ Hz, 4H), 2.01-1.71 (m, 4H), 1.56-1.21 (m, 20H), 1.13-0.77 (m, 6H) ppm.

ESI-TOF-MS: m/z calcd for $C_{28}H_{42}O_2$, $[M+H]^+$: 411.3263, found: 411.3252.

2.5 Synthesis of 4-(butoxy)-4'-[4-(perfluorohexyl)-allyloxy]-1,1'-biphenyl



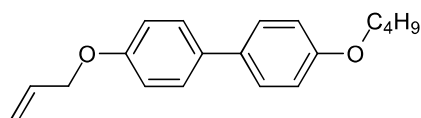
Scheme 2-4. Synthetic route of 4-(butoxy)-4'-[3-(perfluorohexyl)-propoxy]-1,1'-biphenyl

2.5.1 Synthetic procedure for preparation of 4-(ally-2-enyloxy)-4'-(butoxy)-1,1'-biphenyl

4-(Butoxy)-4'-hydroxy-1,1'-biphenyl (10 mmol) was dissolved in 3-pentanone (10 mL), potassium carbonate (2.07 g, 15 mmol) was added, and then 3-bromoprop-1-ene (10 mmol) was dropped into the reaction mixture. The reaction mixture was stirred at

80 °C for one day and separated by filtration. Filtrate was concentrated in *vacuo*, the residue was refined by silica gel column chromatography, and then recrystallized from CH₃OH to give pure product, as a colorless crystalline solid.

Physical data of 4-(ally-2-enyloxy)-4'-(butoxy)-1,1'-biphenyl



Yield = 70%, colorless needles, mp = 146-147 °C, IR (KBr disc) ν = 3427.5, 2956.9, 2933.7, 2873.9, 1606.7, 1500.6, 1273.0, 1246.0, 825.5 cm⁻¹.

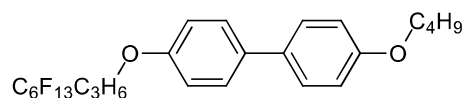
¹H NMR (500 MHz, CDCl₃) δ 7.49-7.29 (m, 4H), 6.95-6.80 (m, 4H), 6.01 (ddt, J = 17.2, 10.5, 5.1 Hz, 1H), 5.37 (d, J = 17.2 Hz, 1H), 5.23 (d, J = 10.5 Hz, 1H), 4.50 (t, J = 5.1 Hz, 2H), 3.92 (t, J = 6.5 Hz, 2H), 1.74-1.69 (m, 2H), 1.49-1.39 (m, 2H), 0.91 (t, J = 7.4 Hz, 3H) ppm.

2.5.2 Synthetic procedure for preparation of D4-4

4-(Butoxy)-4'-(allyloxy)-1,1'-biphenyl (3 mmol), 1-iodoperfluorohexane (1.35 g, 3 mmol), and AIBN (0.50 g, 3 mmol) were dissolved in THF and stirred at 70 °C under nitrogen atmosphere for one day. The reaction was quenched with Na₂CO₃ (aq.), diluted with ethyl acetate and rinsed with water and then with brine. After the organic layer was dried using anhydrous magnesium sulphate, the solvent was evaporated in *vacuo*. The residue without any other refinement was dissolved in THF (anhydrous) to the next step. The mixture with LiAlH₄ (1 *eq.*) stirred at room temperature for one day. The reaction quenched with NH₄Cl (aq.). The mixture was filtered and the filtrate was concentrated in *vacuo*. The residue was purified by silica gel column chromatography,

and then recrystallized from CH₃OH to give pure product (**D4-4**), as a colorless solid.

Physical data of **D4-4**



Yield = 44%, colorless needles, mp = 95-96 °C, IR (KBr disc) ν = 3446.8, 2939.5, 2873.9, 1606.7, 1500.6, 1251.8, 1192.0, 1180.4, 1145.7, 1031.9, 825.5 cm⁻¹.

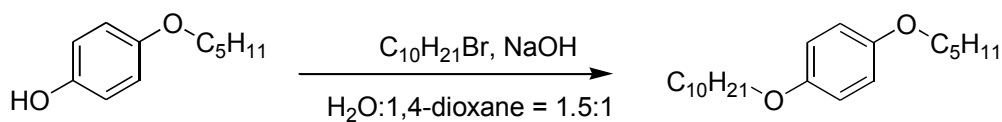
¹H NMR (500 MHz, CDCl₃) δ 7.48-7.45 (m, 4H), 6.96-6.93 (m, 4H), 4.07 (t, J = 5.9 Hz, 2H), 4.00 (t, J = 6.5 Hz, 2H), 2.65-2.26 (m, 2H), 2.15-2.09 (m, 2H), 1.82-1.76 (m, 2H), 1.76-1.45 (m, 2H), 0.99 (t, J = 7.4 Hz, 3H) ppm.

¹³C NMR (126 MHz, CDCl₃) δ 158.43, 157.70, 134.02, 133.16, 127.80, 127.73, 114.80, 114.73, 67.77, 66.39, 31.31, 27.93 (t, J = 22.3 Hz), 20.57, 19.21, 13.78 ppm.

¹⁹F NMR (471 MHz, CDCl₃) δ -80.68, -114.27, -121.80, -122.77, -123.36, -126.04 ppm.

ESI-TOF-MS: m/z calculated for C₂₅H₂₃F₁₃O₂, [M+HCOO]⁻: 647.1467, found: 647.1465.

2.6 Synthesis of 1-(decyloxy)-4-(pentyloxy)benzene



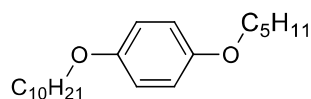
D5-5

Scheme 2-5. Synthetic route of 1-(decyloxy)-4-(pentyloxy)benzene

2.6.1 Synthetic procedure for preparation of 1-(decyloxy)-4-(pentyloxy)benzene

1,4-Dioxane of 4-(pentyloxy)phenol (20 mmol) was dissolved in solution of NaOH (1 mol/L, 20 mL), 40 mL water and 40 mL 1,4-dioxane, then 1-bromodecane (20 mmol) was added and stirred at 70 °C for one day. The reaction solution was poured into 200 mL ice water, diluted with ethyl acetate and rinsed with water twice and then with brine. After the organic layer was dried using anhydrous magnesium sulphate, the solvent was evaporated in *vacuo*, and refined by silica gel column chromatography to obtain a compound, and then recrystallized from CH₃OH to give pure product (**D5-5**).

Physical data of D5-5

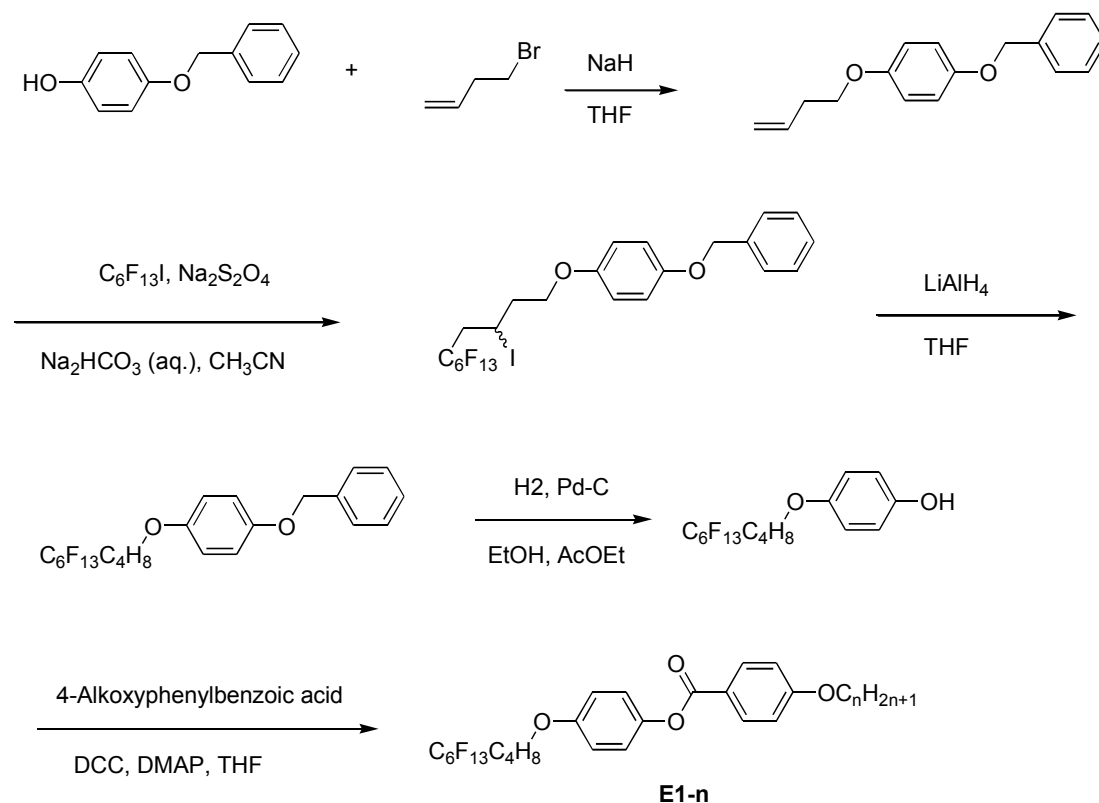


Yield = 25 %, colorless needles, mp = 46-47 °C, IR (KBr disc) ν = 2956.9, 2935.7, 2850.8, 1512.2, 1475.5, 1290.4, 1242.2, 1030.0, 825.5, 771.5 cm⁻¹.

¹H NMR (500 MHz, CDCl₃) δ 6.82 (s, 4H), 3.91-3.88 (m, 4H), 1.77-1.73 (m, 4H), 1.52-1.27 (m, 18H), 0.93 (t, *J* = 7.2 Hz, 3H), 0.88 (t, *J* = 6.8 Hz, 3H) ppm.

ESI-TOF-MS: *m/z* calcd for C₂₁H₃₆O₂, [M+NH₄]⁺: 338.3059, found: 338.3065.

2.7 Synthesis of 4-[4-(perfluorohexyl)butoxy]phenyl 4-alkoxybenzoates



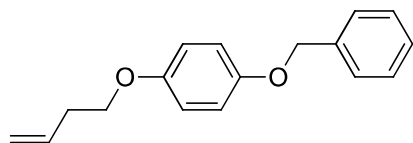
Scheme 2-6. Synthetic route of 4-[4-(perfluorohexyl)butoxy]phenyl 4-alkoxybenzoates

2.7.1 Synthetic procedure for preparation of 1-(benzyloxy)-4-(but-3-enyloxy)benzene

To a suspended solution of 4-benzyloxyphenol (20 g, 0.1 mol) and NaH (6.0 g, 0.15 mol) and catalytic amount of KI in THF (50 ml) was added 4-bromobut-1-ene (20.25 g, 0.15 mol), and the mixture was refluxed for 3 days.³ The reaction mixture was then cooled to room temperature, and quenched with H₂O. The reaction mixture was extracted with ethyl acetate twice. The combined organic layer was washed with brine, dried over anhydrous Na₂SO₄, and removed in *vacuo*. The residue was purified by silica gel chromatography, and then recrystallized from ethanol to give

1-(benzyloxy)-4-(but-3-enyloxy)benzene, as a colorless solid (7.0g, yield: 27%).

Physical data of 1-(benzyloxy)-4-(but-3-en-1-yloxy)benzene



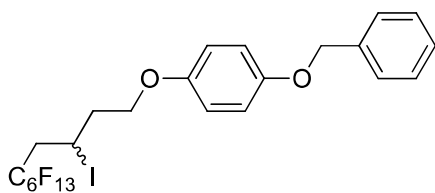
Yield = 27%, colorless needles, mp = 50-52 °C, IR (KBr disc) ν = 3083, 2983, 2945, 2906, 2862, 1508, and 1290 cm^{-1} .

^1H NMR (500 MHz, CDCl_3) δ = 7.43 (d, J = 7.2 Hz, 2H), 7.38 (d, J = 10.3 Hz, 2H), 7.34-7.29 (m, 1H), 6.94-6.87 (m, 2H), 6.86-6.80 (m, 2H), 5.94-5.86 (m, 1H), 5.16 (d, J = 17.2 Hz, 1H), 5.13-5.07 (m, 1H), 5.02 (s, 2H), 3.97 (t, J = 6.7 Hz, 2H), 2.52 (q, J = 6.7 Hz, 2H) ppm.

2.7.2 Synthetic procedure for preparation of 1-(benzyloxy)-4-(3-iodo-4-perfluorohexylbutoxy)benzene

To a mixture of 1-(benzyloxy)-4-(but-3-enyloxy)benzene (7.0 g, 27.5 mmol), sodium hydrogen carbonate (2.3 g, 27.5 mmol), and sodium hydrosulfite (4.8 g, 27.5 mmol) in a mixed solvent of CH_3CN (30 ml) and H_2O (20 ml) was added perfluorohexyl iodide (12.3 g, 27.5 mmol) and the reaction mixture was stirred under shielded light for overnight.⁴ The reaction mixture was diluted with ethyl acetate and washed with H_2O twice, dried over anhydrous MgSO_4 , and the solvent was removed in *vacuo*. The residue was recrystallized from ethanol to give 1-(benzyloxy)-4-(3-iodo-4-perfluorohexylbutoxy)benzene, as a colorless solid (11.2 g, yield: 58%).

Physical data of 1-(benzyloxy)-4-(3-iodo-4-perfluorohexylbutoxy)benzene



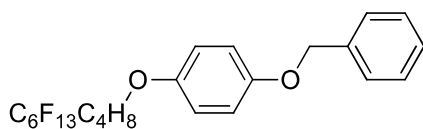
Yield = 58%, colorless needles, mp = 68-72 °C, IR (KBr disc) ν = 1512 and 1242 cm^{-1} .

^1H NMR (500 MHz, CDCl_3) δ = 7.43 (d, J = 7.2 Hz, 2H), 7.38 (t, J = 7.4 Hz, 2H), 7.32 (t, J = 7.2 Hz, 1H), 6.92 (d, J = 9.1 Hz, 2H), 6.85 (d, J = 9.1 Hz, 2H), 5.03 (s, 2H), 4.63-4.58 (m, 1H), 4.14-4.10 (m, 1H), 4.09-4.02 (m, 1H), 3.11-2.79 (m, 2H), 2.33-2.27 (m, 1H), 2.22-2.15 (m, 1H) ppm.

2.7.3 Synthetic procedure for preparation of 1-(benzyloxy)-4-(4-perfluorohexylbutoxy)benzene

LiAlH_4 (1.2 g, 32 mmol) was added dropwisely into a solution of compound 1-(benzyloxy)-4-(3-iodo-4-perfluorohexylbutoxy)-benzene (11.2 g, 16 mmol) in THF (100 ml), and the reaction mixture was stirred overnight. The reaction mixture was quenched with aqueous ammonium chloride and extracted with ethyl acetate twice. The combined organic layer was washed with brine, dried over anhydrous MgSO_4 , and the solvent was removed in *vacuo*. The residue was purified by silica gel chromatography, and then recrystallized from ethanol to give 1-(benzyloxy)-4-(4-perfluorohexylbutoxy)benzene, as a colorless solid (3.6 g, yield: 39%).

Physical data of 1-(benzyloxy)-4-(4-perfluorohexylbutoxy)benzene



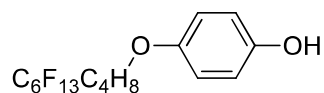
Yield = 39%, colorless needles, mp = 68-77 °C, IR (KBr disc) ν = 1512 and 1242 cm^{-1} .

^1H NMR (500 MHz, CDCl_3) δ = 7.43 (d, J = 7.4 Hz, 2H), 7.38 (d, J = 8.1 Hz, 2H), 7.32 (t, J = 7.2 Hz, 1H), 6.91 (d, J = 9.0 Hz, 2H), 6.82 (d, J = 9.1 Hz, 2H), 5.02 (s, 2H), 3.95 (t, J = 5.7 Hz, 2H), 2.21-2.10 (m, 2H), 1.91-1.74 (m, 4H) ppm.

2.7.4 Synthetic procedure of 4-(4-perfluorohexylbutoxy)phenol

Under hydrogen atmosphere, a mixture of 1-(benzyloxy)-4-(4-perfluorohexylbutoxy)benzene (3.5 g, 6.2 mmol) and Pd-C (0.1g) in a mixed solvent of ethanol (150 ml) and ethyl acetate (150 ml) was vigorously stirred. After the reaction completed, the reaction mixture was filtered and the filtrate was concentrated in *vacuo*. The residue was recrystallized from toluene to give 4-(4-perfluorohexylbutoxy)phenol, as a colorless solid.

Physical data of 4-(4-perfluorohexylbutoxy)phenol



Yield = 66%, colorless needles, mp = 72-74 °C, IR (KBr disc) ν = 3460, 1512 and 1242 cm^{-1} .

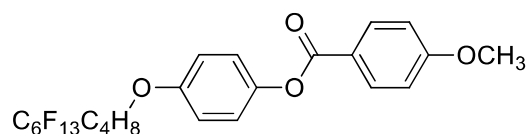
^1H NMR (500 MHz, CDCl_3) δ = 6.92-6.67 (m, 4H), 4.77 (s, 1H), 3.94 (t, J = 5.8 Hz, 2H), 2.26-2.03 (m, 2H), 1.94-1.65 (m, 4H) ppm.

2.7.5 Synthetic procedure for preparation of compounds E1-n

Compounds **E1-n** were prepared by conventional esterification⁵ (DCC method in

THF) with compound 4-(4-perfluorohexylbutoxy)phenol and the corresponding 4-alkoxybenzoic acid for compounds **E1-n**. The products were purified by silica gel chromatography, and then recrystallized from ethanol to give pure product. The spectra data are as follows.

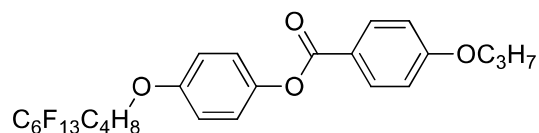
Physical data of E1-1



Yield = 41%, colorless needles, mp = 93-95 °C, IR (KBr disc) ν = 1730, 1512, and 1201 cm^{-1} .

^1H NMR (500 MHz, CDCl_3) δ = 8.15 (d, J = 8.9 Hz, 2H), 7.11 (d, J = 9.0 Hz, 2H), 6.98 (d, J = 8.9 Hz, 2H), 6.92 (d, J = 9.0 Hz, 2H), 4.01 (t, J = 5.8 Hz, 2H), 3.90 (s, 3H), 2.23-2.12 (m, 2H), 1.96-1.76 (m, 4H) ppm.

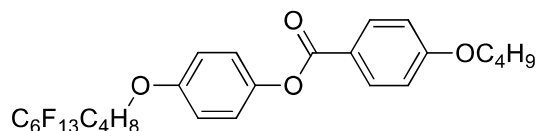
Physical data of E1-3



Yield = 73%, colorless needles, mp = 86-89 °C, IR (KBr disc) ν = 1730, 1512, and 1204 cm^{-1} .

^1H NMR (500 MHz, CDCl_3) δ = 8.13 (d, J = 8.8 Hz, 2H), 7.11 (d, J = 8.9 Hz, 2H), 6.97 (d, J = 8.8 Hz, 2H), 6.92 (d, J = 9.0 Hz, 2H), 4.01 (dd, J = 8.8, 4.5 Hz, 4H), 2.28-2.06 (m, 2H), 1.96-1.77 (m, 6H), 1.06 (t, J = 7.4 Hz, 3H) ppm.

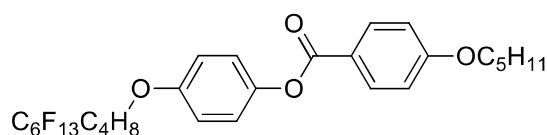
Physical data of E1-4



Yield = 67%, colorless needles, mp = 80-82 °C, IR (KBr disc) ν = 1730, 1512, and 1202 cm^{-1} .

^1H NMR (500 MHz, CDCl_3) δ = 8.13 (d, J = 9.0 Hz, 2H), 7.11 (d, J = 9.0 Hz, 2H), 6.96 (d, J = 8.8 Hz, 2H), 6.92 (d, J = 9.0 Hz, 2H), 4.05 (t, J = 6.5 Hz, 2H), 4.00 (t, J = 5.9 Hz, 2H), 2.23-2.12 (m, 2H), 1.95-1.72 (m, 6H), 1.56-1.46 (m, 2H), 0.99 (t, J = 7.5 Hz, 3H) ppm.

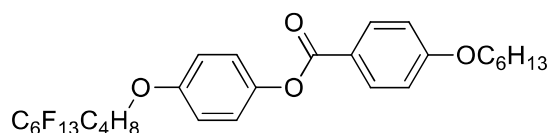
Physical data of E1-5



Yield = 66%, colorless needles, mp = 82-84 °C, IR (KBr disc) ν = 1730, 1512, and 1204 cm^{-1} .

^1H NMR (500 MHz, CDCl_3) δ = 8.13 (d, J = 8.8 Hz, 2H), 7.11 (d, J = 9.0 Hz, 2H), 6.96 (d, J = 8.8 Hz, 2H), 6.92 (d, J = 8.9 Hz, 2H), 4.04 (t, J = 6.6 Hz, 2H), 4.00 (t, J = 5.8 Hz, 2H), 2.22-2.12 (m, 2H), 1.99-1.78 (m, 6H), 1.51-1.35 (m, 4H), 0.94 (t, J = 7.1 Hz, 3H) ppm.

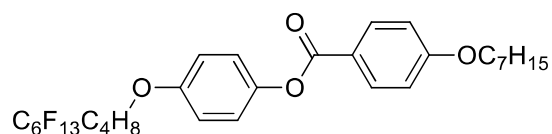
Physical data of E1-6



Yield = 59%, colorless needles, mp = 75-77 °C, IR (KBr disc) ν = 1724, 1521, and 1202 cm^{-1} .

^1H NMR (500 MHz, CDCl_3) δ = 8.13 (d, J = 8.8 Hz, 2H), 7.11 (d, J = 9.1 Hz, 2H), 6.96 (d, J = 8.8 Hz, 2H), 6.92 (d, J = 9.0 Hz, 2H), 4.04 (t, J = 6.6 Hz, 2H), 4.00 (t, J = 5.8 Hz, 2H), 2.23-2.12 (m, 2H), 2.01-1.75 (m, 6H), 1.57-1.44 (m, 2H), 1.37-1.34 (m, 4H), 0.92 (t, J = 7.0 Hz, 3H).

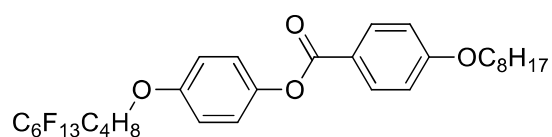
Physical data of E1-7



Yield = 72%, colorless needles, mp = 71-73 °C, IR (KBr disc) ν = 1730, 1512, and 1201 cm^{-1} .

^1H NMR (500 MHz, CDCl_3) δ = 8.13 (d, J = 9.0 Hz, 2H), 7.11 (d, J = 8.9 Hz, 2H), 6.96 (d, J = 8.7 Hz, 2H), 6.92 (d, J = 9.0 Hz, 2H), 4.04 (t, J = 6.6 Hz, 2H), 4.00 (t, J = 5.8 Hz, 2H), 2.23-2.14 (m, 2H), 1.90-1.79 (m, 6H), 1.50-1.44 (m, 2H), 1.43-1.27 (m, 6H), 0.90 (t, J = 6.7 Hz, 3H) ppm.

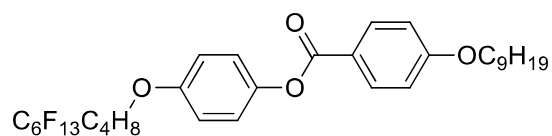
Physical data of E1-8



Yield = 69%, colorless needles, mp = 66-68 °C, IR (KBr disc) ν = 1730, 1512, and 1201 cm^{-1} .

^1H NMR (500 MHz, CDCl_3) δ = 8.13 (d, J = 8.7 Hz, 2H), 7.11 (d, J = 9.1 Hz, 2H), 6.96 (d, J = 9.0 Hz, 2H), 6.92 (d, J = 8.9 Hz, 2H), 4.04 (t, J = 6.6 Hz, 2H), 4.00 (t, J = 5.9 Hz, 2H), 2.22-2.12 (m, 2H), 1.96-1.74 (m, 6H), 1.52-1.42 (m, 2H), 1.41-1.19 (m, 8H), 0.89 (t, J = 6.9 Hz, 3H) ppm.

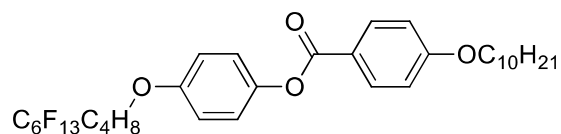
Physical data of E1-9



Yield = 65%, colorless needles, mp = 71-74 °C, IR (KBr disc) $\nu=1730$, 1512, and 1201 cm^{-1} .

^1H NMR (500 MHz, CDCl_3) δ = 8.13 (d, J = 8.7 Hz, 2H), 7.11 (d, J = 9.0 Hz, 2H), 6.96 (d, J = 9.0 Hz, 2H), 6.92 (d, J = 9.0 Hz, 2H), 4.04 (t, J = 6.6 Hz, 2H), 4.00 (t, J = 5.9 Hz, 2H), 2.18 (dt, J = 18.3, 9.5 Hz, 2H), 2.00-1.76 (m, 6H), 1.53-1.43 (m, 2H), 1.43-1.22 (m, 10H), 0.89 (t, J = 6.9 Hz, 3H) ppm.

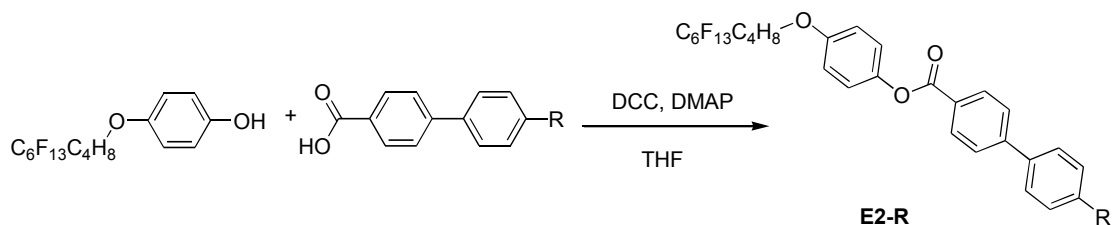
Physical data of E1-10



Yield = 64%, colorless needles, mp = 73-75 °C, IR (KBr disc) ν = 1730, 1512, and 1201 cm^{-1} .

^1H NMR (500 MHz, CDCl_3) δ = 8.13 (d, J = 8.8 Hz, 2H), 7.11 (d, J = 9.0 Hz, 2H), 6.96 (d, J = 9.0 Hz, 2H), 6.92 (d, J = 9.1 Hz, 2H), 4.04 (t, J = 6.5 Hz, 2H), 4.00 (t, J = 5.8 Hz, 2H), 2.23-2.12 (m, 2H), 1.97-1.71 (m, 6H), 1.50-1.44 (m, 2H), 1.42-1.14 (m, 12H), 0.89 (t, J = 6.9 Hz, 3H) ppm.

2.8 Synthesis of compounds 4-[4-(perfluorohexyl)butoxy]phenyl 4-phenylbenzoate derivatives

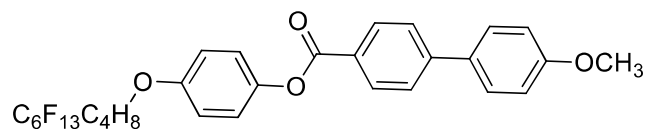


Scheme 2-7. Synthetic route of 4-[4-(perfluorohexyl)butoxy]phenyl 4-phenylbenzoate derivatives (**E2-R**)

2.8.1 Synthetic procedure for preparation of **E2-R**

Compounds **E2-R** were prepared by conventional esterification (DCC method in THF) with compound 4-(4-(perfluorohexyl)butoxy)phenol and the corresponding 4-alkoxybibenzoic acid for compounds **E2-R**. The products were purified by silica gel chromatography, and then recrystallized from ethanol to give pure product, as a colorless crystalline solid. The spectra data are as follows.

Physical data of **E2-OCH₃**

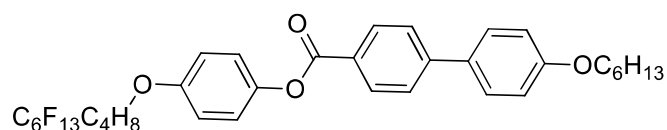


Yield = 48%, colorless needles, mp = 95-97 °C, IR (KBr disc) ν = 1146, 1198, and 1734 cm^{-1} .

^1H NMR (500 MHz, CDCl_3) δ = 8.23 (d, J = 8.3 Hz, 2H), 7.69 (d, J = 8.3 Hz, 2H), 7.61 (d, J = 8.7 Hz, 2H), 7.15 (d, J = 8.9 Hz, 2H), 7.02 (d, J = 8.7 Hz, 2H), 6.94 (d, J = 8.9 Hz, 2H), 4.01 (t, J = 5.8 Hz, 2H), 3.87 (s, 3H), 2.23-2.13 (m, 2H), 1.98-1.76 (m,

4H) ppm.

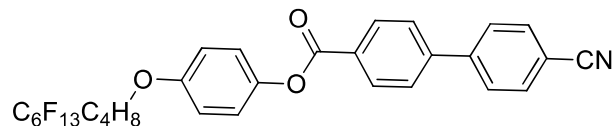
Physical data of E2-OC₆H₁₃



Yield = 25%, colorless needles, mp = 97-99°C, IR (KBr disc) ν = 1144, 1194, and 1736 cm^{-1} .

¹H NMR (500 MHz, CDCl₃) δ = 8.23 (d, J = 8.3 Hz, 2H), 7.69 (d, J = 8.4 Hz, 2H), 7.60 (d, J = 8.6 Hz, 2H), 7.15 (d, J = 9.0 Hz, 2H), 7.01 (d, J = 8.8 Hz, 2H), 6.94 (d, J = 9.0 Hz, 2H), 4.03-4.00 (m, 4H), 2.23-2.13 (m, 2H), 1.98-1.73 (m, 6H), 1.54-1.44 (m, 2H), 1.43-1.26 (m, 4H), 0.92 (t, J = 7.0 Hz, 3H) ppm.

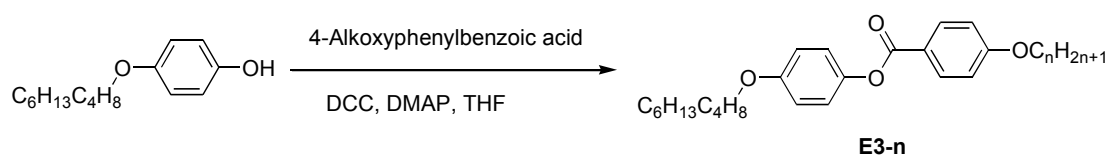
Physical data of E2-CN:



Yield = 46%, colorless needles, mp = 130-133 °C, IR (KBr disc) ν = 1142, 1192, and 1732 cm^{-1} .

¹H NMR (500 MHz, CDCl₃) δ = 8.30 (d, J = 8.3 Hz, 2H), 7.80-7.72 (m, 6H), 7.15 (d, J = 8.9 Hz, 2H), 6.95 (d, J = 8.9 Hz, 2H), 4.02 (t, J = 5.8 Hz, 2H), 2.23-2.13 (m, 2H), 1.92-1.88 (m, 2H), 1.87-1.79 (m, 2H) ppm.

2.9 Synthesis of 4-alkoxyphenyl 4-alkoxybenzoates



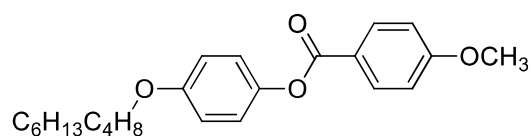
Scheme 2-8. Synthetic route of 4-alkoxyphenyl 4-(4-decyloxy)benzoates (**E3-n**)

2.9.1 Synthetic procedure for preparation of **E3-n**

Compounds **E3-n** were prepared by conventional esterification (DCC method in THF) with compound 4-decyloxyphenol and the corresponding 4-alkoxybenzoic acid for compounds **E3-n**. The products were purified by silica gel chromatography, and then recrystallized from ethanol to give pure product, as a colorless crystalline solid.

The spectra data are as follows.

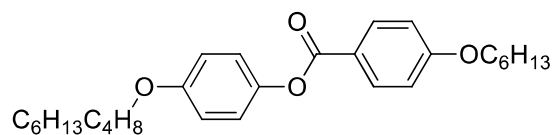
Physical data of **E3-OCH₃**



Yield = 72%, colorless needles, mp = 70-73 °C, IR (KBr disc) ν = 1730, 1512, and 1201 cm^{-1} .

^1H NMR (500 MHz, CDCl_3) δ = 8.15 (d, J = 9.0 Hz, 2H), 7.10 (d, J = 9.0 Hz, 2H), 6.98 (d, J = 8.7 Hz, 2H), 6.92 (d, J = 8.9 Hz, 2H), 3.95 (t, J = 6.6 Hz, 2H), 3.89 (s, 3H), 1.83-1.70 (m, 2H), 1.51-1.40 (m, 2H), 1.40-1.20 (m, 12H), 0.88 (t, J = 6.8 Hz, 3H) ppm.

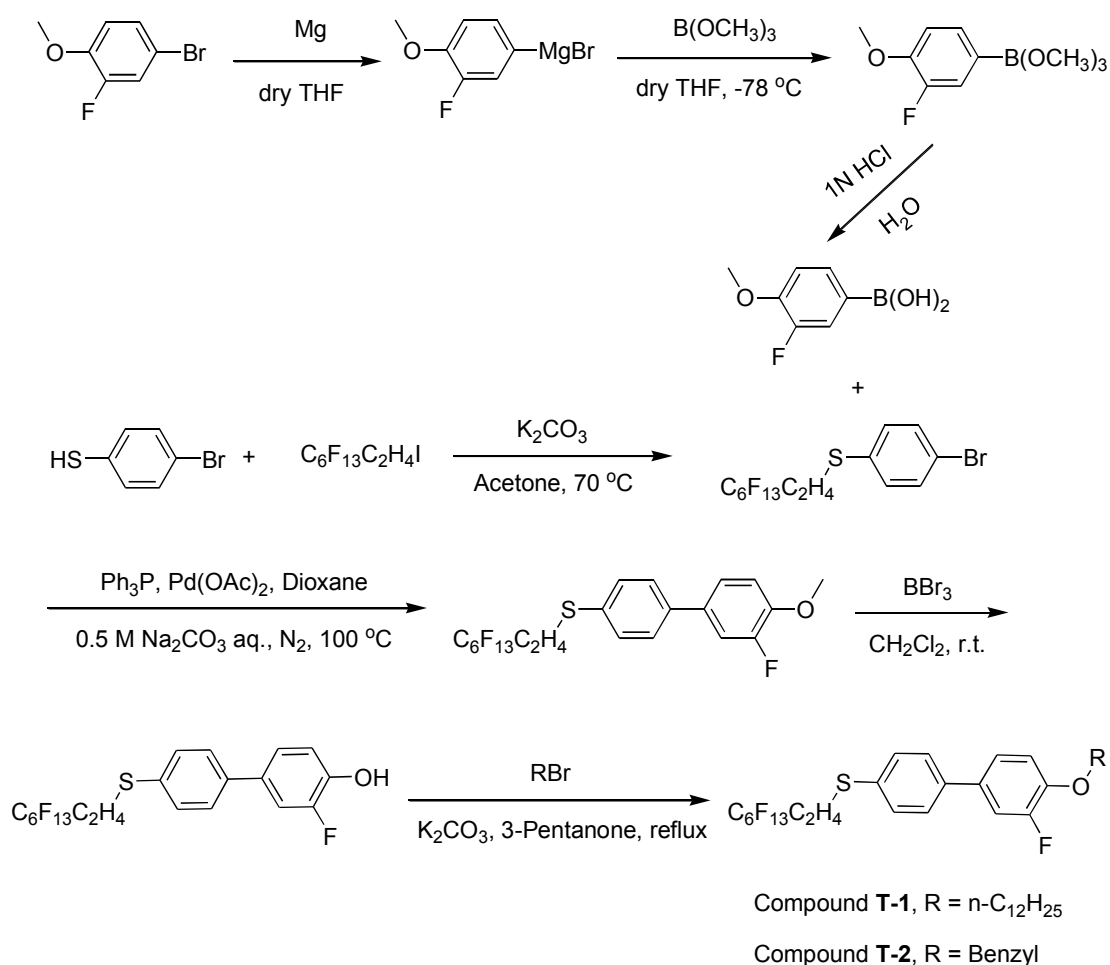
Physical data of **E3-OC₆H₁₃**



Yield = 54%, colorless needles, mp = 60-62 °C, IR (KBr disc) ν = 1730, 1512, and 1201 cm^{-1} .

^1H NMR (500 MHz, CDCl_3) δ = 8.13 (d, J = 8.9 Hz, 2H), 7.09 (d, J = 9.1 Hz, 2H), 6.96 (d, J = 8.9 Hz, 2H), 6.92 (d, J = 9.1 Hz, 2H), 4.03 (t, J = 6.6 Hz, 2H), 3.95 (t, J = 6.5 Hz, 2H), 1.87-1.72 (m, 4H), 1.52-1.41 (m, 4H), 1.41-1.20 (m, 16H), 0.91-0.87 (m, 6H) ppm.

2.10 Synthesis of 4-[2-(perfluorohexyl)ethylthio]-3'-fluoro-4'-alkoxy-1,1'-biphenyl

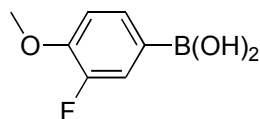


Scheme 2-9. Synthetic route of 4-[2-(perfluorohexyl)ethylthio]-4'-alkoxy-1,1'-biphenyl

2.10.1 Synthetic procedure for preparation of 2-fluoro-4-methoxyphenylboronic acid

Luminous magnesium powder (0.43 g, 17.5 mmol) and THF (anhydrous, 10 mL) were added into flask with two necks under nitrogen protection. 4-Bromo-2-fluoro-1-methoxybenzene (2.10 g, 10.2 mmol) was dissolved into THF (anhydrous, 10 mL) and then dropped into flask. The reaction mixture was stirred for 2 hours, and then cooled into -78 °C before trimethyl borate (1.11 g, 10.7 mmol) in THF (10 mL) was added. The reaction mixture was stirred at -78 °C for 2.5 hours. The reaction quenched with HCl (1 N, 50 mL). The mixture was filtered and the filtrate was evaporated in *vacuo*. The residue was recrystallized from CHCl₃ to give pure product, as a colorless crystalline solid. The spectra data are as follows.

Physical data of 2-fluoro-4-methoxyphenylboronic acid



Yield = 88%, colorless needles, mp = 208-211 °C, IR (KBr disc) ν = 1134, 2936, and 3431 cm⁻¹.

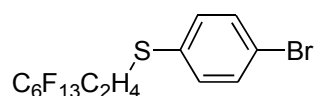
¹H NMR (500 MHz, CDCl₃) δ = 7.64 (d, J = 6.6 Hz, 1H), 7.57 (d, J = 7.8 Hz, 1H), 7.18 (t, J = 6.70 Hz, 1H), 3.90 (s, 3H) ppm.

2.10.2 Synthetic procedure for preparation of 4-[2-(perfluorohexyl)ethylthio]bromobenzene

4-Bromothiophenol (3.63 g, 19.2 mmol) was dissolved in acetone (50 mL), potassium carbonate (3.17 g, 23 mmol) was added, and then perfluorohexylethyl

iodide (10.0 g, 21.1 mmol) was dropped into the reaction mixture. The reaction mixture was stirred at 70 °C for one day and separated by filtration. Filtrate was concentrated in *vacuo*, the residue was purified by silica gel column chromatography, and then recrystallized from CH₃OH to give pure product, as a colorless crystalline solid.

Physical data of 4-[2-(perfluorohexyl)ethylthio]bromobenzene



Yield = 91%, colorless needles, mp = 38-40 °C, IR (KBr disc) ν = 1140, 1217, and 2936 cm⁻¹.

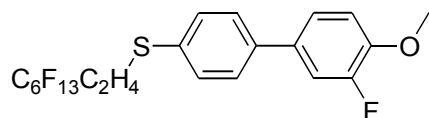
¹H NMR (500 MHz, CDCl₃) δ = 7.46 (d, *J* = 8.5 Hz, 2H), 7.23 (d, *J* = 8.5 Hz, 2H), 3.12-3.10 (m, 2H), 2.43-2.33 (m, 2H) ppm.

2.10.3 Synthetic procedure for preparation of 4-[2-(perfluorohexyl)ethylthio]-3'-fluoro-4'-methoxyl-1,1'-biphenyl

4-[2-(Perfluorohexyl)ethylthio]-bromobenzene (1.31 g, 2.45 mmol) and 2-fluoro-4-methoxyphenylboronic acid (0.50 g, 2.49 mmol) were dissolved in 1,4-dioxane (50 mL), sodium carbonate (0.5 N, 25 mL), triphenylphosphine (0/06 g, 0.23 mmol) and palladium(II) acetate (0.01 g, 0.045 mmol) were added into the reaction mixture. The reaction mixture was stirred at 70 °C for two days under nitrogen protection. The reaction quenched with water (50 mL) and HCl (1 N, 50 mL). The mixture was filtered and the filter mass was purified by silica gel column chromatography to give pure product, as a colorless crystalline solid. The spectra data

are as follows.

Physical data of 4-[2-(perfluorohexyl)ethylthio]-3'-fluoro-4'-methoxy-1,1'-biphenyl



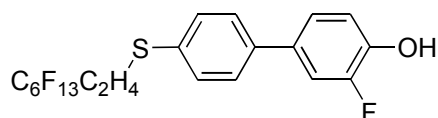
Yield = 83%, colorless needles, mp = 104-106 °C, IR (KBr disc) ν = 1141, 1207, and 2936 cm^{-1} .

^1H NMR (500 MHz, CDCl_3) δ = 7.52 (d, J = 8.5 Hz, 2H), 7.42 (d, J = 8.5 Hz, 2H), 7.28 (d, J = 6.6 Hz, 1H), 7.18 (d, J = 7.8 Hz, 1H), 6.98 (t, J = 6.7 Hz, 1H), 3.86 (s, 3H), 3.30-3.23 (m, 2H), 2.42 (m, 2H) ppm.

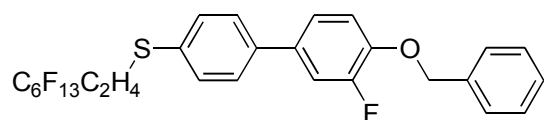
2.10.4 Synthetic procedure for preparation of 4-[2-(perfluorohexyl)ethylthio]-3'-fluoro-4'-hydroxy-1,1'-biphenyl

4-[2-(perfluorohexyl)ethylthio]-3'-fluoro-4'-methoxy-1,1'-biphenyl (1.15 g, 1.98 mmol) was dissolved in CH_2Cl_2 (50 mL) in an ice bath to cool, and boron tribromide (10.0 g, 39.9 mmol) was added. The reaction mixture was stirred at 0 °C for 30 min, and at room temperature for 30 hours. The crude product was extracted with ethyl acetate. The extractant was evaporated in *vacuo*, and the residue was purified by silica gel column chromatography to give pure product.

Physical data of 4-[2-(perfluorohexyl)ethylthio]-3'-fluoro-4'-hydroxy-1,1'-biphenyl



Yield = 98%, colorless needles, mp = 138-140 °C, IR (KBr disc) ν = 1074, 1123,



Yield = 59%, colorless needles, mp = 108-110 °C, IR (KBr disc) ν = 1065, 1141, 1207 and 2936 cm^{-1} .

^1H NMR (500 MHz, CDCl_3) δ = 7.47 (d, J = 8.5 Hz, 2H), 7.42-7.39 (m, 5H), 7.32 (d, J = 7.9 Hz, 2H), 7.21 (d, J = 7.9 Hz, 2H), 7.15 (d, J = 7.8 Hz, 1H), 7.01 (t, J = 6.7 Hz, 1H), 5.10 (s, 2H), 3.10-3.06 (m, 2H), 2.40-2.31 (m, 2H) ppm.

2.11 References

1. Iuchi, A.; Morita, Y.; Hirakawa, T.; Kasatani, K.; Okamoto, H. *ECS Transactions* **2009**, *16* (24), 65.
2. Hartmann, P. C.; Collet, A.; Viguier, M.; Blanc, C. *Journal of Fluorine Chemistry* **2004**, *125* (12), 1909.
3. Shindo, T.; Fukuyama, Y.; Sugai, T. *Synthesis* **2004**, *2004* (05), 692.
4. Wu, K.; Chen, Q. *Chinese Journal of Chemistry*, **2004**, *22*, 371.
5. Neises, B.; Steglich, W. *Angewandte Chemie* **1978**, *17*(7), 522.

Chapter 3 Liquid crystals based on 4-alkoxy-4'-[4-(perfluorohexyl)butoxy]-1,1'-biphenyl derivatives

3.1 Introduction

Liquid crystalline physical gel which contains two components was reported by Kato et al. in 1999.¹ Literatures containing the word of liquid crystalline physical gels are up to 259 on scholar google until Sep. 2016. Different types of mesophases can be found in liquid crystalline physical gels. Because the properties of liquid crystals and gels come from different components, the properties can be easily changed by adjusting components of liquid crystals and/or organogelators.

In liquid crystals, very few special molecules can self-assemble into three dimensions in particular cases. For example, Twieg and co-workers reported that semifluorinated *n*-alkanes gelatinize hydrocarbon liquids in 1985.² The liquid crystalline properties of semifluorinated *n*-alkanes were explored in 2001 and 2006.

In 2003, Mori and co-workers explored the 5-substituted-2-(3,4,5-trialkoxy-benzoyl-amino)tropones derivatives to investigate the intermolecular interactions at self-assemble process (**Figure 3-1**).³ They found that an intramolecular hydrogen bond between the amide proton and the tropone carbonyl group played a key role in liquid crystalline property and gelation ability.

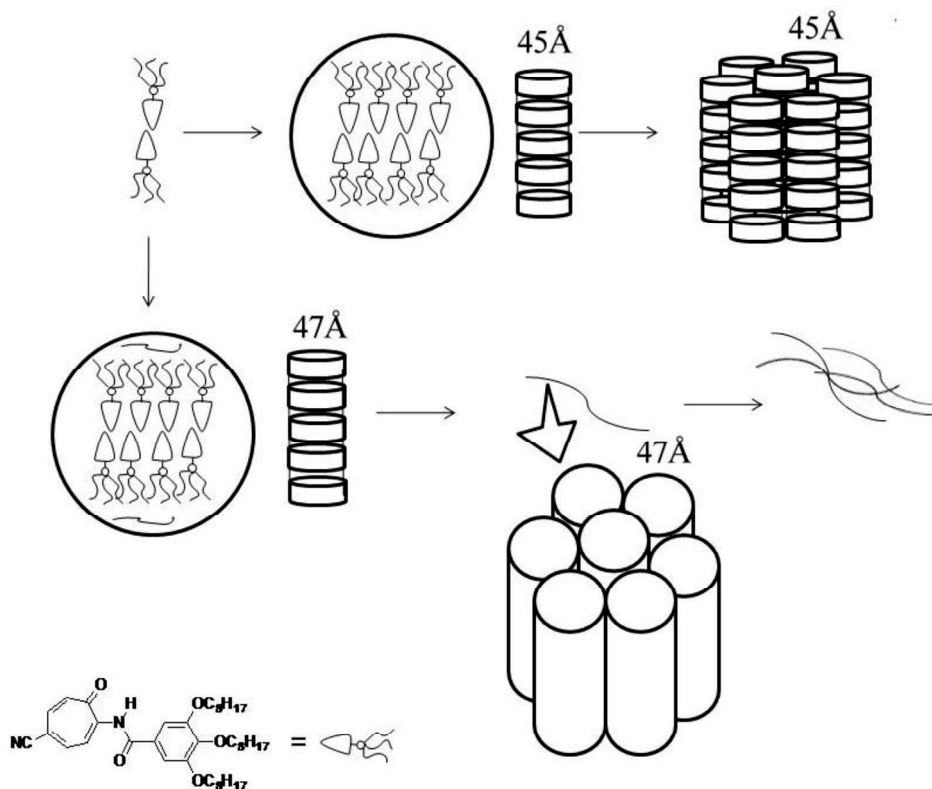


Figure 3-1. Illustration of intermolecular interactions in liquid crystals and supramolecular gels

Fluorinations have been introduced into varieties of structures as means of enhancing functions of materials. The effect of fluorination applied to aromatic rings or aliphatic is different. Compounds with 4-(perfluorohexyl)butoxyl groups have been used as structural units in the construction of self-assembly system. 4-(Perfluorohexyl)butoxyl derivatives perform a significant effect on liquid crystalline properties such as thermal stability and viscosity.⁴

In the past years, our group has reported a lot of liquid crystals with 4-(perfluorohexyl)butoxyl group to explore liquid crystalline properties.⁵ Herein we synthesized 4-semifluoroalkoxybiphenyl derivatives to explore their liquid crystalline properties. Synthetic routes and physical datum of 4-semifluoroalkoxybiphenyl derivatives were shown in Chapter 2. 4-Semifluoroalkoxybiphenyl derivatives are

named **D1-n**, **D3-n** and **D4-4** (Figure 3-2). Compounds **D2-n** and **D5-5** were also synthesized to investigate the change of liquid crystalline properties as liquid crystalline core changes.

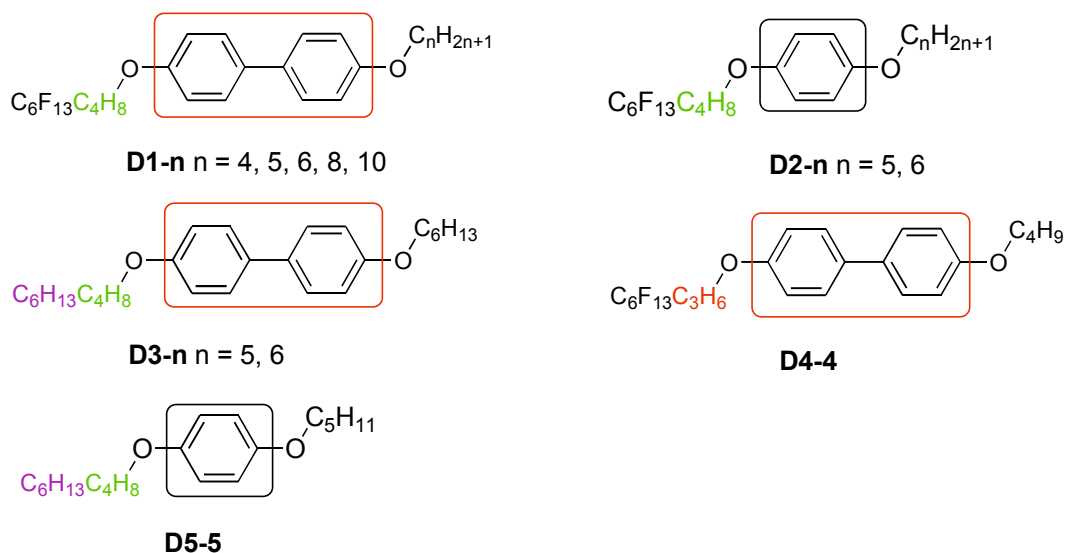


Figure 3-2. Chemical structures of compounds **D1-n**, **D2-n**, **D3-n**, **D4-4** and **D5-5**

3.2 Liquid crystalline properties

Liquid crystalline properties of 4-semifluoroalkoxybiphenyl derivatives were achieved by polarized optical microscopy (POM) and differential scanning calorimetry (DSC). Characteristic textures and defect structures, which change when passing a mesophase transition, reveal the mesophase type observed by POM. Compounds **D2-5** and **D2-6** are in liquid state at room temperature and compounds **D3-5** and **D5-5** do not show any mesophase in cooling process by POM. The textures of mesophases for compounds **D1-n**, **D3-6** and **D4-4** are shown as followed from **Figure 3-3** to **Figure 3-9** respectively.

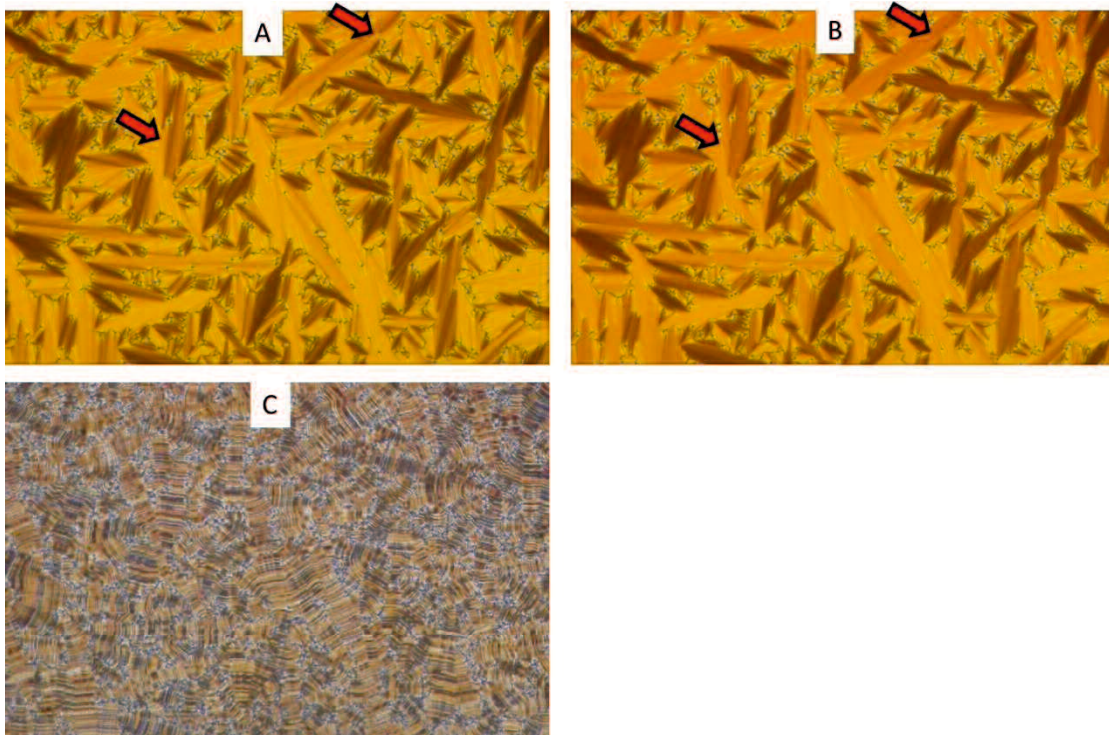


Figure 3-3. Polarized photomicrographs of compound **D1-4** in cooling process at: A 160 °C, B 114 °C and C 110 °C

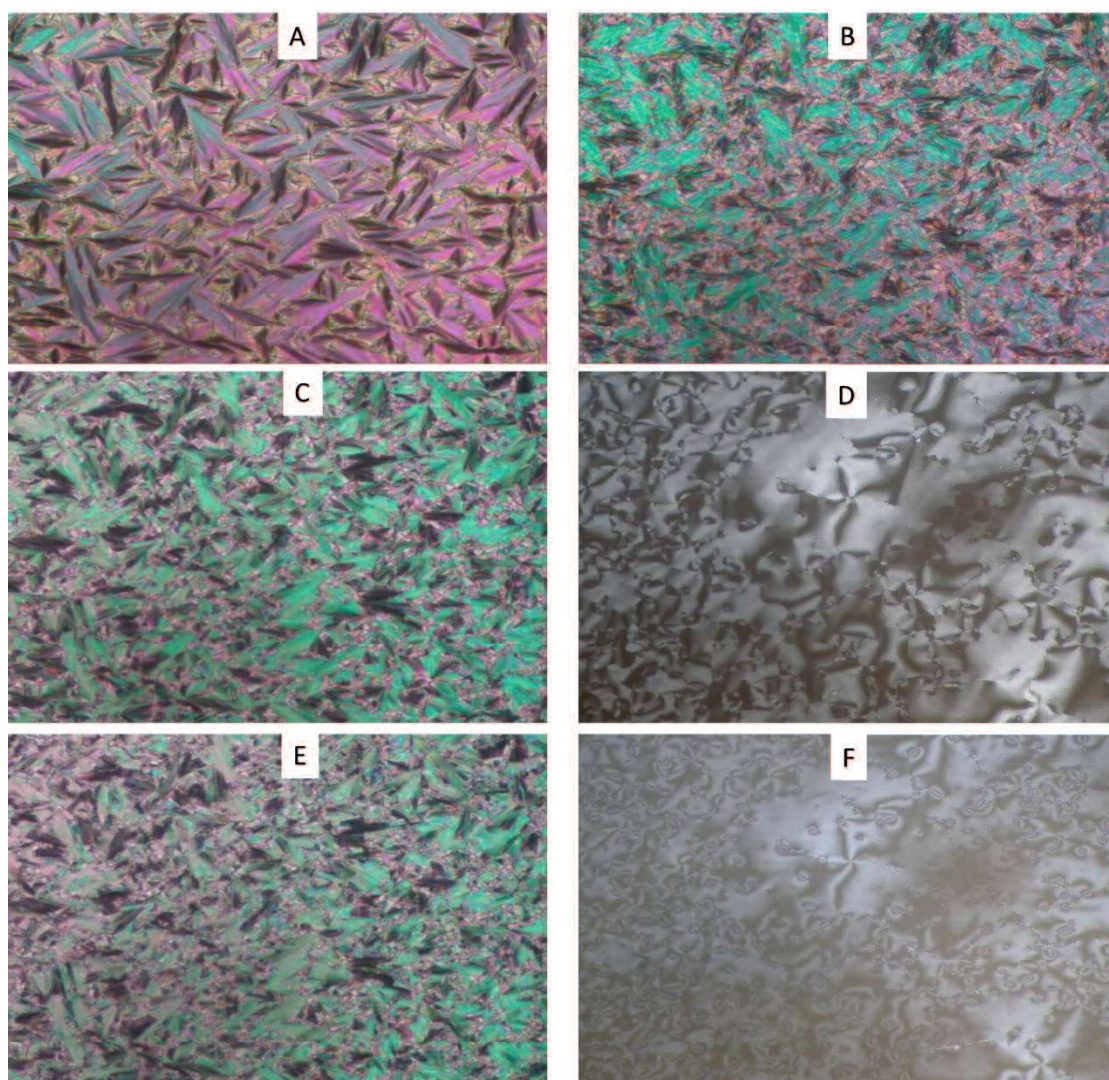


Figure 3-4. Polarized photomicrographs of compound **D1-5** in cooling process at: A 120 °C, B 110 °C, C & D 100 °C and E & F 90 °C

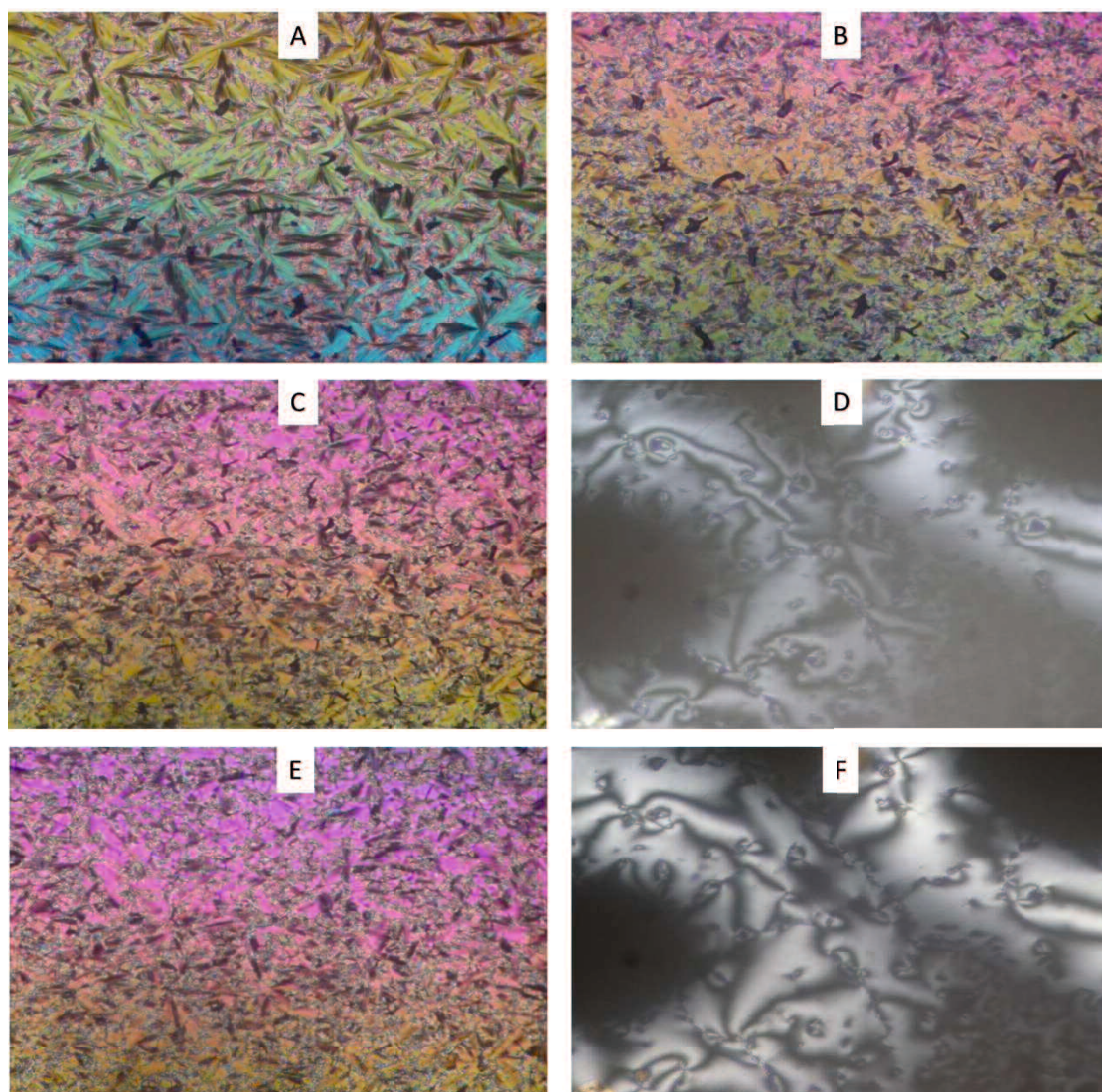


Figure 3-5. Polarized photomicrographs of compound **D1-6** in cooling process at: A 120 °C, B 110 °C, C & D 100 °C and E & F 85 °C

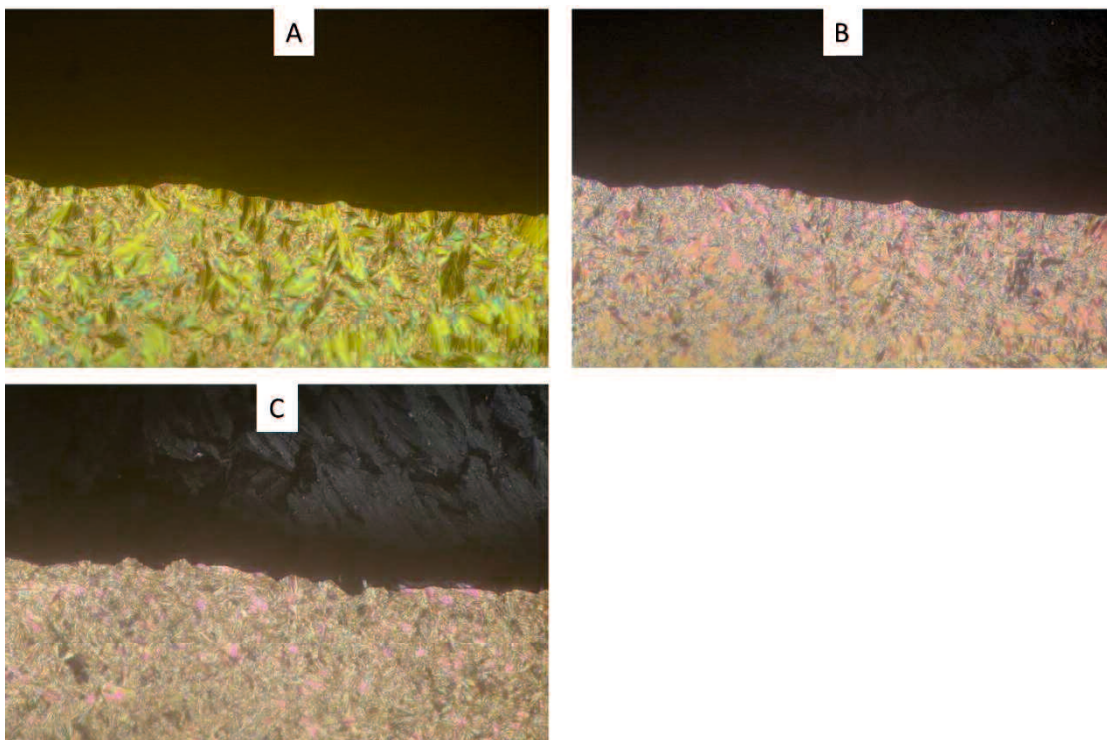


Figure 3-6. Polarized photomicrographs of compound **D1-8** in cooling process at: A 125 °C, B 110 °C and C 95 °C

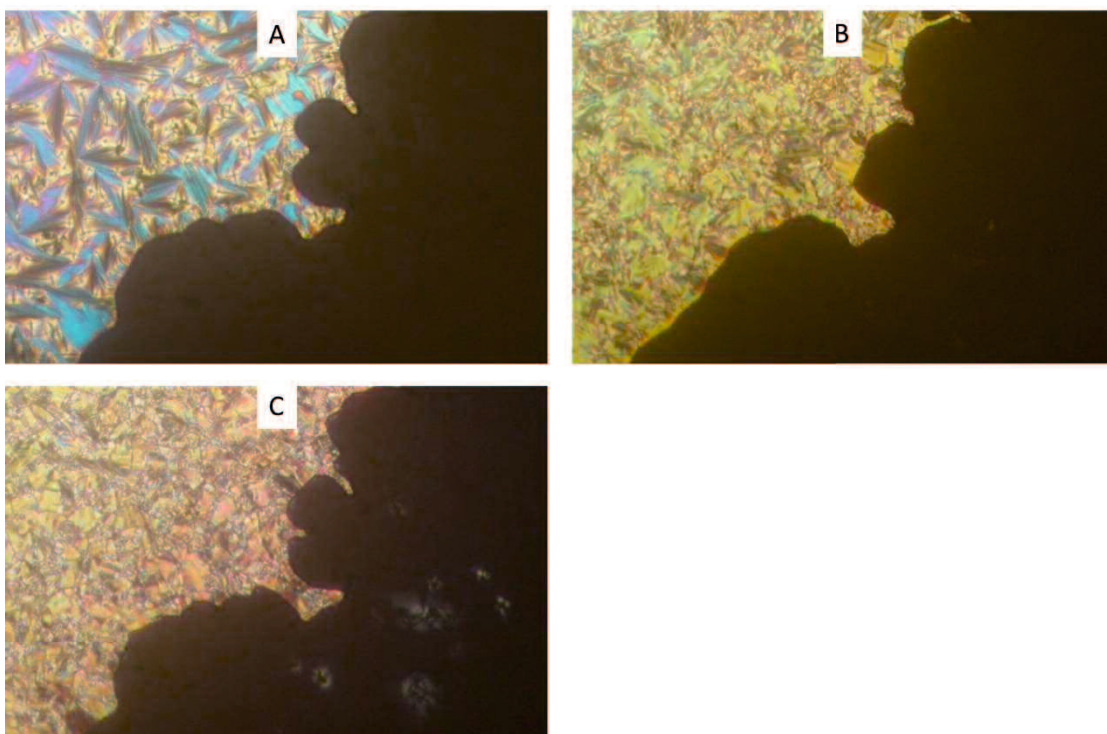


Figure 3-7. Polarized photomicrographs of compound **D1-10** in cooling process at: A 130 °C, B 110 °C and C 102 °C



Figure 3-8. Polarized photomicrographs of compound **D3-6** in cooling process at: A 108 °C and B 107 °C

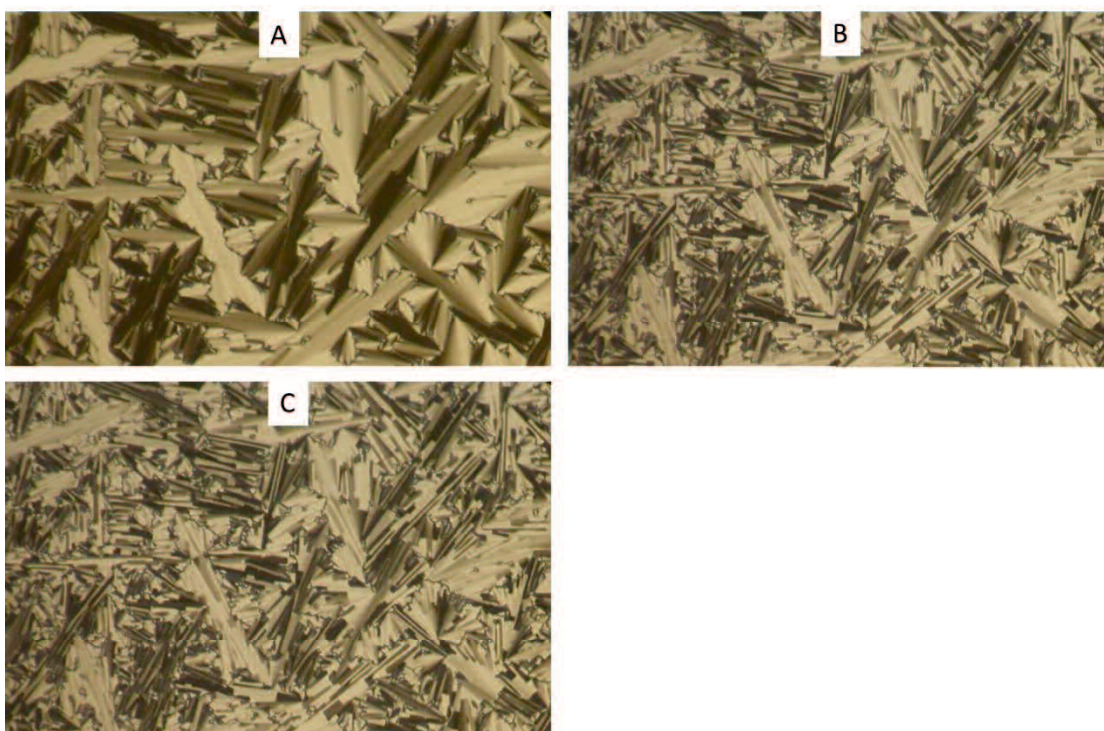


Figure 3-9. Polarized photomicrographs of compound **D4-4** in cooling process at: A 155 °C, B 115 °C and C 108 °C

In cooling process of compound **D1-4**, a fan texture was observed at 171 °C under homogeneous alignments (**Figure 3-3-A**), and then the texture changed to another texture at 117 °C (**Figure 3-3-B**), at last changed to a broken-fan

texture at 98 °C (**Figure 3-3-C**). Polarized photomicrographs of compound **D1-4** at 160 °C and 114 °C were taken. The textures of mesophases for compound **D1-4** at 160 °C and 114 °C are too hard to tell their differences. The slight differences of the textures between **Figure 3-3-A** and **Figure 3-3-B** were marked by red arrows. Fan textures of **Figure 3-3-A** have slopes while fan textures of **Figure 3-3-B** are planes. The latent heat change is 0.7 kJ/mol at 118 °C also proved that smectic mesophases have changed at 118 °C (**Figure 3-10**).

In cooling process of compound **D1-5**, a typical focal conic fan texture was observed at 163 °C under homogeneous alignments (**Figure 3-4-A**), and then the texture changed to a broken-fan texture at 112 °C (**Figure 3-4-B**). Both mesophases have an orthogonal characteristic. These results suggest that compound **D1-5** shows two kinds of smectic A mesophases (SmA) which were named SmA(2) and SmA(1), respectively. The latent heat change of SmA(1)-SmA(2) also supports the assignment of the SmA.⁹ At 100 °C, a schlieren texture was observed under homeotropic alignment (**Figure 3-4-D**), which suggests the mesophase is assigned to be smectic C mesophase (SmC). The latent heat change is agreed to the assignment of SmC-SmA.¹⁰ However, the lower tilted mesophase was unidentified. The similar results of compound **D1-6** were showed in **Figure 3-5** and **Table 3-1**.

The mesophase transition temperatures and thermodynamic datum of compounds **D1-5** and **D1-6** are collected in **Table 3-1**, **Figure 3-11** and **Figure 3-12**.

Table 3-1. The transition temperature (°C) and the associated latent heats [kJ mol⁻¹] of compounds **D1-5**, **D1-6** and **D3-6** during the first scanning process^[a]

Compound	Heating/Cooling	Transition temperature (°C) and ΔH [kJ mol ⁻¹]
	process	
D1-5	Heating	Cryst 87[11.7] SmX 97[2.3] SmC 108[2.3] SmA(1) 112[-] ^[b] SmA(2) 163[11.2] Iso
	Cooling	Cryst 79[4.1] SmX 94[2.4] SmC 105[2.3] SmA(1) 110[-] ^[b] SmA(2) 160[11.3] Iso
D1-6	Heating	Cryst 93[13.0] Sm C 108[2.7] SmA(1) 118[0.5] SmA(2) 159[10.4] Iso
	Cooling	Cryst 79[10.1] SmX 86[1.7] SmC 106[2.8] SmA(1) 115[0.5] SmA(2) 156[10.7] Iso
D3-6	Heating	Cryst 111[25.3] Iso
	Cooling	Cryst 106[22.6] SmA 108[7.2] Iso

^[a] Peak temperatures from DSC at a rate of 5 °C min⁻¹; ^[b] The latent heat change was contained in Sm A(1)→Sm A(2); Cryst, SmX, SmC, SmA and Iso

indicated crystalline solid, unidentified smectic mesophase, smectic C mesophase, smectic A mesophase and isotropic liquid.

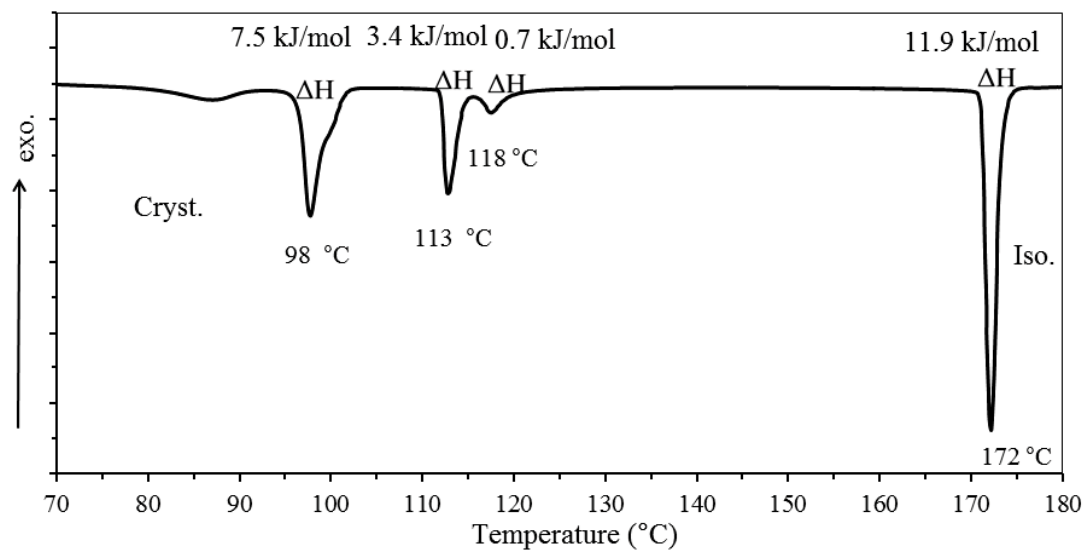


Figure 3-10. Differential scanning calorimetry during the first heating process for compound **D1-4**

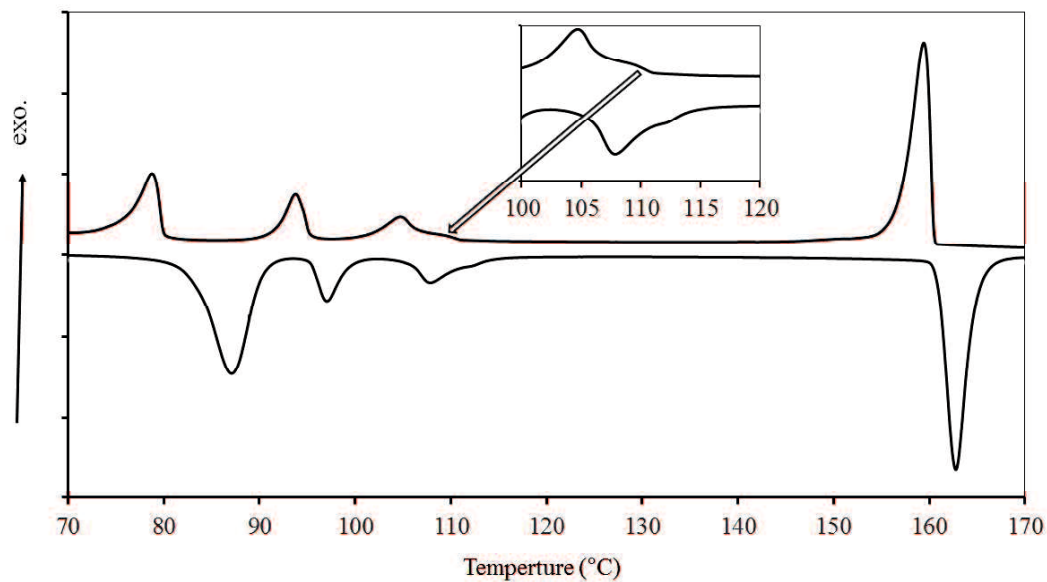


Figure 3-11. Differential scanning calorimetry during the first process for compound **D1-5**

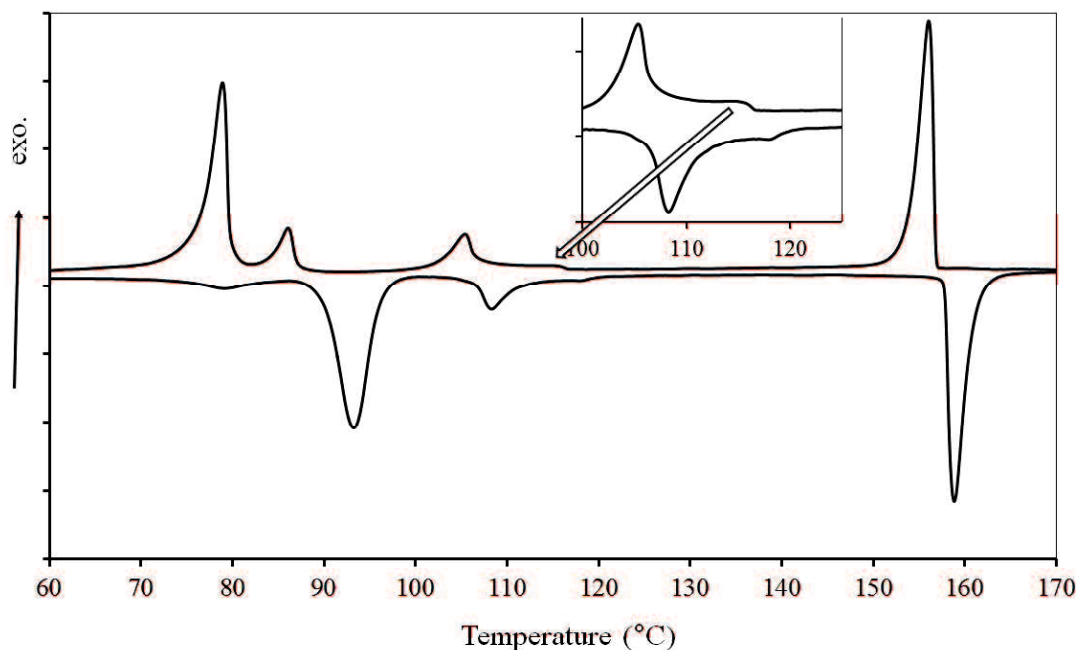


Figure 3-12. Differential scanning calorimetry during the first process for compound **D1-6**

The textures of mesophases for compounds **D1-8** and **D1-10** are different from compounds **D1-5** and **D1-6**. The schlieren textures of compounds **D1-8** and **D1-10** are also observed under homeotropic alignment (**Figure 3-6-C** and **Figure 3-7-C**). The thermodynamic datum of compounds **D1-8** and **D1-10** are shown in **Figure 3-13** and **Figure 3-14**.

Compound **D3-6** only shows SmA with a narrow range of temperature from 106 °C to 108 °C. The mesophase transition temperatures and thermodynamic datum of compound **D3-6** are shown in **Figure 3-8**, **Table 3-1** and **Figure 3-15**.

Compound **D4-4** shows three texture types of mesophases (**Figure 3-9**). The thermodynamic data of compound **D4-4** are shown in **Figure 3-16**.

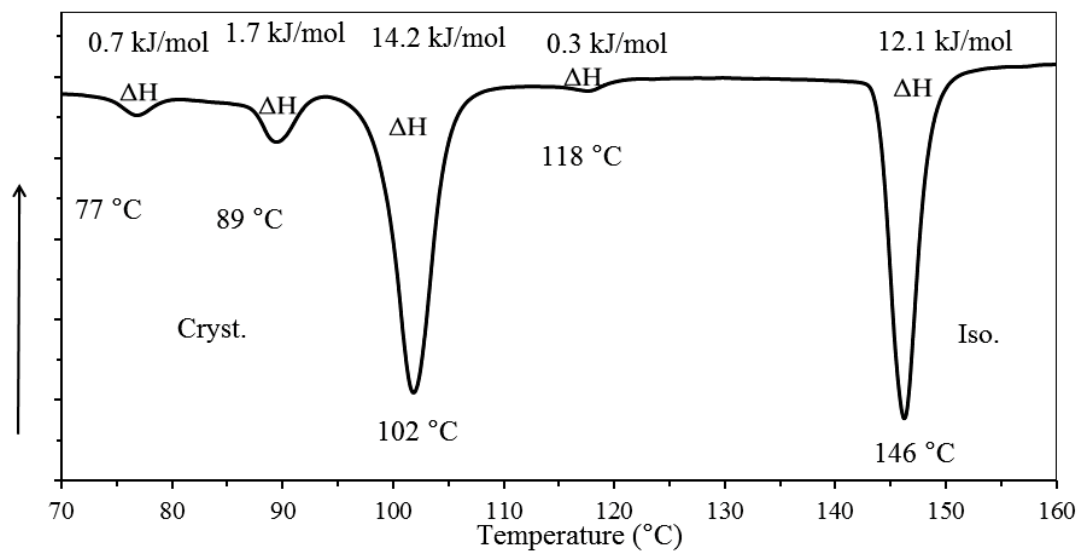


Figure 3-13. Differential scanning calorimetry during the first heating process for compound **D1-8**

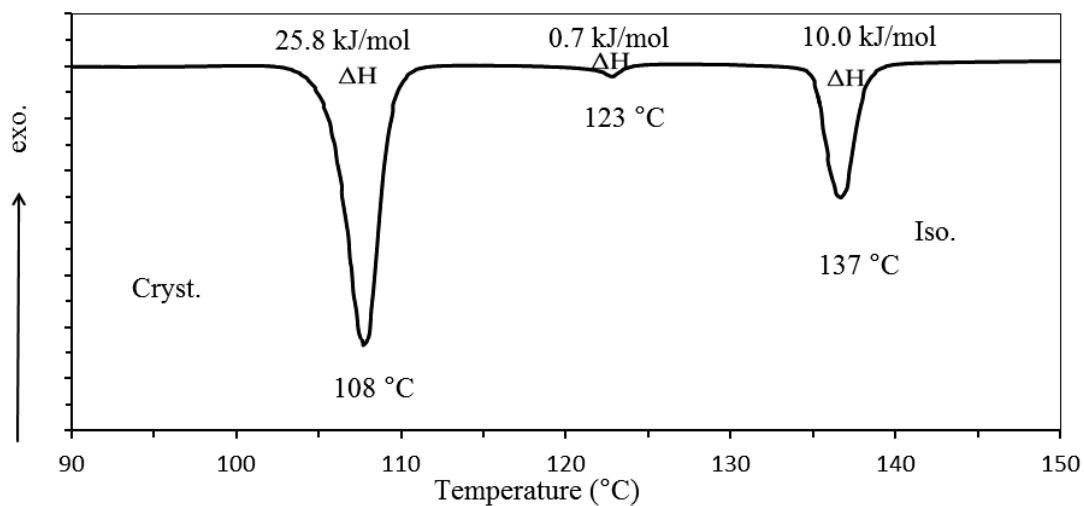


Figure 3-14. Differential scanning calorimetry during the first heating process for compound **D1-10**

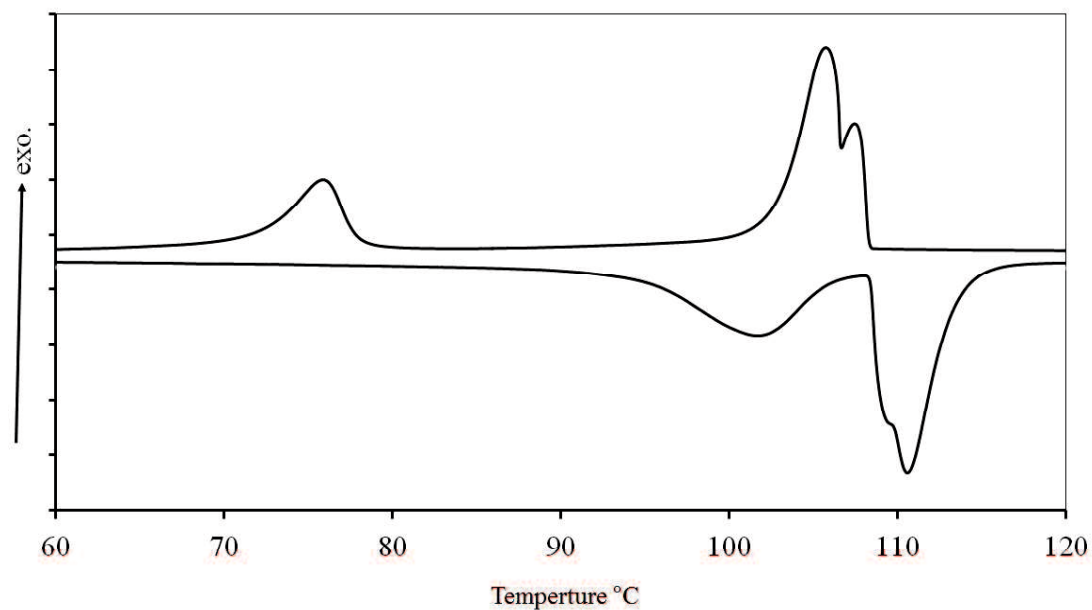


Figure 3-15. Differential scanning calorimetry during the first process for compound **D3-6**

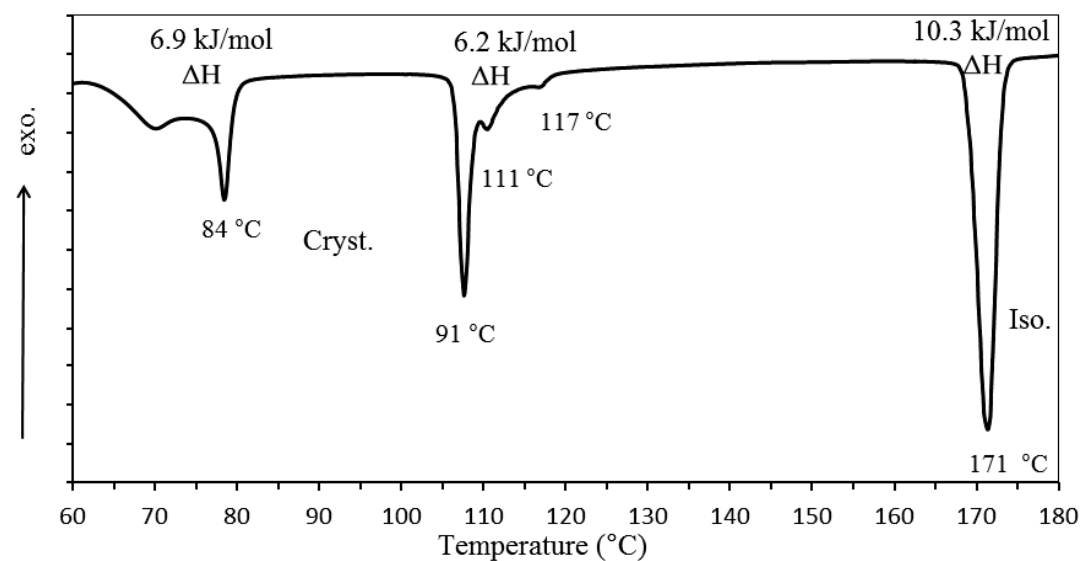


Figure 3-16. Differential scanning calorimetry during the first heating process for compound **D4-4**

3.3 Conclusions

Liquid crystals based on 4-semifluoroalkoxybiphenyl derivatives have been developed. Compounds **D1-n**, **D3-6** and **D4-4** with a biphenyl as a core group have

liquid crystalline properties while compounds **D2-n** and **D5-5** with a benzene group as a core group do not show liquid crystalline properties. The thermal ranges of mesophase for compounds **D1-n** sharply decrease as carbon number of terminal group slight increases. Thermotropic liquid crystalline property is also changed as 4-(perfluorohexyl)butoxyl group changes to decyloxyl group. So, the liquid crystalline properties depending on the core group, 4-(perfluorohexyl)butoxyl group and terminal group, which can be proved.

The intermolecular interactions and crystal packing will be explored in the future.

3.4 References

1. Mizoshita, N.; Hanabusa, K.; Kato, T. *Advanced Materials* **1999**, *11* (5), 392.
2. Twieg, R. J.; Russell, T. P.; Siemens, R.; Rabolt, J. F. *Macromolecules* **1985**, *18* (6), 1361.
3. Hashimoto, M.; Ujiie, S.; Mori, A. *Advanced Materials* **2003**, *15* (10), 797.
4. Hird, M. *Chemical Society Reviews* **2007**, *36*, 2070.
5. (a) Okamoto, H.; Murai, H.; Takenake, S. *Bulletin of the Chemical Society of Japan* **1997**, *70*, 3163; (b) Okamoto, H.; Yamada, N.; Takenaka, S. *Journal of Fluorine Chemistry* **1998**, *91*, 125; (c) Duan, M.; Okamoto, H.; Petrov, V. F. *Bulletin of the Chemical Society of Japan* **1998**, *71*, 2735; (d) Duan, M.; Okamoto, H.; Petrov, V. F. *Bulletin of the Chemical Society of Japan* **1999**, *72*, 1637; (e) Yano, M.; Taketsugu, T.; Hori, K.; Okamoto, H.; Takenaka, S. *Chemistry-A European Journal* **2004**, *10*, 3991.

Chapter 4 Gelation abilities of 4-alkoxy-4'-[4-(perfluorohexyl)butoxy]-1,1'-biphenyl derivatives

4.1 Introduction

LMWG is a family of organogelator that can gelatinize organic solvents at low concentrations. Although the self-assembly process of organogelator molecules into three dimensional nanofiber networks is complex, the molecular mode of organogelator can be easily illustrated as follow (**Figure 4-1**).¹ Most of time organogelator molecules can be divided into three functional units, such as terminal groups, core groups and alkyl or alkoxy chains. The core groups usually provide non-covalent interactions such as hydrogen bonds, halogen bonds, π - π interactions and van der Waals interactions. The terminal groups and alkyl or alkoxy chains can adjust the solvability of organogelator in solvents to keep a balance at supersaturation.

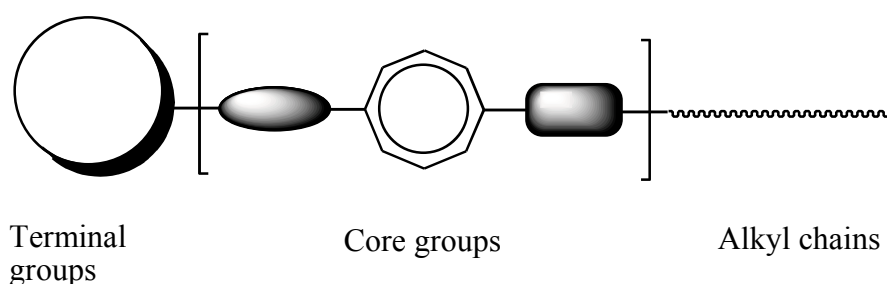


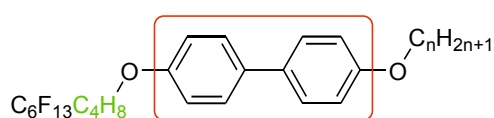
Figure 4-1. Illustration of molecular mode of organogelator

New functional fluorinated materials are quickly developed to meet the demanding requirements of advanced applications in fields such as biomedicine, biology, catalysis, electronic devices and environmental protections.² Fluorinated materials have special characteristics such as low optical loss, excellent thermal

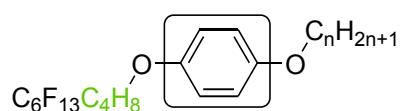
stability, highly effective and recyclable absorbents, excellent electrical property and high-performance catalyst. The special characteristics of per- and/or semifluorinated groups such as per- and/or semifluoroalkoxyl groups are introduced by characteristics of fluorination. Non-covalent interaction between a fluorine atom and a hydrogen atom is similar to hydrogen bond, but with a much lower energy.

In the past years, several LMWGs having per- and/or semifluoroalkyl groups (R_f) without a hydrogen bond group were published.³ It is well proved that soft materials containing R_f can show particular properties by the interplay of structural variations, such as the lengthened arms, the type and orientation of the linking groups and the terminal chains.⁴ Characteristics of R_f groups showing properties of hydrophobic or fluorophilic/solvophobic interactions have been widely used in the design of soft materials, but they are always used as terminal groups.⁵

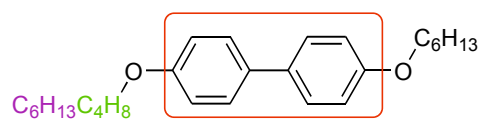
In our group, R_f as terminal groups affect their gelation ability, which have been reported.^{3b, 3c} In order to deepen the understanding of the relation between molecular structure and gelation ability, 4-semifluoroalkoxybiphenyl derivatives compounds **D1-n**, **D2-n**, **D3-n** and **D4-4** have been synthesized and explored.



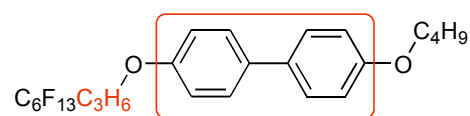
D1-n $n = 4, 5, 6, 8, 10$



D2-n $n = 5, 6$



D3-n $n = 5, 6$



D4-4

Figure 4-2. Chemical structures for compounds **D1-n**, **D2-n**, **D3-n** and **D4-4**

4.2 General gelation abilities

To clarify the relation between molecular structure and gelation ability, exactly speaking, the relation between the alkoxy chain length and gelation ability, the gelation abilities of compounds **D1-n** as LMWGs in various organic solvents (polar and non-polar) were investigated and the results were showed in **Table 4-1**. The alkoxy chain of **D1-n** is prolonged from butoxy to decyloxy to clarify the relation between gelation ability and the alkoxy chain length. Gelation tests were achieved as follows:

A weighed compound was mixed with an organic solvent in a micro tube (11 mm), and the mixture was heated until the solid dissolved. The resulting solution was cooled to room temperature and then the gelation was checked visually. When inverting the glass tube, no fluid flew down from the walls of the tube, we judged it “successful gel”. When the gel was formed, we evaluated quantitatively the gel forming property by determining the CGC, which is the critical concentration of the compound necessary for gelation at room temperature.

Table 4-1. Gelation abilities of compounds **D1-n** (wt%) at room temperature ^{[a], [b]}

Solvents	D1-4	D1-5	D1-6	D1-8	D1-10
PE	P(5.0)	P(5.0)	P(5.0)	P(5.0)	G(5.0)
DPMNP	P(5.0)	G(4.0)	G(4.0)	G(3.0)	G(2.0)
THF	S(5.0)	S(5.0)	S(5.0)	S(5.0)	S(5.0)

Toluene	S(5.0)	S(5.0)	S(5.0)	S(5.0)	S(5.0)
Cyclohexane	S(5.0)	G(4.0)	G(4.0)	G(5.0)	G(3.0)
Octane	G(3.0)	G(3.0)	G(2.0)	G(2.0)	G(1.0)
Acetone	P(5.0)	P(5.0)	P(5.0)	P(5.0)	P(5.0)
Acetonitrile	P(5.0)	P(5.0)	P(5.0)	P(5.0)	P(5.0)
3-Pentanone	S(5.0)	S(5.0)	S(5.0)	S(5.0)	G(5.0)
GBL	G(4.0)	G(0.5)	G(0.5)	G(0.8)	G(0.8)
1-Octanol	G(4.0)	G(0.7)	G(0.6)	G(0.8)	G(0.7)
Ethanol	P(5.0)	P(5.0)	P(5.0)	P(5.0)	P(5.0)
Methanol	P(5.0)	P(5.0)	P(5.0)	P(5.0)	P(5.0)
Ethyl acetate	P(5.0)	S(5.0)	S(5.0)	P(5.0)	G(5.0)
PC	G(4.0)	G(0.6)	Ins(5.0)	G(0.5)	G(0.5)
DMF	P(5.0)	G(2.0)	G(1.0)	G(4.0)	G(1.0)
DMSO	P(5.0)	G(2.0)	Ins(5.0)	G(1.0)	G(0.7)
HMPA	S(5.0)	S(5.0)	G(5.0)	G(5.0)	G(4.0)

^[a] G, P, S and Ins indicated gel, precipitate, soluble and insoluble; for gels, the critical gelation concentrations at room temperature were shown in parentheses, for P, S and Ins, compounds **D1-n** were precipitated, soluble and insoluble respectively at the concentrations in parentheses; ^[b] PE, DPMNP, THF, GBL, PC, DMF, DMSO and HMPA indicated petroleum ether, dipropylene glycol propyl ether, tetrahydrofuran, γ -butyrolactone, propylene carbonate, *N,N*-dimethyl formamide, dimethyl sulfoxide and hexamethylphosphoric triamide, respectively.

The results indicate that compounds **D1-n** as LMWGs can gelatinize most of tested solvents like cyclohexane, octane, GBL, 1-octanol, DMF and butyrolactone. Compounds **D1-n** tend to precipitate in petroleum ether, acetonitrile, acetone, methanol and ethanol, while dissolving in ethyl acetate, 3-pentanone, chloroform, 1,2-dichloromethane, toluene and tetrahydrofuran.

From **Table 4-1**, compound **D1-10** gelatinizes most of organic solvents which were tested in this paper. The gelation abilities of compounds **D1-n** become effective as the carbon chains of alkoxy groups prolong in generally organic solvents. For example, compound **D1-10** can gelatinize 3-pentanone at 5.0 wt%, compounds **D1-n** except **D1-10** are dissolved in 3-pentanone. In octane, the CGCs of **D1-n** where n is varying from 4 to 10 are changing from 3.0 wt% to 1.0 wt%.

In some cases, the critical gelation concentration value ranges within 0.7-1.0 wt%, indicate that **D1-10** is an effective organogelator. Among all the organogelators, the lowest CGC value (0.5 w%) is observed in PC gels gelatinized by **D1-8** and **D1-10**.

Although chemical structures of compounds **D1-n** are similar, and the gelation ability tend to be effective with elongation of the alkoxy chains, some results are out of the tendency. For example, in DMSO and propylene carbonate (PC), compound **D1-5** can respectively form gels even CGCs at 2.0 wt% and 1.0 wt%, and meanwhile compound **D1-6** can't gelatinize in DMSO and PC even at 5.0 wt%.

4.3 Particular gelation abilities

Gelation ability of **D1-10** was investigated with organic acids and some particular

organic compounds. Acetic acid is one of the simplest carboxylic acid and is classified as a weak acid. At the same time, acetic acid not only has a distinctive sour taste and pungent smell, but also has a corrosive effect. If acetic acid can be gelatinized, it maybe decrease its criticality. Compound **D1-10** showed effective gelation ability in acetic acid (**Table 4-2**). Caproic acid as a precursor for the synthesis of fine chemicals was investigated and even gelatinized at a general CGC value (2.0 wt%).⁶

Volatile organic compounds (VOCs) such as alkanes, arenes, phosphines, ketones, amines, carboxylic acids, esters, and aldehydes may have toxic effects on the human host after intestinal absorption and delivery to the liver via the portal vein.⁷ Fatty acid esters as a kind of VOCs are widely used in food, textile, cosmetic, rubber and metal processing, synthetic lubricant industries, and so on.⁸ From the results showed in **Table 4-1**, we know that **D1-10** gelatinize ethyl acetate at CGC of 5 wt%. Gelation test was carried out with dibutyl oxalate, methyl laurate or dibutyl adipate using **D1-10**, and the results were shown in **Table 4-2**.

Table 4-2. Gelation abilities of **D1-10** with VOCs at room temperature ^[a]

Solvents	Acetic acid	Caproic acid	Dibutyl oxalate	Methyl laurate	Dibutyl adipate
D1-10/wt%	G(0.4)	G(2.0)	G(2.0)	G(2.0)	G(2.0)

^[a] G: gel, for gels, the critical gelation concentrations (CGC) at room temperature were shown in parentheses.

Some VOCs are not very stable when they are heated in air. For example, methacrylic acid may be polymerized, phenols and aldehydes are easily oxidized. 10 wt% **D1-10** Solutions in THF was dropped into VOCs until the weight concentration of **D1-10** declined from 10% to 3%. All of the tested VOCs were quickly gelatinized at room temperature (**Table 4-3** and **Figure 4-3**).

Table 4-3. Gelation abilities of **D1-10** solution with some particular VOCs at room temperature ^{[a], [b]}

Solvents	MAA	C6:O	2LP	Guaiacol	HEXANAL	Decanal	BzH
D1-10/wt%	G(3.0)	G(3.0)	G(3.0)	G(3.0)	G(3.0)	G(3.0)	G(3.0)

^[a] G: gel, for gels, the gelation weight concentrations at room temperature were shown in parentheses; ^[b] C6:O, MAA, 2LP, HEXANAL and BzH indicated *n*-caproic acid, methacrylic acid, 2-allylphenol, *n*-Hexylaldehyde and benzaldehyde.

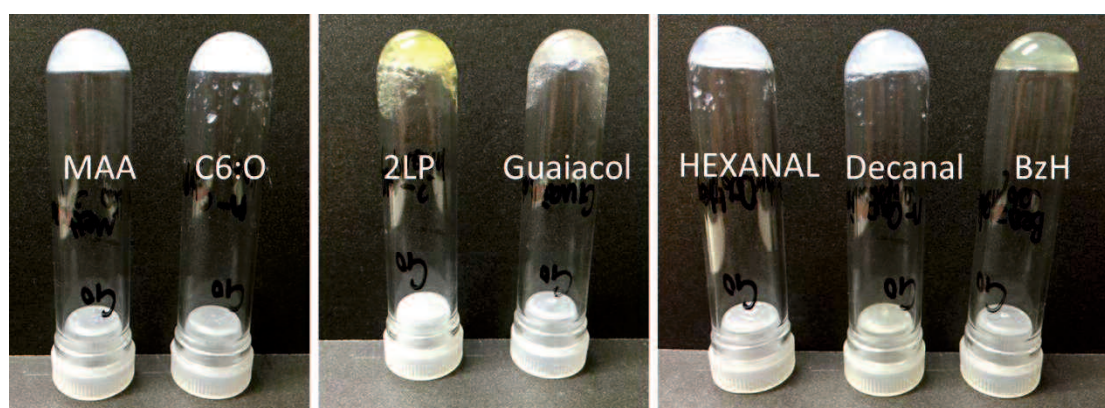


Figure 4-3. Gelation abilities of solution **D1-10** at CGC with some VOCs at room temperature

Formalin is widely used in chemical industry as an important precursor for many

chemical compounds and other materials, especially for polymers.⁹ Formalin is toxic and allergenic, according to the US National Toxicology Program describing formalin as “known to be a human carcinogen”. Gelation abilities of 10 wt% **D1-10** solution in THF with formalin was investigated (**Figure 4-4**). Formaldehyde was selectively gelatinized out of formalin, and water in formalin was still liquid.



Figure 4-4. Gelation ability of solution **D1-10** in THF with formalin at room temperature

4.4 The driving force for self-assembly

To gain visual insights into the aggregation mode, we selected the gel which was formed by compounds **D1-5** and **D1-10** at different concentrations in PC system as samples to study using scanning electron microscope (**Figure 4-5** and **Figure 4-6**). The SEM image shows that three dimensional nanofiber networks are formed by self-assembly of organogelator molecules. The average diameters of nanofiber formed by compound **D1-5** at 5 wt% are in a range of 750-250 nm, while formed by compound **D1-10** at 1 wt% are in a range of 600-250 nm.

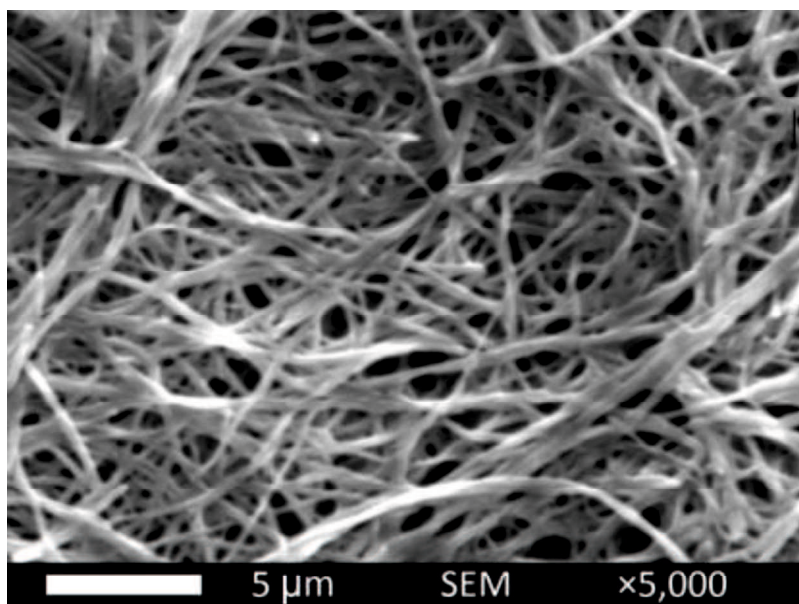


Figure 4-5. SEM image of PC xerogel system formed by compound **D1-5** (scale bar = 5 μm)

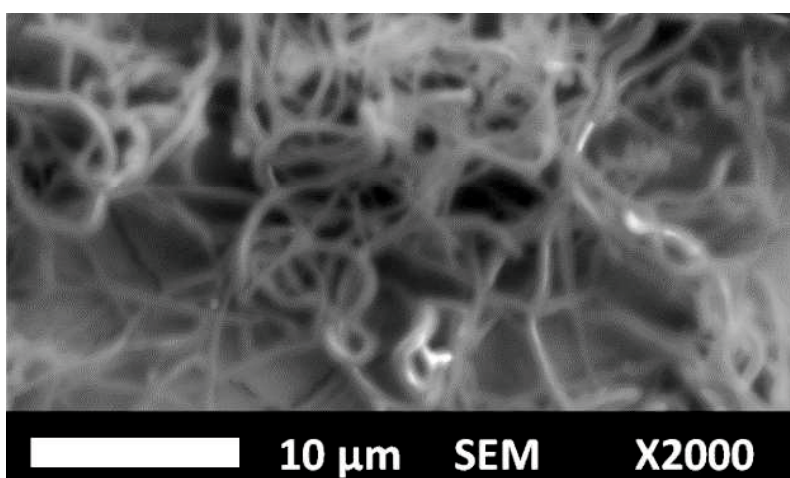


Figure 4-6. SEM image of PC xerogel system formed by compound **D1-10** (scale bar = 10 μm)

In order to explore the driving force for self-assemble, molecules similar with compounds **D1-n** with different frameworks have been synthesized and named as compounds **D2-n** ($n = 5, 6$) and compounds **D3-n** ($n = 5, 6$) (**Figure 4-2**). Compounds **D2-n** is different with compounds **D1-n** on core groups, with one benzene ring. While

compounds **D3-n** are different from compounds **D1-n** on terminal groups, having two alkoxy groups without 4-(perfluorohexyl)butoxy groups.

Compounds **D2-n** did not form gels in the tested solvents, which prove that the core groups with biphenyl is necessary. Benzene groups often provide π - π interactions on self-assemble process between intermolecules. The π - π interactions of **D2-n** molecules with only a benzene group maybe too weak to drive **D2-n** molecules to assemble.

Fluorinated materials generally have properties very different from those of hydrogen carbonyl materials, eg., good thermal stability, low coefficients, low refractive index and oxidative resistance. Herein, the gelation abilities of compounds **D3-5** and **D3-6** without 4-(perfluorohexyl)butoxy groups also have been explored. Unfortunately, compounds **D3-5** and **D3-6** did not show gelation ability. That means the 4-(perfluorohexyl)butoxy group may provide a feasible driving force which maybe hydrophobic and solvophobic interactions for molecular assembly.

Compound with carbon number decreasing from four to three between perfluoroalkoxy group and biphenyl group was synthesized and named as **D4-4**. Compound **D4-4** did not form any supramolecular gel with the tested solvents. The number of carbon between perfluoroalkoxy group and biphenyl group acts as a nonnegligible factor effecting gelation ability.

Through changing molecular structure of compounds **D1-n**, the driving force of self-assemble was indirectly turned out to be π - π interaction, molecular interaction,

hydrophobic and solvophobic interactions. The essential driving force for gelation of compounds **D1-n** was also studied by IR and ^1H NMR.

Infrared spectra of xerogels of compounds **D1-5** and **D1-6** in cyclohexane and pure compounds **D1-5** and **D1-6** were carried out and showed in **Figure 4-7** and **Figure 4-8**. From **Figure 4-7** and **Figure 4-8**, infrared spectra of xerogels of compounds **D1-5** and **D1-6** are the same as pure compounds respectively. Hydrogen bonds formed by hydroxyl groups can be proved by infrared spectra peak only at 3300 cm^{-1} . Mostly, infrared spectra peaks of water show at 3300 cm^{-1} and 1630 cm^{-1} . Infrared spectra of xerogels have a large peak at 3300 cm^{-1} , at the same time, a sharp peak at 1630 cm^{-1} can be found. Infrared spectra of pure organogelator also show the same two peaks. So it can be proved that hydrogen bonds do not form the peak at 1630 cm^{-1} when molecules of compounds **D1-5** and **D1-6** form three dimensional nanofiber networks by self-assembly.

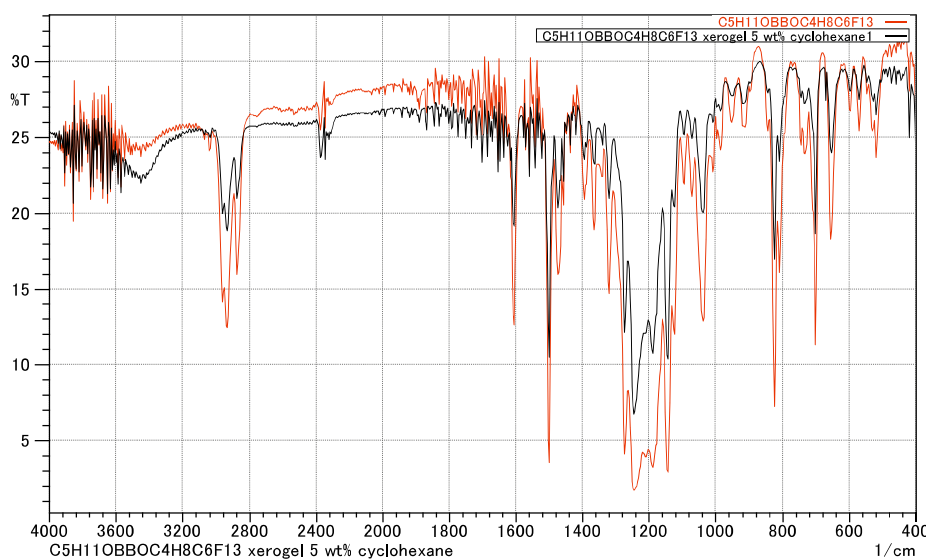


Figure 4-7. Infrared spectra of the xerogels of compound **D1-5** compared with compound **D1-5** (Red one is compound **D1-5**, black one is xerogel of compound **D1-5** at 5 wt% in cyclohexane.)

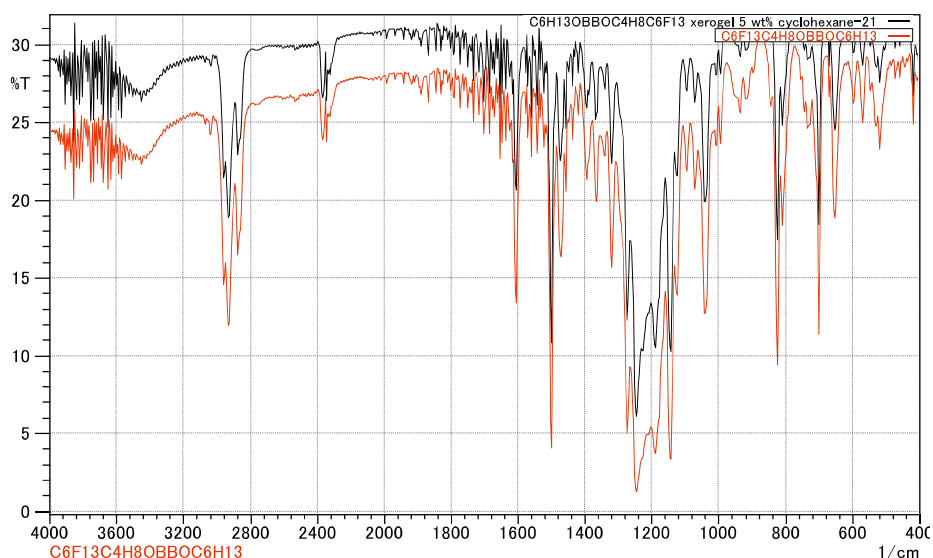


Figure 4-8. Infrared spectra of the xerogels of compound **D1-6** compared with compound **D1-6** (Red one is compound **D1-6**, black one is xerogel of compound **D1-6** at 5 wt% in cyclohexane.)

At the same time, from ¹H NMR spectra of compound **D1-5** in *d*₆-DMSO at different temperatures and concentrations in **Figure 4-9** and **Figure 4-10**, we thought that hydrogen bonds do not play any significant role in gel self-assembly.

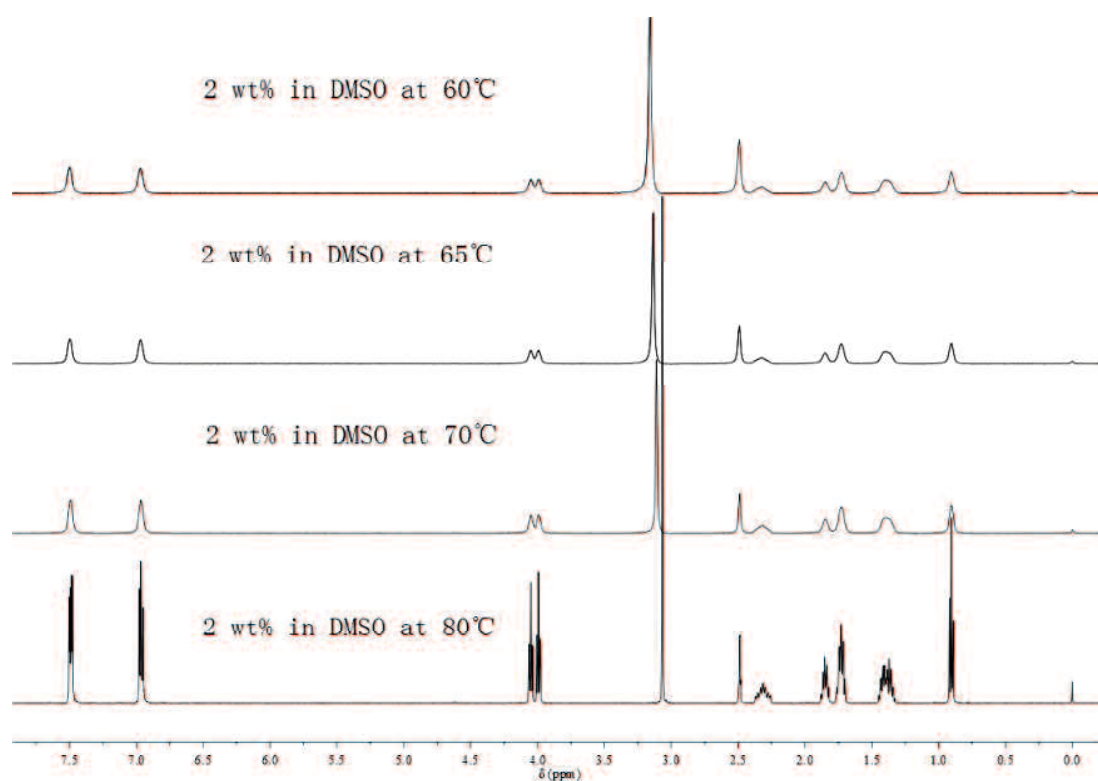


Figure 4-9. ^1H NMR spectra of compound **D1-5** in d_6 -DMSO at different temperatures

As reported in the past, the presence of long alkyl chains and rigid rodlike aromatic segments has been considered to be essential for the stable LMWG assemblies. In compounds **D1-n**, **D2-n**, **D3-n** and **D4-4**, only compounds **D1-n** showed gelation abilities. Not only the formation of π - π stacking interactions, but also the weaker intermolecular interaction between perfluoroalkoxyl chains affect the gelation abilities of compounds **D1-n**.

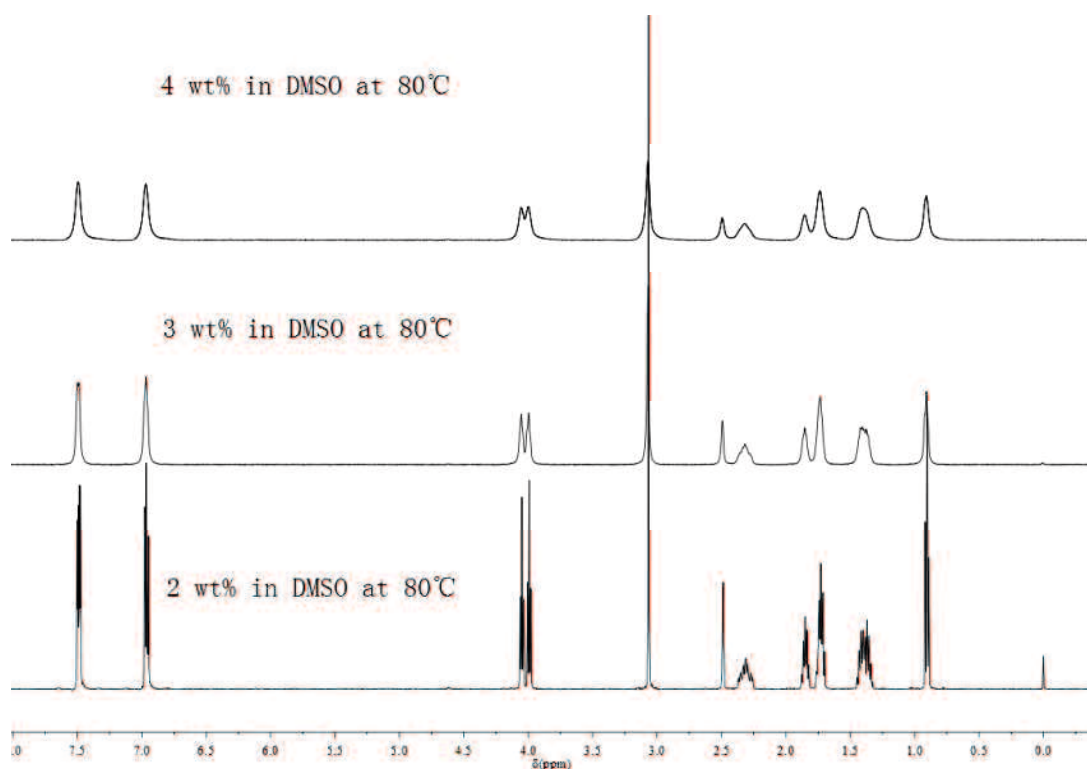


Figure 4-10. ^1H NMR spectra of compound **D1-5** in d_6 -DMSO at different concentrations

4.5 Rheological property of gels

The gels formed by **D1-n** were thermoreversible. Hence the gel to sol transition temperature (T_{gel}) was plotted against the organogelator weight concentration (wt%) in DMSO, GBL or PC (**Figure 4-11**). **Figure 4-10** shows that in GBL at the same concentration, the T_{gel} values of **D1-10** are similar to those of **D1-8**, meanwhile, in DMSO the T_{gel} values of **D1-10** are about 20 °C higher than those of **D1-8**. The T_{gel} values of **D1-8** show an order of PC > GBL > DMSO at the same concentration. For **D1-10**, the T_{gel} values in DMSO are similar to those in PC, and both of them are higher than it in GBL. The T_{gel} values rapidly decreased below at concentrations of 2 wt%.

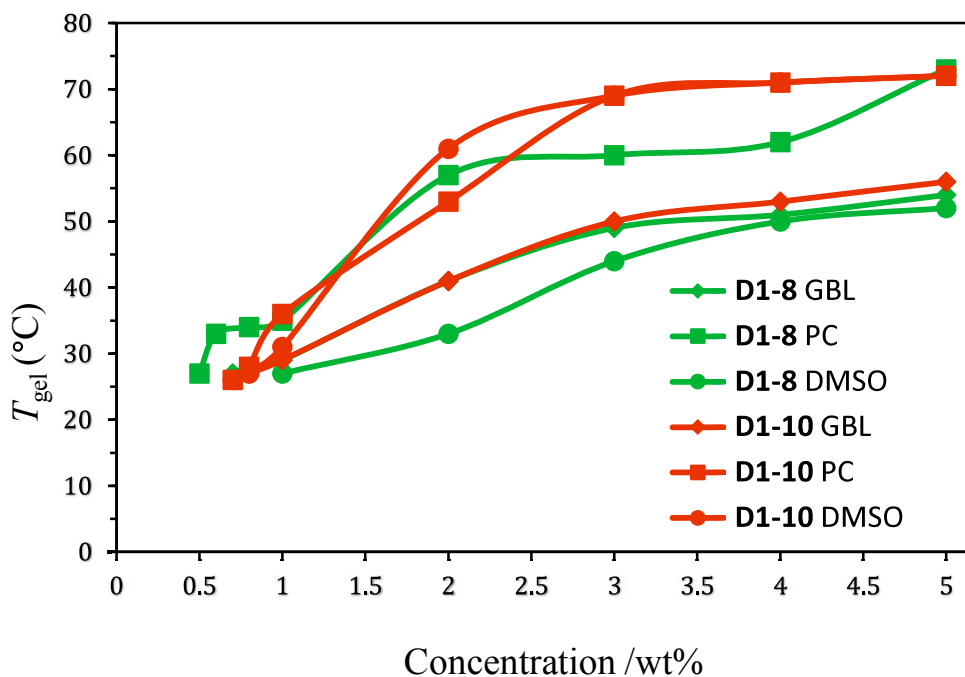


Figure 4-11. Plots of T_{gel} vs. concentration for **D1-8** and **D1-10** in PC, GBL and DMSO

The supramolecular gel characterization is principally related with rheological properties, even it has been defined.¹⁰ The rigidity and flow behaviors are shown in rheological measurement by storage modulus (G') and loss modulus (G''), respectively. As a supramolecular gel, G' should hold the line with frequency up to a particular yield point and should be stronger than G'' .

From **Figure 4-12**, we know that G' of gels formed by **D1-8** and **D1-10** are nearly a line, and the values of storage modulus and G'' of gel formed by **D1-8** are larger than that formed by **D1-10**, respectively. The results mean that supramolecular gels are showing rigidity and elastic characters and different supramolecular gels formed by different organogelators are showing different strengths of the gel networks in same solvents.

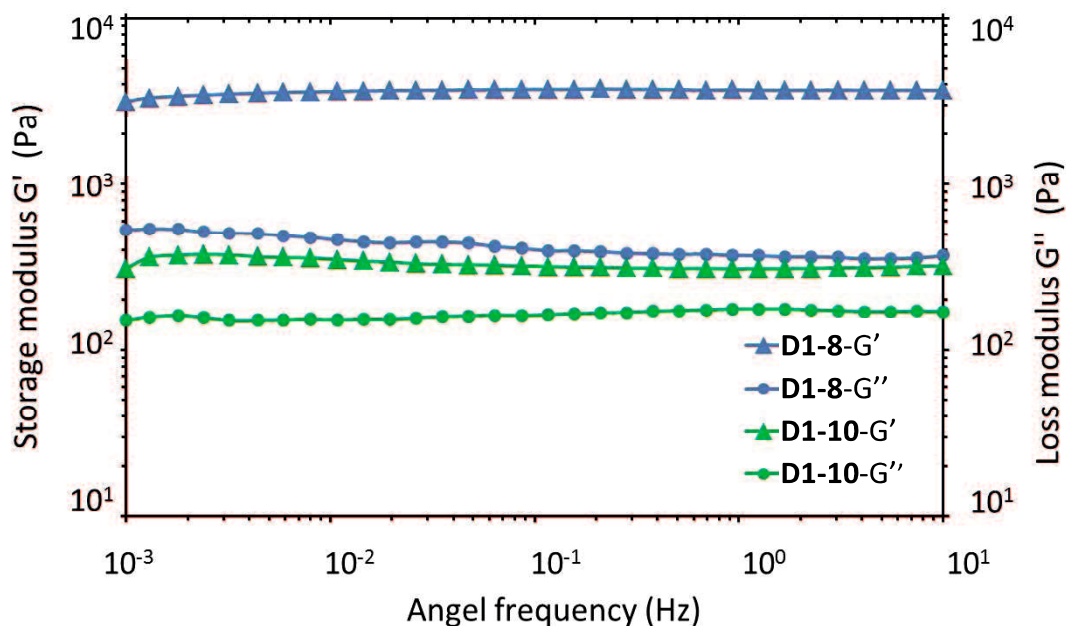


Figure 4-12. Frequency sweep rheometry data for supramolecular gels were gelatinized by **D1-8** and **D1-10** at 1 wt% with PC at room temperature

4.6 Conclusions

4-Alkoxy-4'-[4-(perfluorohexyl)butoxy]-1,1'-biphenyl derivatives as LMWGs show effective gelation abilities. Compounds **D1-5** and **D1-6** can gelatinize with γ -butyrolactone even at critical gelation concentration of 0.5 wt%. At the same critical gelation concentration, compounds **D1-8** and **D1-10** also gelatinize with propylene carbonate.

The aggregation mode was explored by using scanning electron microscope, infrared spectra and ¹H NMR spectra. In propylene carbonate xerogel system formed by compound **D1-5**, organogelator molecules form three dimensional nanofiber networks without hydrogen bonding.

The thermodynamical properties and rheological properties of supramolecular gels were explored, too. Supramolecular gels formed by compounds **D1-8** and **D1-10** in propylene carbonate are more thermodynamically stable than other solvents such as γ -butyrolactone and DMSO, and show good rheological properties.

4.7 References

1. Mohmeyer, N.; Schmidt, H. W. *Chemistry—A European Journal* **2005**, *11* (3), 863.
2. Pagliaro, M.; Ciriminna, R. *Journal of Materials Chemistry* **2005**, *15* (47), 4981.
3. (a) Twieg, R. J.; Russell, T. P.; Siemens, R.; Rabolt, J. F. *Macromolecules* **1985**, *18* (6), 1361; (b) Yoshida, T.; Hirakawa, T.; Nakamura, T.; Yamada, Y.; Tatsuno, H.; Hirai, M.; Morita, Y.; Okamoto, H. *Bulletin of Chemical Society Japan* **2015**, *88* (10), 1447; (c) Yoshida, T.; Nakamura, T.; Morita, Y.; Okamoto, H. *Chemistry Letters* **2015**, *44* (4), 512.
4. (a) Krieg, E.; Weissman, H.; Shimoni, E.; Bar On, A.; Rybtchinski, B. *Journal of the American Chemical Society* **2014**, *136* (26), 9443; (b) Johansson, G.; Percec, V.; Ungar, G.; Zhou, J. *Macromolecules* **1996**, *29* (2), 646; (c) Percec, V.; Johansson, G.; Ungar, G.; Zhou, J. *Journal of the American Chemical Society* **1996**, *118* (41), 9855.
5. (a) Shen, J.; Hogen-Esch, T. *Journal of the American Chemical Society* **2008**, *130* (33), 10866; (b) Hird, M. *Chemical Society Reviews* **2007**, *36* (12), 2070; (c) Okamoto, H.; Murai, H.; Takenaka, S. *Bulletin of Chemical Society Japan* **1997**, *70* (12), 3163; (d) Okamoto, H.; Yamada, N.; Takenaka, S. *Journal of Fluorine Chemistry* **1998**, *91* (2), 125; (e) Yano, M.; Taketsugu, T.; Hori, K.; Okamoto, H.; Takenaka, S. *Chemistry—A European Journal* **2004**, *10* (16), 3991; (f) Yoshida, T.; Hirakawa, T.; Nakamura, T.; Yamada, Y.; Tatsuno, H.; Morita, Y.; Okamoto, H. *ECS Transactions* **2013**, *50* (48), 95.
6. Kenealy, W.; Cao, Y.; Weimer, P. *Applied Microbiology and Biotechnology* **1995**,

44 (3-4), 507.

7. Raman, M.; Ahmed, I.; Gillevet, P. M.; Probert, C. S.; Ratcliffe, N. M.; Smith, S.; Greenwood, R.; Sikaroodi, M.; Lam, V.; Crotty, P. *Clinical Gastroenterology and Hepatology* **2013**, *11* (7), 868.

8. Haas, M. J.; Scott, K. M.; Marmer, W. N.; Foglia, T. A. *Journal of the American Oil Chemists' Society* **2004**, *81* (1), 83.

9. Huang, H.; Leung, D. Y.; Ye, D. *Journal of Materials Chemistry* **2011**, *21* (26), 9647.

10. Piepenbrock, M.-O. M.; Lloyd, G. O.; Clarke, N.; Steed, J. W. *Chemical Reviews* **2009**, *110* (4), 1960.

Chapter 5 Supramolecular phase-selective gelation abilities by 4-alkoxy-4'-[4-(perfluorohexyl)butoxy]-1,1'-biphenyl derivatives

5.1 Introduction

The impacts of environmental risk factors on human health are extremely varied and complex. Water is not only an abundant natural resource, but also a major part of human body which occupies 60% or more by weight of human body. As industry develops, the scarcity of safe water becomes a serious challenge confronting humankind in the 21st century.¹ For example, hazardous waste such as dyes, pharmaceuticals, petroleum products and heavy metals are discharging into environment with water. There is a huge and terrible task to protect environment especially water. Marine pollution is mostly occurred with accidental or discharge of crude oil and petrochemicals. Oils spill destroys ocean environment, which usually happens everywhere in the world. The pollution source impacts on human health through biological concentration in food chain.

Now activated carbon, zeolites, chitosans and some other nonconventional adsorbents are used to remove dyes and heavy metals from waste water. However, there are shortages such as lack of selectivity, low pollutant uptake and costly regeneration processes. So it is a necessary to develop new methods to remove pollution source from environment for human health and environmental safety.

Supramolecular gels were explored in environment recovery. Supramolecular gels as a kind of soft materials have liquid-like property of highly fluidness and solid-like

property of rigidity. Supramolecular gels are widely applied in cosmetics, pharmaceutical preparation, greases and other food industry. In order to recover crude oil and reduce damage, supramolecular gel which is potentially efficient, recyclable, economically viable for large scale application, and without second pollution method, becomes a hotspot (Figure 5-1).¹

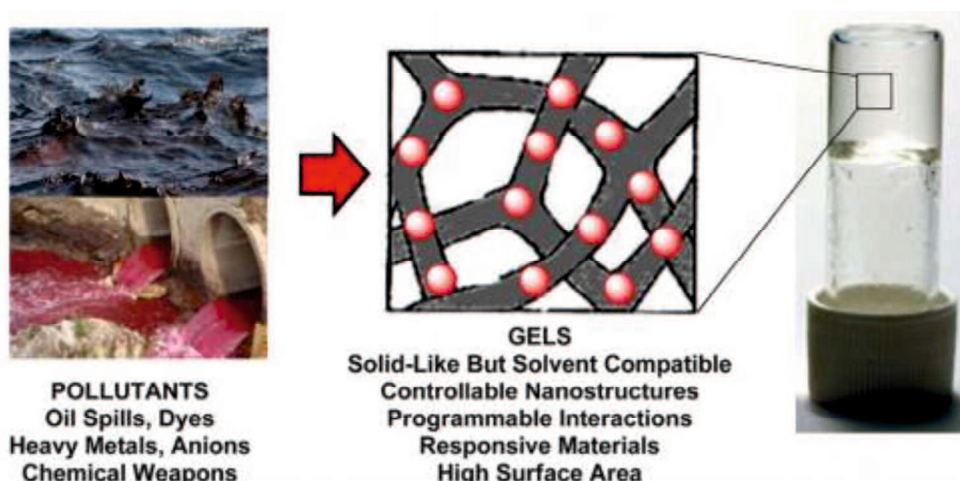


Figure 5-1. Self-assembled gel-phase soft materials for environmental remediation¹

Since Bhattacharya and Krishnan-Ghosh used a simple amino acid amphiphile *N*-lauroyl-L-alanine (Figure 5-2) to selectively gelatinize commercial oils and aromatic hydrocarbons, different kinds of gelators have been reported.²

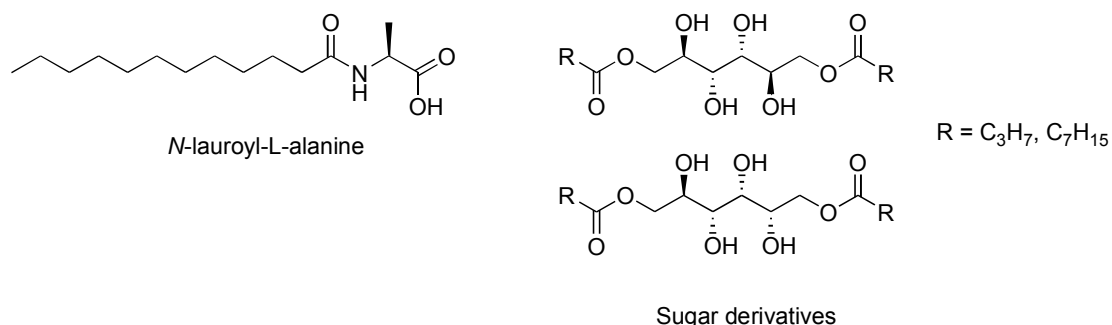


Figure 5-2. Chemical structure of *N*-lauroyl-L-alanine and sugar derivatives

For example, John and co-workers combining 12 key principles of green

chemistry reported a kind of sugar-derived gelators (**Figure 5-2**) which is an ideal candidate for ecofriendly oil spill recovery. In order to fit for real-life application, the sugar-based gelators dissolved in ethanol at high concentration were explored at room temperatures.³

To apply at scale in the real-world, the ideal system of LMWG must have properties as follows:

The source of gelators must be firstly wide, cheap, reusable and ecofriendly, which means gelators can be gotten easily by avoiding secondary pollution. The gelation process without heating-cooling cycles is necessary. Then the supramolecular gels must be stable in a wide temperature range and shear forces.

In this work, phase selective gelation abilities of compounds **D1-n** and **D4-4** were investigated. The chemical structures of compounds **D1-n** and **D4-4** were shown in

Figure 5-3.

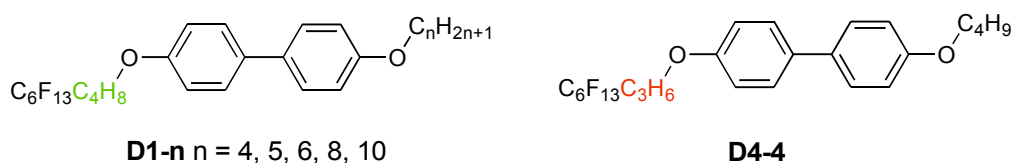


Figure 5-3. Chemical structures of compounds **D1-n** and **D4-4**

5.2 Phase selective gelation abilities

5.2.1 Phase selective gelation abilities of **D1-n** with heating-cooling cycle

Aromatic amines are widely used as a precursor of pesticides, pharmaceuticals, and dyes. Amines as an important organic base are widely used in industry and may

spill into nature and pollute our rivers and oceans.⁴ Although amines themselves may be not the major risk for environment, from the past researches, amines as the precursor of toxic compounds can destroy environment through degradation reactions.⁵ In order to protect human health and environmental safety, it is important to reduce amines in environment, especially in water. Although approaches like adsorbents and chemical dispersants which remove pollutants out of environment have been researched, those approaches still have some limitations in practice.⁶

So, representative examples of amines were chosen and investigated with compounds **D1-n** and **D4-4** by the “stable to inversion in a test tube” method firstly. The results of CGCs are shown below in **Table 5-1**. Compounds **D1-5** and **D1-6** could rapidly gelatinize primary amines (e.g. aniline, benzylamine, β -phenylethylamine). The time of secondary amine (e.g. piperidine) forming gel at 1 wt% was longer than that of primary amines in heating-cooling cycle at room temperature. Hexamethylphosphoric triamide (HMPA) could be gelatinized only by compound **D1-6** at 5 wt% while *N*-ethyl-diisopropylamine only by compound **D1-5** at the same concentration. Except some cases (i.e. CGCs of **D1-6** with *N,N*-diisopropylethylamine (DIEA), **D1-8** with benzylamine or piperidine), for gelators **D1-n** with the long alkoxy chains, gelation abilities have become strong.

Table 5-1. Gelation abilities of compounds **D1-n** and **D4-4** with amines at room temperature ^{[a],[b]}

Solvents	D1-4	D1-5	D1-6	D1-8	D1-10	D4-4
----------	-------------	-------------	-------------	-------------	--------------	-------------

Aniline	G(4.0)	G(1.0)	G(1.0)	G(1.0)	G(0.2)	P(5.0)
Benzylamine	G(5.0)	G(1.0)	G(1.0)	G(2.0)	G(0.6)	P(5.0)
1-PEA	P(5.0)	G(2.0)	G(2.0)	G(1.0)	G(1.0)	P(5.0)
2-PEA	G(5.0)	G(1.0)	G(1.0)	G(1.0)	G(0.6)	P(5.0)
Piperidine	P(5.0)	G(1.0)	G(1.0)	G(5.0)	G(3.0)	P(5.0)
DIEA	G(3.0)	G(5.0)	S(5.0)	G(5.0)	G(3.0)	P(5.0)
DMA	P(5.0)	G(5.0)	G(5.0)	G(5.0)	G(4.0)	P(5.0)
Pyridine	G(5.0)	G(5.0)	G(5.0)	G(5.0)	G(5.0)	P(5.0)

^[a] G and P indicated gel and precipitate; for gels, the critical gelation concentrations (CGCs) at room temperature were shown in parentheses, for P and S, compounds **D1-n** and **D4-4** were precipitated and soluble respectively at the concentrations in parentheses; ^[b] 1-PEA, 2-PEA, DIEA and DMA indicated 1-phenylethylamine, 2-phenylethylamine, *N,N*-diisopropylethylamine and *N,N*-dimethylaniline, respectively.

Phase selective gelators that can selectively solidify organic layer from a biphasic mixture of water and organic layer are studied to offer a potential and effective solution to this pollution problem. Generally, phase selective gelators with CGCs at 5 wt% showing phase-selective property have potential applications in environment

recovery. In the meantime compounds **D1-5** and **D1-6** showing efficient gelation abilities even at 1 wt% encourage us to analyze their phase-selective property. We dropped water (1 mL) into test tubes containing gel formed by compounds **D1-5** and **D1-6** in aniline, benzylamine, 2-PEA, DIEA and pyridine at CGCs. The mixtures were heated and shaken sharply to ensure homogeneous dispersion of amine in water. After cooling the mixture to room temperature, compound **D1-5** could selectively gelatinize the aniline, benzylamine and 2-phenylethylamine in aqueous-amine biphasic systems (**Figure 5-4**). The gels formed by compound **D1-6** in benzylamine, 2-phenylethylamine and HMPA were destroyed after water was dropped, but in aniline it gelatinized again.

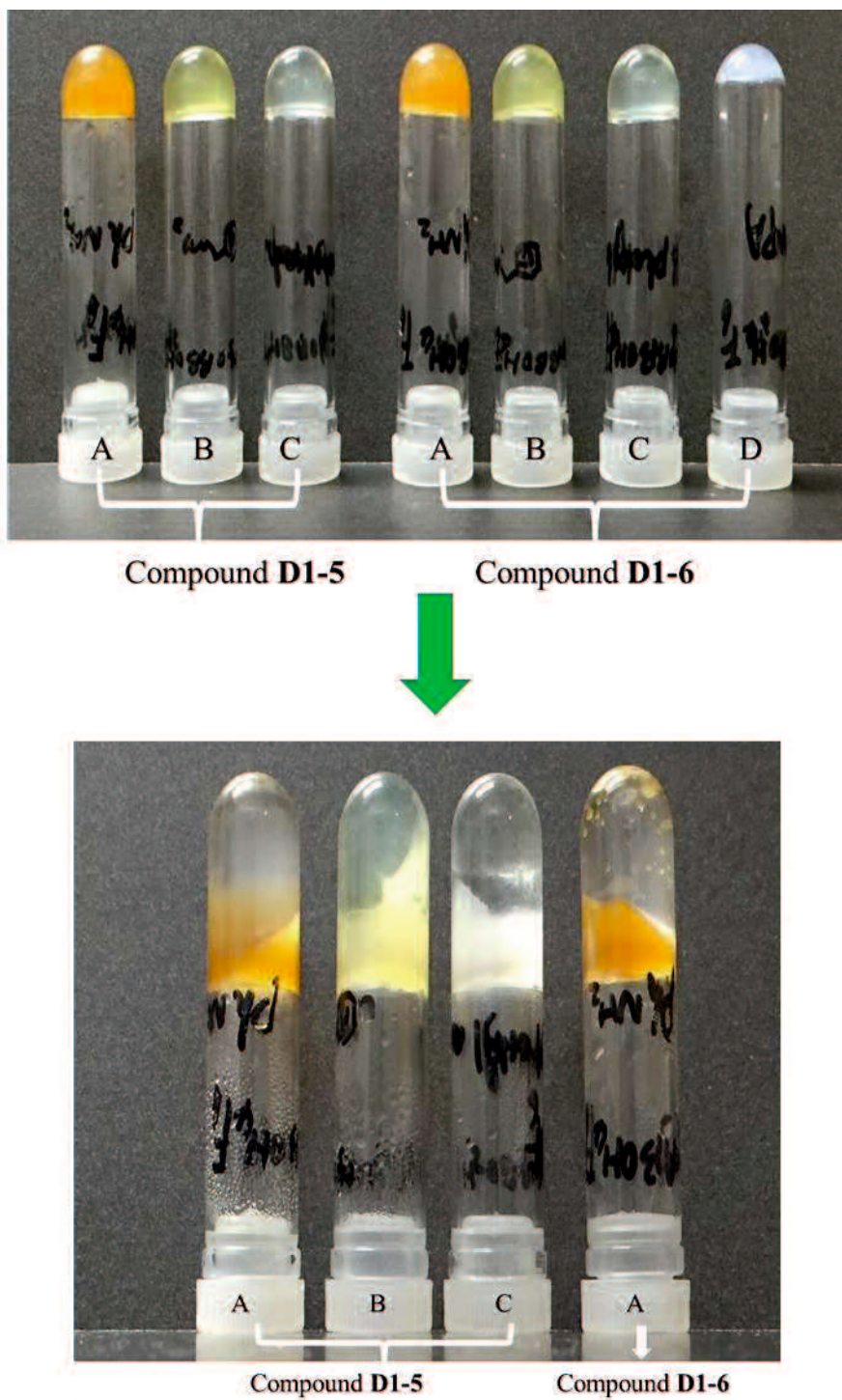


Figure 5-4. Phase selective gelation of **D1-5** and **D1-6** in A: aniline, B: benzylamine, C: 2-phenylethylamine, D: *N,N*-diisopropylethylamine

Oil is one of the important materials not only in our daily life, but also in industry. For example, synthetic lubricant is used in automobile engines, generators and other

machines; mineral oil is used in biomedicine, veterinary medicine, mechanical and electrical industries.⁷ So every year many tons of oil are used and even thrown into environment.⁸ Meanwhile almost every year, accidents of oil spills happen in oceans and rivers.⁹ Herein, gelation abilities of **D1-n** and **D4-4** with synthetic lubricant, mineral oil, lamp oil, polyolefin and rape oil were investigated. The results are shown in **Table 5-2**.

Table 5-2. Gelation abilities of compounds **D1-n** and **D4-4** with oils at room temperature ^{[a],[b]}

Solvents	D1-4	D1-5	D1-6	D1-8	D1-10	D4-4
Synth. Lub.	G(1.0)	G(1.0)	G(1.0)	G(1.0)	G(0.7)	G(5.0)
Mineral oil	G(1.0)	G(1.0)	G(1.0)	G(1.0)	G(0.7)	G(5.0)
Lamp oil	G(5.0)	G(5.0)	G(5.0)	G(3.0)	G(2.0)	G(5.0)
Poly- α -olefin	G(4.0)	G(0.8)	G(1.0)	G(0.7)	G(0.7)	G(5.0)
Rape oil	G(4.0)	G(0.8)	G(0.8)	G(0.7)	G(0.7)	G(5.0)

^[a] G: gel, for gels, the critical gelation concentrations (CGCs) at room temperature were shown in parentheses; ^[b] Synth. Lub. indicated synthetic lubricant.

As can be seen from **Table 5-2**, it proves that the slight longer the alkoxy chains, the better the gelation abilities. Compound **D1-10** shows the best gelation ability

among **D1-n** and **D4-4**.

The property of phase selectively gelatinize in aqueous-oil biphasic systems was also tested. Because oil spills often happen in ocean and pH of seawater is about 8.0, we replaced water with 1 mL of saturated solution where NaCl was added into a saturated solution of NaHCO₃ until NaCl was undissolved. Similar test like the test in aqueous-amine biphasic systems was carried out. All of those gels formed by compounds **D1-n** at CGCs in synthetic lubricant, mineral oil, lamp oil, polyolefin and rape oil selectively solidified in the aqueous-oil biphasic systems after heating-cooling cycle process (**Figure 5-5**).

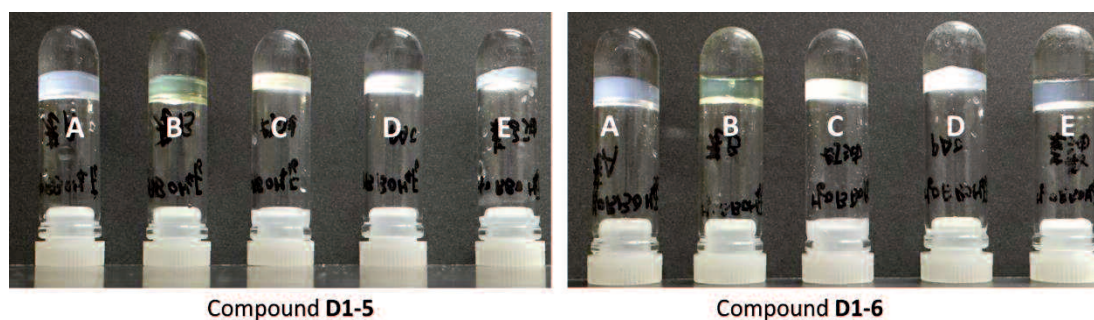


Figure 5-5. Photograph of gel formed in aqueous-amine biphasic systems using compound **D1-5** (left) and **D1-6** (right) as gelators. A: synthetic lubricant, B: mineral oil, C: lamp oil, D: polyolefin, E: rape oil

We adjusted the aqueous from basic to acidic by 0.5 mL of 1M HCl(aq.) and found that compounds **D1-n** still can selectively solidify oil layer (**Figure 5-6**).

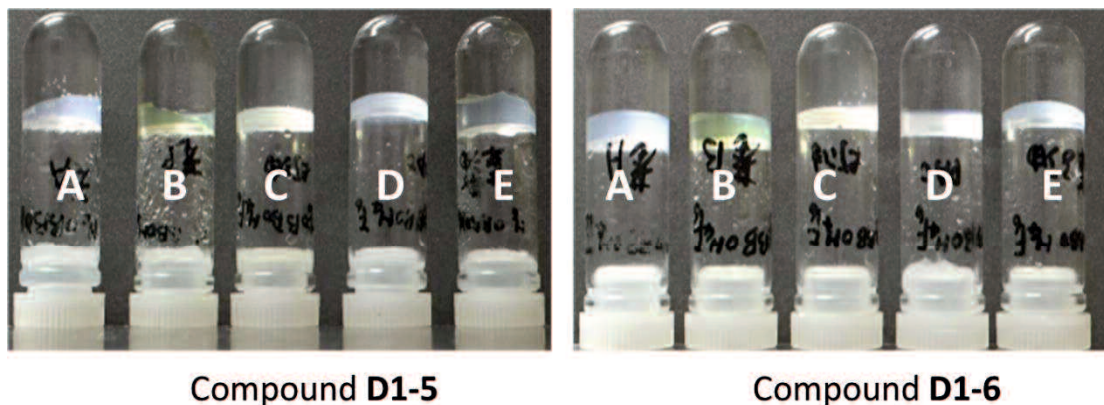


Figure 5-6. Photograph of gel formed at acidic solution using compound **D1-5** (left) and **D1-6** (right) as gelators. A: synthetic lubricant, B: mineral oil, C: lamp oil, D: polyolefin, E: rape oil

Factually, oil pollution usually happens in lakes and sea.⁹ So we also investigated the selective gelation abilities of **D1-8** and **D1-10** at CGC from marine water which was picked up from Tokiwa beaches in Yamaguchi prefecture of Japan, too. Marine water (1 g) was dropped into a sealed tube containing gel at CGC and the mixture was heated until the gel dissolved. Then, the aqueous-oil biphasic mixture was shaken about 1 min with heating and then cooled to room temperature. The tube was subsequently inverted to judge the gel formation. The gels gelatinized by **D1-8** and **D1-10** can selectively gelatinize oil phase from aqueous-oil biphasic mixture (**Figure 5-7** and **Figure 5-8**).

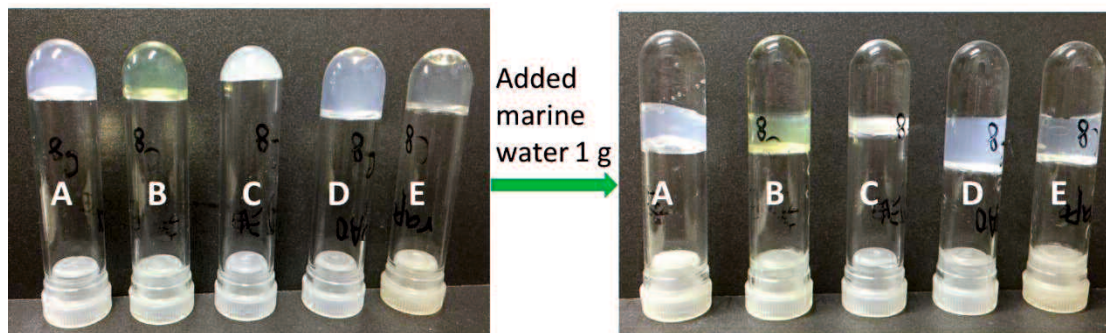


Figure 5-7. Phase selective gelation of **D1-8** with aqueous-oils. A: synthetic lubricant, B: mineral oil, C: lamp oil, D: polyolefin, E: rape oil

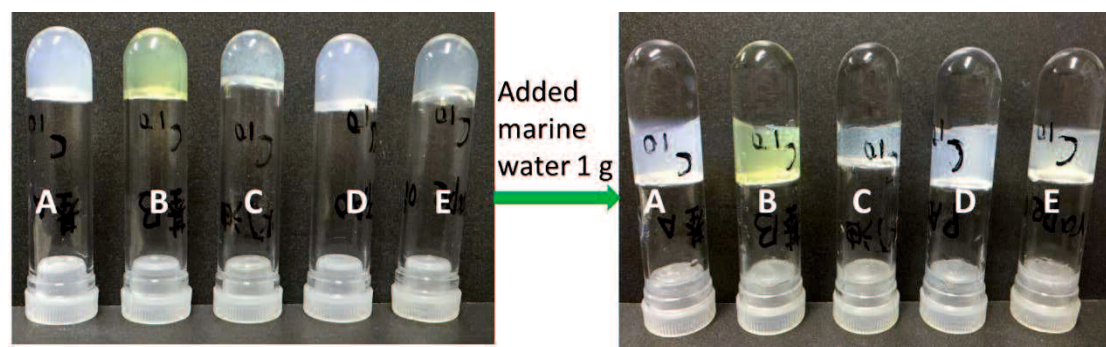


Figure 5-8. Phase selective gelation of **D1-10** with aqueous-oils. A: synthetic lubricant, B: mineral oil, C: lamp oil, D: polyolefin, E: rape oil

5.2.2 Phase selective gelation abilities of **D1-n** without heating-cooling cycle

Compounds **D1-n** perform excellent selective gelation abilities even at CGCs of 1 wt% in the aqueous-aniline and aqueous-oil biphasic systems by heating-cooling process that was inspiring us to research their selective gelation abilities at room temperature. The process of forming supramolecular gels through heating-cooling cycle limits gel potential applications in practice, and adding a co-solvent to prepare gelator solution is a quite feasible method to cover the disadvantage.¹⁰ Gelator **D1-10** was inspiring us to research selective gelation ability at room temperature. According

to **Table 4-1**, 10 wt% **D1-10** solutions in toluene or THF were prepared and their gelation abilities in other organic liquid at room temperature were investigated.

We prepared solution of 10 wt% of compound **D1-5** in toluene by heating. The warm toluene solution was dropped into aqueous-aniline biphasic mixture until weight percentage of compound **D1-5** in organic layer decreased to 5 wt%. Then the mixture was shaken sharply to make sure that aniline can mix with the solution. To our surprise, the solution of compound **D1-5** can fast selectively solidify aniline from a biphasic mixture. Compound **D1-6** presents the same result as compound **D1-5** (**Figure 5-9**).

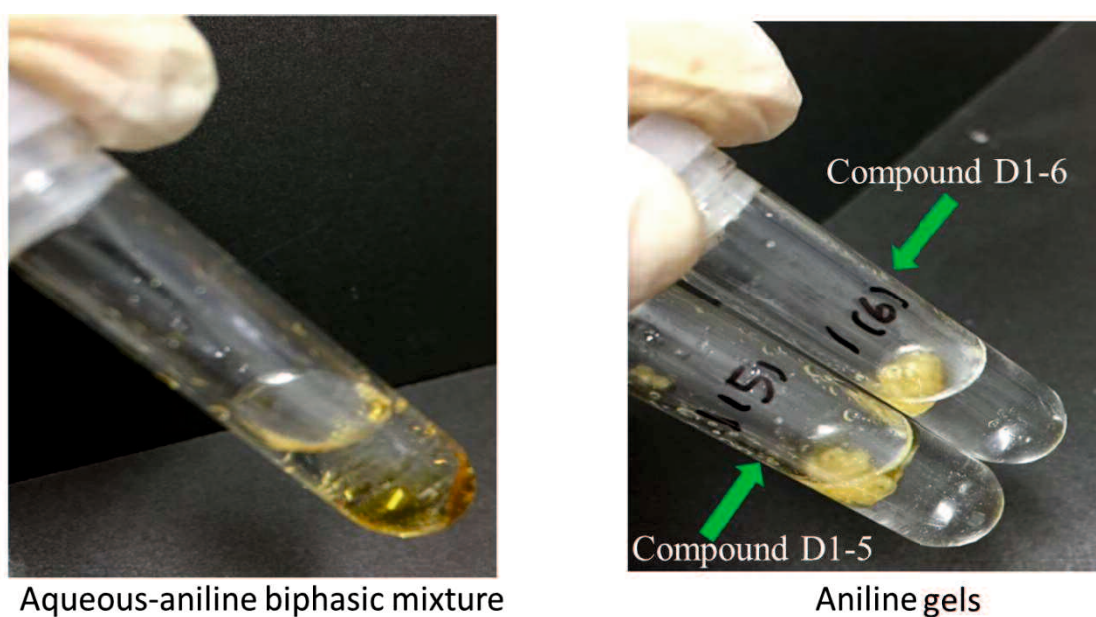


Figure 5-9. Photograph of gel formed with **D1-5** or **D1-6** in toluene solutions at room temperature

Biphasic systems (aqueous/synthetic lubricant = 4:1) were also researched with warm solution of 10 wt% of compound **D1-5** in toluene. The organic layer was

quickly and selectively gelatinized in 1 min. Unfortunately there was a sharp slowdown in gelation speed for solution of compound **D1-5** in toluene at room temperature.

According to **Table 4-1**, a 10 wt% **D1-10** solution in THF was prepared. The selective phasic property of 10% **D1-10** solution in THF was studied with synthetic lubricant at room temperature. We prepared two different kinds of aqueous-oil mixtures (A and B). Mixture A contained 1g marine water and 0.1 g synthetic lubricant, and B contained 1g marine water and 0.2g synthetic lubricant. Aqueous-oil mixtures A and B were mixed respectively by ultrasonic wave without heating at room temperature about 1 min. Then, the solution of **D1-10** in THF was added into A and B to make the weight concentration of **D1-10** decrease to 3% and 1% in organic components, respectively (**Figure 5-10**). Synthetic lubricant was gelatinized at 3 wt% about 10 seconds. The organic component of aqueous-oil mixture was selectively gelatinized at weight concentration of 1% over night.

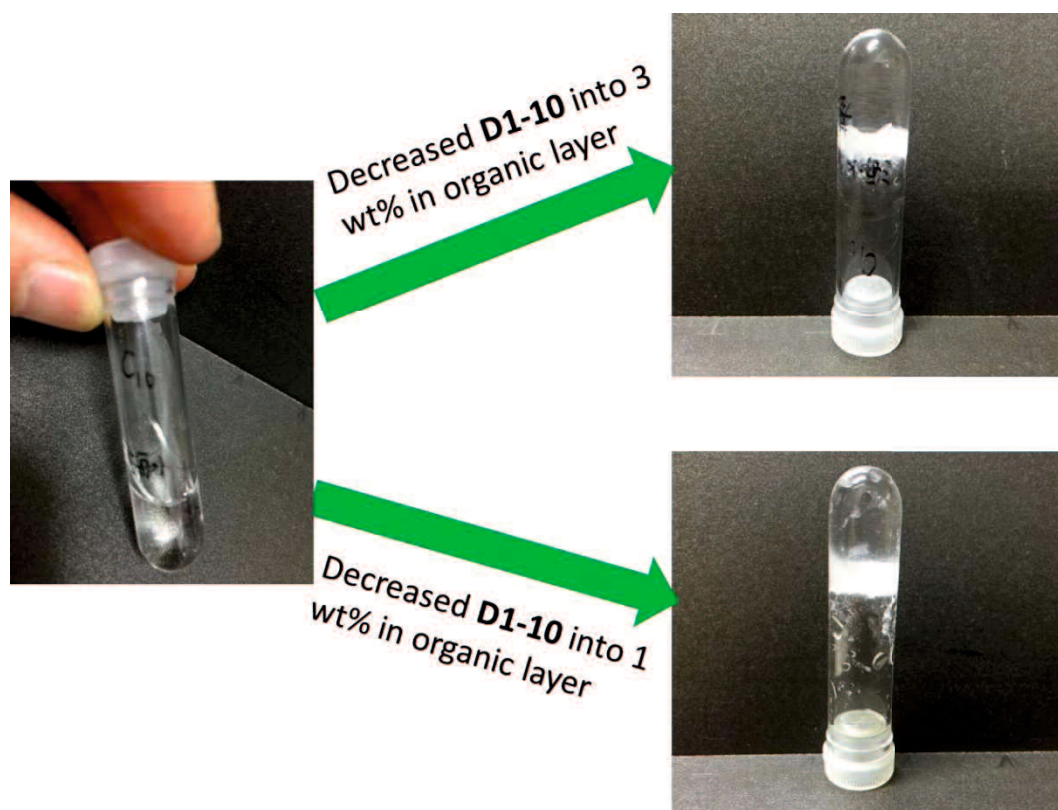


Figure 5-10. The selective phase properties of **D1-10** solution in THF at different concentrations

5.3 The effect of phase selective properties

In this work, we found that gelation ability of **D1-6** solution in toluene was disturbed by its temperature. So herein, we prepared a 10 wt% **D1-10** solution by ultrasonic wave without heating at room temperature in a sealed tube. The selective gelation abilities of **D1-10** solution in toluene or THF were studied with aqueous-aniline biphasic mixture as follows. Firstly, aqueous-aniline biphasic mixture (0.1 g aniline and 1 g marine water) was put into a sealed tube and mixed by ultrasonic wave without heating about 1 min. Secondly, **D1-10** solution was dropped into the tube and then shaken to be intensively mixed. After 1 min, we found that the 10 wt% **D1-10** solution in THF could selectively gelatinize aniline layer, while the

same concentration solution in toluene gelatinized a part of aniline, and liquid aniline was easily found by visual observation (**Figure 5-11**). Thus, the 10 wt% **D1-10** solution in THF for researching gelation ability in further examinations is more effective than that in toluene at room temperature.

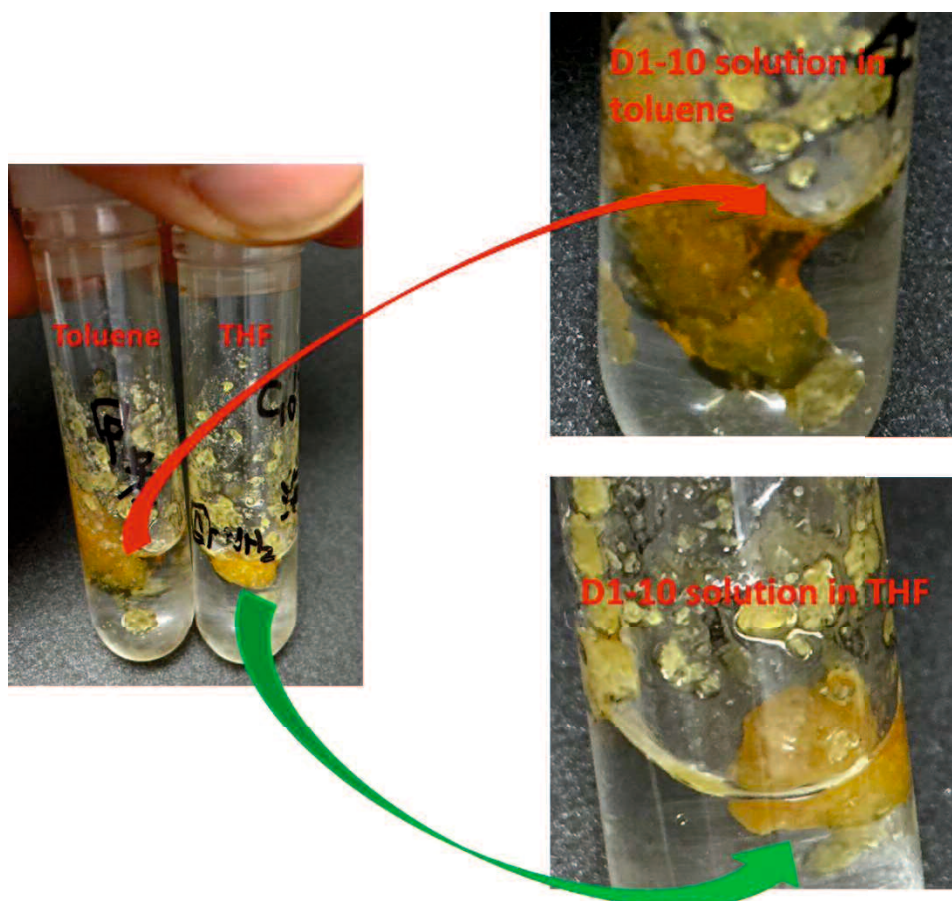


Figure 5-11. Gelation abilities of **D1-10** in THF or toluene at room temperature

We try to find out what the reason of low effective gelation ability of **D1-10** in toluene is. Compound **D1-5** successfully gelatinized in toluene overnight at 10 wt%, but it failed to gelatinize at 5 wt%. The morphology of xerogel gelatinized by compound **D1-5** at 10 wt% was investigated by SEM. There were many three dimensional nanofiber networks (**Figure 5-12-A**), at the same time, clusters (**Figure**

5-12-B) and zero-dimensional (0D) nano dots (**Figure 5-12-C)** also were found in the same sample in different parts. We proposed that the stability of gel gelatinized by compound **D1-5** in toluene is not very good.

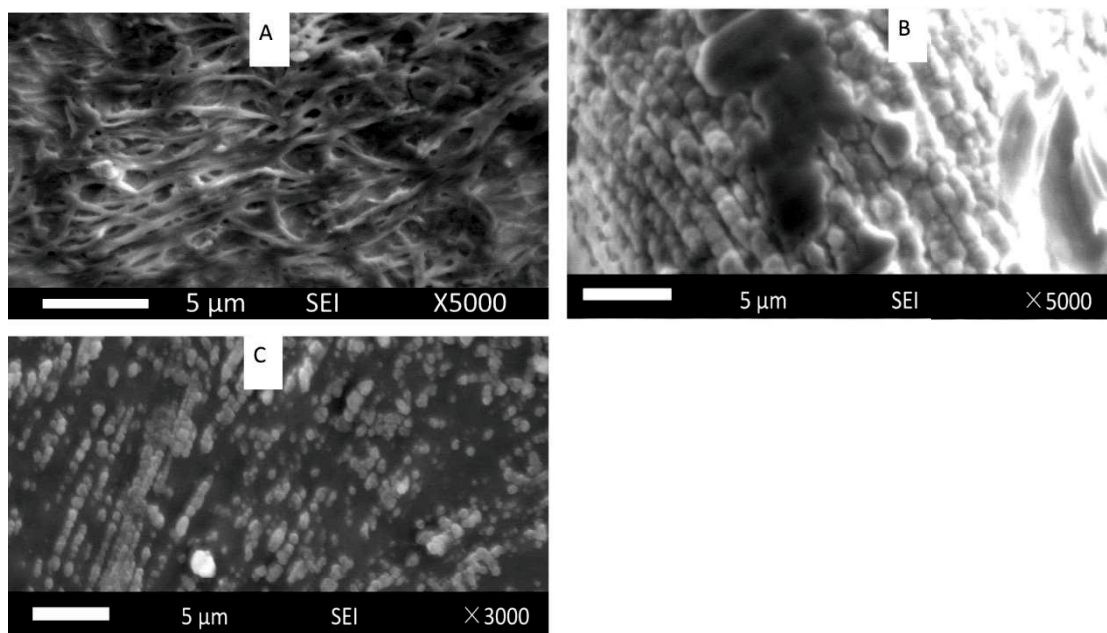


Figure 5-12. SEM image of compound **D1-5** in toluene (10 wt%)

5.4 Conclusions

Compounds **D1-n** show effective gelation abilities in tested amine and oils. Most of supramolecular gels formed by tested amine and oil can gelatinize again from biphasic mixture using heating-cooling cycle even at extreme pH value. **D1-n** solutions in toluene and THF were explored. **D1-5** and **D1-6** solutions in toluene can selectively gelatinize amine from aqueous-amine, but the temperature of solution plays a key role in phase selectivity gelation ability. The phase selective properties of 10 wt% **D1-10** in toluene and THF at room temperature were researched. The **D1-10** solution in THF shows more effective phase selectivity than in toluene. The three

dimensional nanofiber networks found in the 10 wt% **D1-5** solution in toluene also proves that the gelation ability is not very strong.

5.5 References

1. Okesola, B. O.; Smith, D. K. *Chemical Society Reviews* **2016**, *45*, 4226.
2. Bhattacharya, S.; Krishnan-Ghosh, Y. *Chemical Communications* **2001**, (2), 185.
3. Jadhav, S. R.; Vemula, P. K.; Kumar, R.; Raghavan, S. R.; John, G. *Angewandte Chemie* **2010**, *122* (42), 7861.
4. Pinheiro, H.; Touraud, E.; Thomas, O. *Dyes and pigments* **2004**, *61* (2), 121.
5. Poste, A. E.; Grung, M.; Wright, R. F. *Science of the Total Environment* **2014**, *481*, 274.
6. Zhang, X.; Song, J.; Ji, W.; Xu, N.; Gao, N.; Zhang, X.; Yu, H. *Journal of Materials Chemistry A* **2015**, *3*(37), 18953.
7. (a) Nagendramma, P.; Kaul, S. *Renewable and Sustainable Energy Reviews* **2012**, *16* (1), 764; (b) Shkol'nikov, V.; Bronshtein, L.; Shekhter, Y. N.; Drozdova, O. *Chemistry and Technology of Fuels and Oils* **1977**, *13* (7), 479; (c) Rudnick, L. R. *Synthetics, Mineral Oils, and Bio-based Lubricants: Chemistry and Technology*, CRC press **2013**, p14.
8. Higgins, T. E. *Pollution prevention handbook*, CRC Press **1995**, p177-198.
9. Blumer, M. *Persistence and degradation of spilled fuel oil*, *Science* **1972**, *176*, 1120.
10. (a) Mukherjee, S.; Shang, C.; Chen, X.; Chang, X.; Liu, K.; Yu, C.; Fang, Y. *Chemical Communications* **2014**, *50* (90), 13940; (b) Basak, S.; Nanda, J.; Banerjee,

A. *Journal of Materials Chemistry* **2012**, 22 (23), 11658.

Chapter 6 Liquid crystalline property and gelation ability of

4-[4-(perfluorohexyl)butoxy]phenyl 4-alkoxybenzoates

6.1 Introduction

Although many molecular structures have been synthesized for liquid crystals, the relations between molecular structure and liquid crystalline properties are still not very clear.¹ As the investigation developed, some rules between molecular structure and liquid crystalline properties have been found. For example, some liquid crystalline compounds, with a molecular structure fitting closely with a simple rod-like shape are easy to form mesophase.² Molecular polarizabilities and refractive also have relations with liquid crystalline properties.

In the past years, our group investigated some alky benzoate derivatives having a semifluoroalkyl group (**Figure 6-1**).³ All of them have a single benzene ring as the liquid crystalline core. Most of single-benzene ring compounds are difficult to form mesophase because of the low molecular anisotropy. Semifluoroalkyl groups tend to enhance the thermal stability of liquid crystalline properties owing to fluorination.

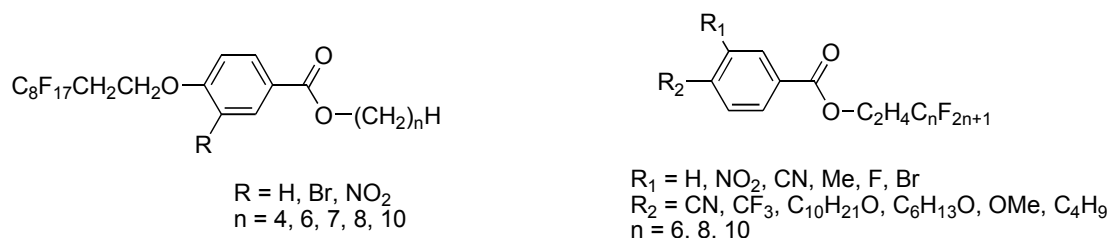


Figure 6-1. Chemical structures of alky benzoate derivatives having a semifluoroalkyl group

As we know, the typical core structures such as benzene, biphenyl, triphenyl and

pyrenyl, due to their extraordinary abilities of self-assembly through π - π interaction, are usually used in liquid crystalline molecular structures.⁴

In this work, benzene was introduced into the alky benzoate derivatives to explore the relation between molecular structures and physical properties such as liquid crystalline properties and supramolecular gel properties. Compounds like 4-[4-(perfluorohexyl)butoxy]phenyl 4-alkoxybenzoates were synthesized according to Chapter 2. The chemical structures of 4-[4-(perfluorohexyl)butoxy]phenyl 4-alkoxybenzoates are shown in **Figure 6-2**.

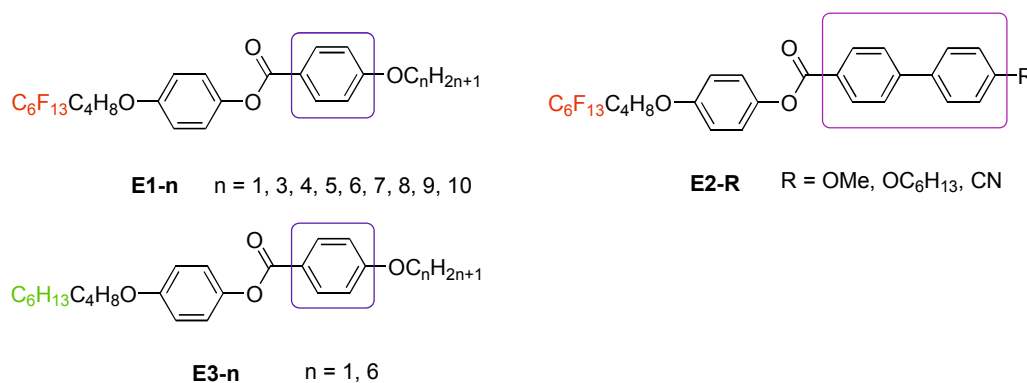


Figure 6-2. Chemical structures of 4-[4-(perfluorohexyl)butoxy]phenyl 4-alkoxybenzoates

6.2 Liquid crystalline properties

Liquid crystalline properties of 4-[4-(perfluorohexyl)butoxy]phenyl 4-alkoxybenzoates derivatives were achieved by polarized optical microscopy (POM) and differential scanning calorimetry (DSC). Characteristic textures and defect structures change when passing a mesophase transition, which reveals the mesophase type observed by POM.

Compounds **E1-n** show exclusively smectic A mesophases (SmA) which are characterized using a polarized microscope and DSC measurements. Textures of mesophase of **E1-n** are shown in **Figure 6-3** and **Figure 6-4**.

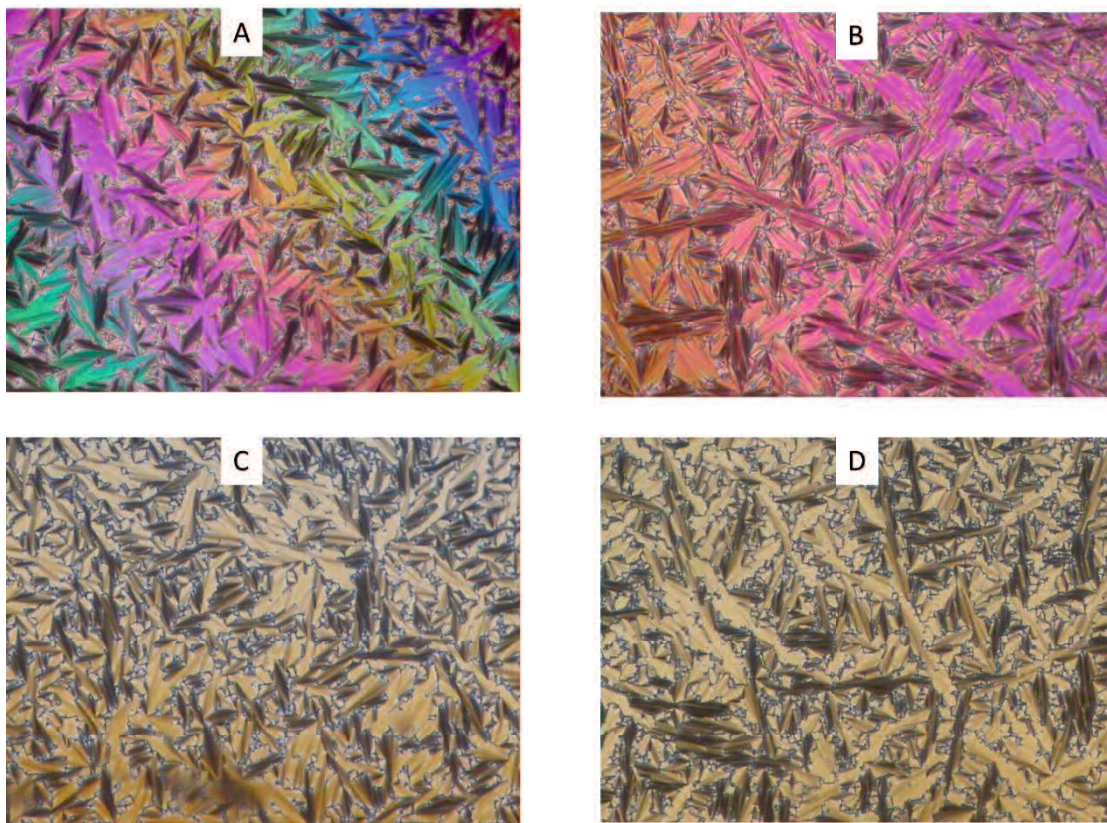


Figure 6-3. Polarized micrographs for A: compound **E1-1** at 130°C, B: compound **E1-3** at 145°C, C: compound **E1-4** at 145°C, D: compound **E1-5** at 145°C

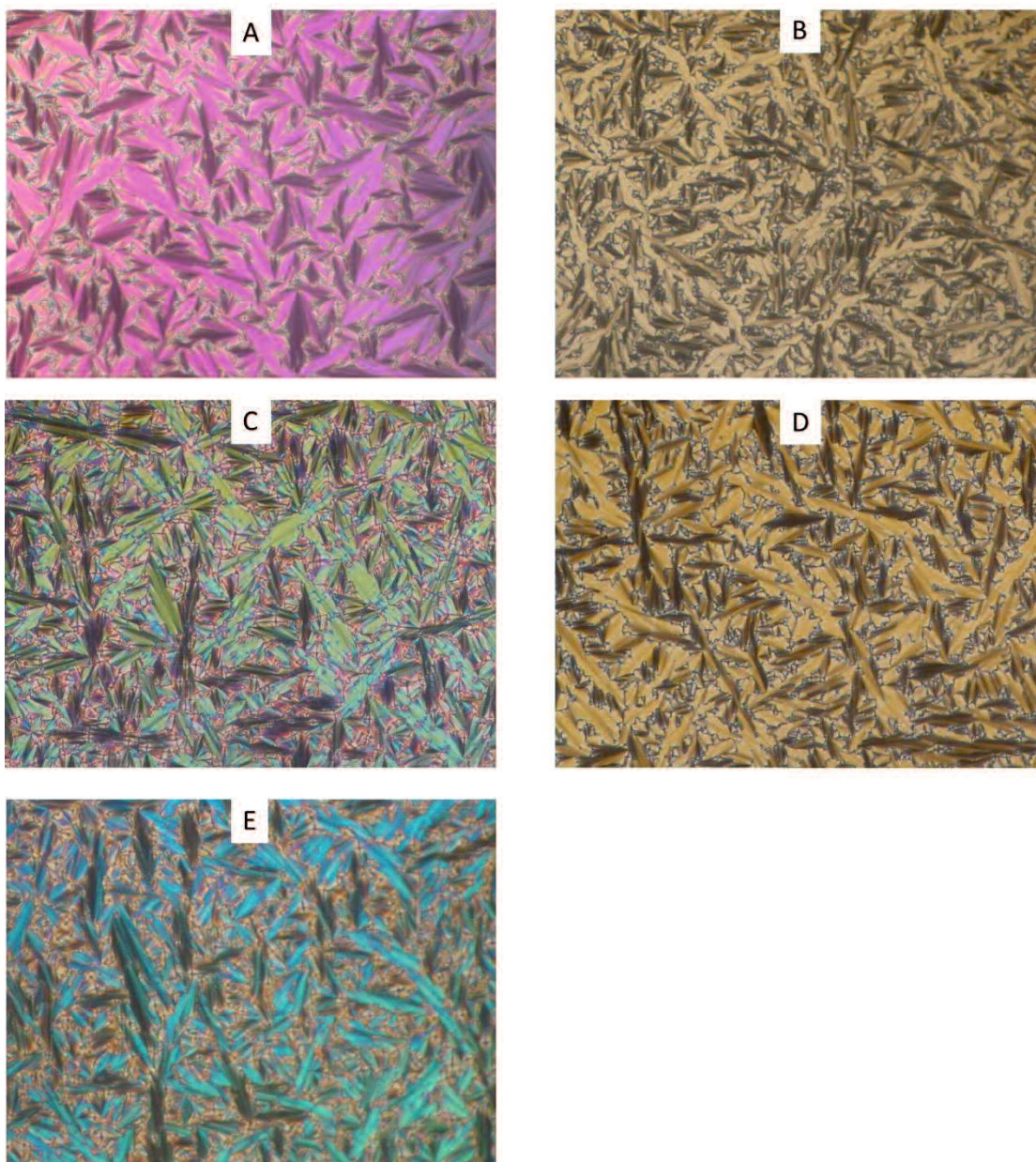


Figure 6-4. Polarized micrographs for A: compound **E1-6** at 130°C, B: compound **E1-7** at 135°C, C: compound **E1-8** at 135°C, D: compound **E1-9** at 130°C, E: compound **E1-10** at 125°C

The results of DSC analysis have been summarized in **Table 6-1**. According to **Table 6-1**, compounds **E1-n** show similar thermodynamic properties. The SmA-Iso mesophase transition temperatures change from 134 °C to 152 °C. The associated latent heats with SmA-Iso transition change from 5.2 kJ mol⁻¹ to 10.4 kJ mol⁻¹.

Table 6-1. Transition temperatures [$^{\circ}\text{C}$] and the associated latent heats [kJ mol^{-1}] of compounds **E1-1** in first heating process

Compounds	Transition temperatures ($^{\circ}\text{C}$)			ΔH (kJ mol^{-1})	
	Cryst	SmA	Iso	mp	SmA-Iso
E1-1	• 96	• 142	•	40.6	5.2
E1-3	• 88	• 148	•	30.5	6.7
E1-4	• 81	• 152	•	30.7	7.2
E1-5	• 83	• 148	•	34.5	7.9
E1-6	• 77	• 147	•	30.6	8.3
E1-7	• 73	• 144	•	29.0	9.2
E1-8	• 67	• 141	•	41.1	10.2
E1-9	• 73	• 138	•	34.1	10.3
E1-10	• 75	• 134	•	51.6	10.4

Cryst, SmA and Iso indicate crystal, smectic A mesophase and isotropic liquid, respectively. Parentheses indicate a monotropic transition.

The mesophase of compounds **E1-n** only simply shows SmA. According to liquid crystalline properties of 4-[4-(perfluorohexyl)butoxy]phenyl 4-alkoxybenzoates, compounds **E2-R** having a biphenyl core were designed and synthesized. The terminal groups (R) of compounds **E2-R** are methoxyl group (-OMe), hexyloxy group (-OC₆H₁₃) and cyano group (-CN). Terminal group affecting thermodynamic properties of liquid crystals is usually studied. Methoxyl group as a short alkoxy group, hexyloxy group as a general alkoxy group and cyano group as an electron withdraw group were used to investigate the terminal group effect. The liquid crystalline properties were explored by POM and DSC. Textures of mesophase of **E2-R** are shown in **Figure 6-5** and **Figure 6-6**.

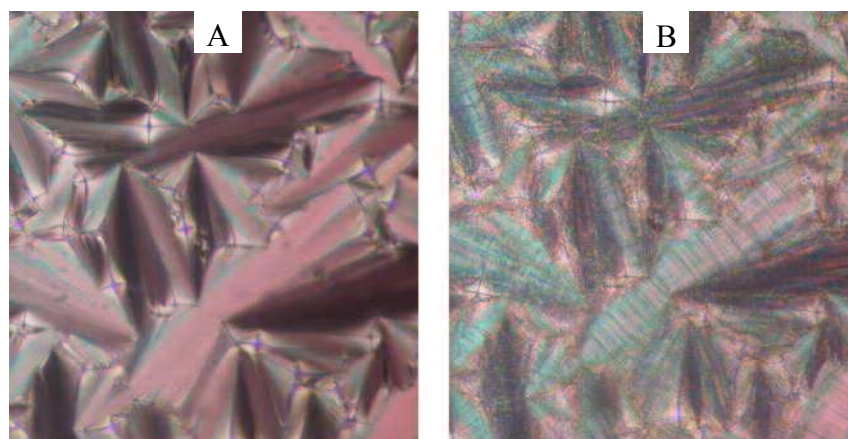


Figure 6-5. Polarized micrographs of compound **E2-OMe** at 149 °C (A) and 59 °C (B)

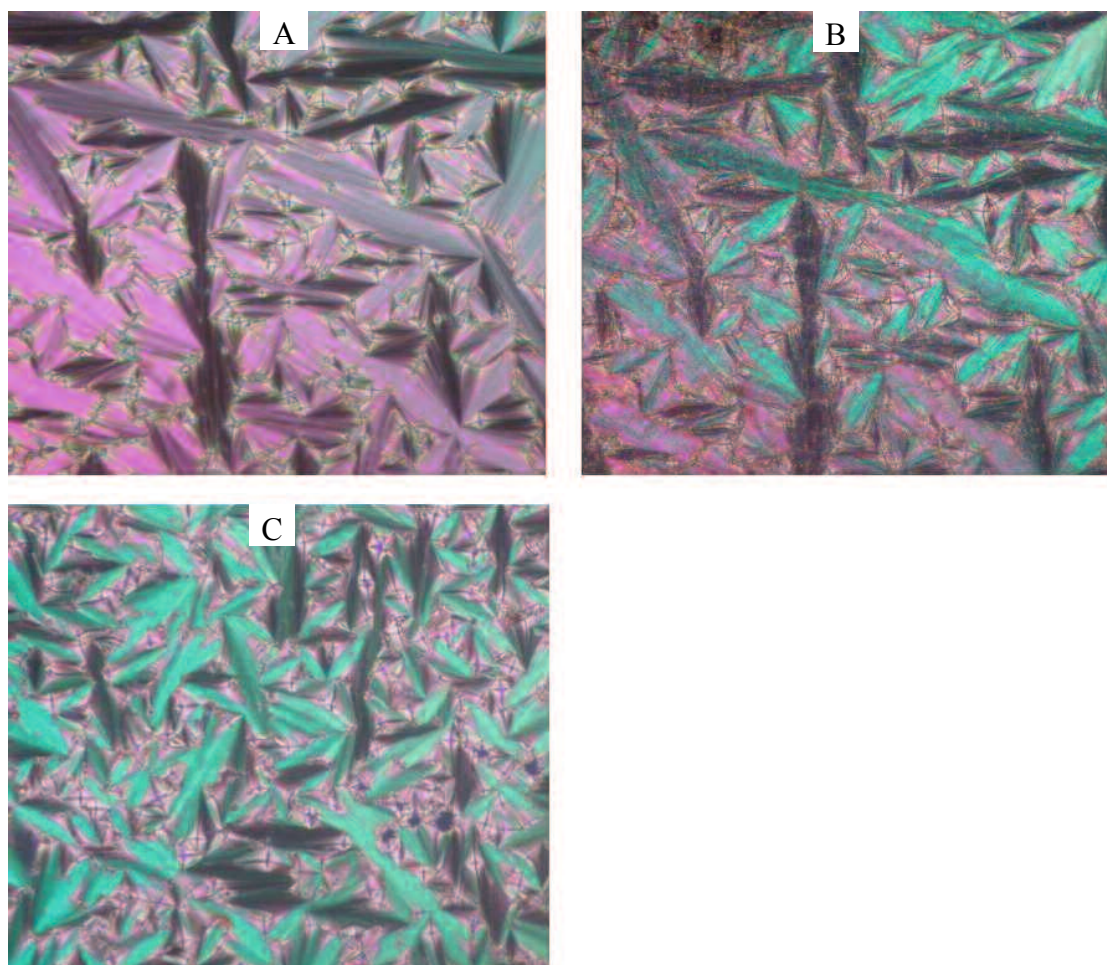


Figure 6-6. Polarized micrographs for A: compound **E2-OC₆H₁₃** at 260 °C, B: compound **E2-6** at 59 °C, C: compound **E2-CN** at 216 °C

The results of DSC analysis have been summarized in **Table 6-2**. According to **Table 6-2**, compounds **E2-OMe** and **E2-OC₆H₁₃** show liquid crystalline properties such as SmC and SmA from 100 °C to 260 °C while compound **E2-CN** shows liquid crystalline properties such as SmA from 132 °C to 256 °C. The results proved that the inductive effective of terminal group in compounds **E2-R** can change their liquid crystalline properties. Comparing with compounds **E1-n** which show liquid crystalline properties until 155 °C, the transition temperature range of compound **E2-R** is wider.

Table 6-2. Transition temperatures [$^{\circ}\text{C}$] and the associated latent heats [kJ mol^{-1}] of compounds **E2-R**

Compounds	Transition temperatures ($^{\circ}\text{C}$)				ΔH (kJ mol^{-1})		
	Cryst	SmC	SmA	Iso	mp	SmC-SmA	SmA-Iso
E2-OMe	• 97	• 121	• 263	•	20.1	2.2	8.7
E2-OC₆H₁₃	• 99	• 124	• 265	•	22.8	2.4	11.1
E2-CN	• 132	-	• 256	•	24.2		6.2

Cryst, SmC, SmA and Iso indicate crystal, smectic C mesophase, smectic A mesophase and isotropic liquid, respectively. Parentheses indicate a monotropic transition.

Replacing 4-(perfluorohexyl)butoxy group by decyloxy group was applied to investigating the fluorophobic effect in this work. Compounds **E3-n** ($n = 1$ and 6) were synthesized and their liquid crystalline properties were explored. For compounds **E3-1**, a schlieren texture was observed in cooling process and the mesophase was assigned to be a nematic (N) mesophase as shown in **Figure 6-7**.

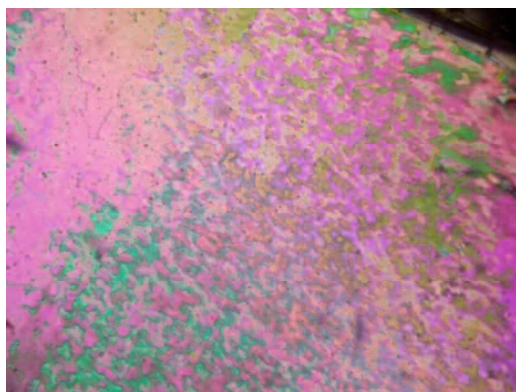


Figure 6-7. Polarized micrograph for compound **E3-1** at 70°C

The results of DSC analysis have been summarized in **Table 6-3**. Transition temperatures of **E3-6** are cited from B. Heinrich's work.⁵ Comparing with **Table 6-1**, the thermodynamic properties of compounds **E3-1** and **E3-6** are more unstable than compounds **E1-n**.

Table 6-3. Transition temperatures [°C] and the associated latent heats [kJ mol⁻¹] of compounds **E3-1** and **E3-6**

Compounds	Transition temperatures (°C)				ΔH (kJ mol ⁻¹)		
	Cryst	SmC	N	Iso	mp	SmC-N	N-Iso
E3-1	• 71	–	• 73	•	45.3	–	1.3
E3-6 ⁵	• 61	(• 55)	• 87	•	48.5	1.9	1.8

Cryst, SmC, N, and Iso indicate crystal, smectic C mesophase, nematic mesophase and isotropic liquid, respectively. Parentheses indicate a monotropic transition.

6.3 Gelation abilities

Supramolecular gels usually consist of three dimensional nanofiber networks through non-covalent force such as hydrogen bond and π - π interaction. 4-Alkoxy-4'-semifluoroalkoxybiphenyl compounds show not only liquid crystalline properties but also effective gelation abilities to encourage us to explore the gelation ability of semifluorinated 4-alkoxyphenyl 4-alkoxybenzoates.

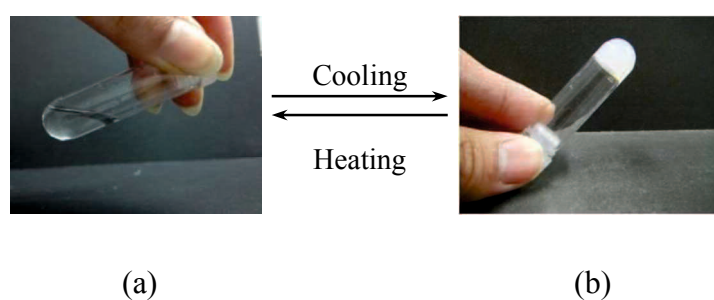


Figure 6-8. Physical supramolecular gel; (a) sol state, (b) supramolecular gel state

Interestingly, compound **E2-6** formed a physical supramolecular gel (i.e. thermoreversible gel) in several organic solvents as shown in **Figure 6-8**. Therefore, we carried out the gelation tests of compounds **E1-n** in several organic solvents and the results were shown in **Table 6-4**. The photographs of supramolecular gels formed by compounds **E1-6** were shown in **Figure 6-9**.

Table 6-4. Critical gel concentration for compounds **E1-n**^{[a],[b]}

Solvents	Compounds (concentration, wt%)									
	E1-1	E1-3	E1-4	E1-5	E1-6	E1-7	E1-8	E1-9	E1-10	

<i>n</i> -Octane	P (5.0)	P (5.0)	P (5.0)	P (5.0)	G (3.5)	G (5.0)	G (5.0)	G (5.0)	G (5.0)
Toluene	S (5.0)								
Ethanol	P (5.0)	P (5.0)	P (5.0)	P (5.0)	G (2.5)	G (5.0)	G (5.0)	G (5.0)	G (5.0)
1-Octanol	P (5.0)	G (2.0)	G (2.0)	G (2.0)	G (1.0)				
AcOEt	S (5.0)								
Acetonitrile	S (5.0)	P (5.0)	P (5.0)	P (5.0)	G (5.0)				
PC	P (5.0)	G (2.0)	G (2.0)	G (2.0)	G (1.5)				
GBL	P (5.0)	P (5.0)	P (5.0)	P (5.0)	G (4.5)	G (4.5)	G (1.0)	G (2.0)	G (1.0)

^[a] G, S and P are gel, sol and precipitated states, respectively. For gels, the critical gelation concentrations (CGCs) at room temperature were shown in parentheses, for P and S, compounds **E1-n** were precipitated and soluble respectively at the concentrations in parentheses; ^[b] PC and GBL indicated propylene carbonate and γ -Butyrolactone, respectively.

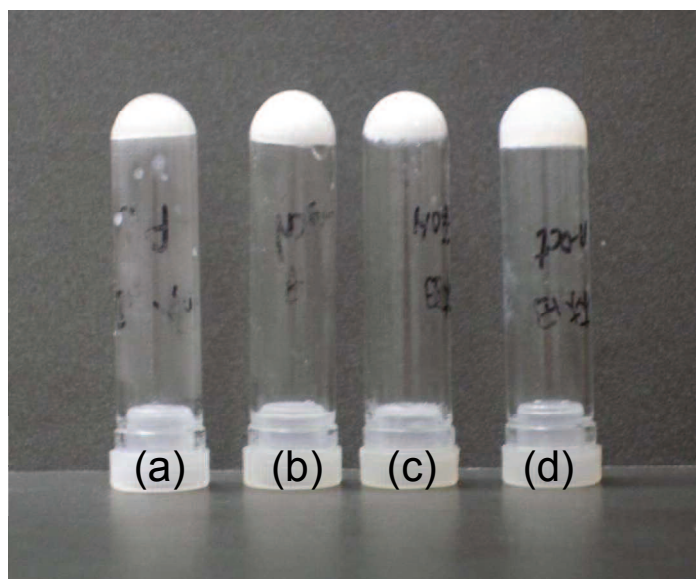


Figure 6-9. Photographs for organic gels formed by compound **E1-6**; (a) γ -butyrolactone supramolecular gel (4.5wt%), (b) acetonitrile supramolecular gel (5.0wt%), (c) ethanol supramolecular gel (5.0wt%), (d) *n*-octane supramolecular gel (3.5wt%)

Figure 6-9 shows a photograph of organic supramolecular gels (GBL, acetonitrile, ethanol, and *n*-octane gels) formed by compound **E1-6** at room temperature by cooling from an isotropic liquid state, and the supramolecular gels are cloudy.

The gelation phenomena are also confirmed by means of scanning electron microscope (SEM) observation, and the result for a xerogel prepared from *n*-octane supramolecular gel is shown in **Figure 6-10**. It is apparent in the figure that the supramolecular gel consists of several rod-like fibers aligned to form the network structures with bundles with diameters of less μm order.

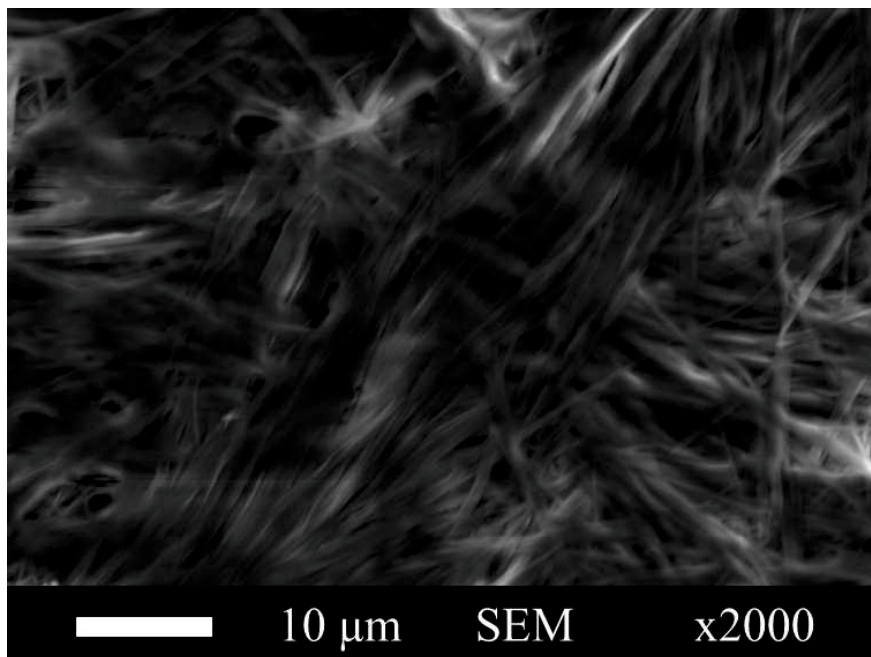


Figure 6-10. SEM image for xerogel prepared from *n*-octane gel (x2,000)

The thermodynamic stabilities of supramolecular gels formed by compounds **E1-n** have been explored using the gel to sol transition temperature (T_{gel}). Unfortunately, all the T_{gel} is just above room temperature. T_{gel} of compound **E1-n** in *n*-octane, ethanol, acetonitrile and GBL were shown in **Figure 6-11**.

The gelation abilities of compounds **E2-R** and **E3-n** were investigated. Among compounds **E2-R**, only compound **E2-OC₆H₁₃** gelatinized with *n*-Octane, 1-Octanol and GBL, others did not show gelation ability in tested solvents. On the other hand, compounds **E3-1** and **E3-6** were precipitated or soluble in the tested solvents as shown in **Table 6-5**. These results indicate that both of a semifluoroalkoxyl chain and a subtle long alkoxy chain in the molecular structure are indispensable to form the organic gels.

Table 6-5. Critical gel concentration for compounds **E2-R** and **E3-n**^{[a],[b]}

Solvents	Compounds (concentration, wt%)				
	E2-OMe	E2-OC₆H₁₃	E2-CN	E3-1	E3-6
<i>n</i> -Octane	P (5.0)	G (2.0)	P (5.0)	P (5.0)	P (5.0)
Toluene	P (5.0)	P (5.0)	P (5.0)	S (5.0)	S (5.0)
Ethanol	I (5.0)	I (5.0)	I (5.0)	P (5.0)	P (5.0)
1-Octanol	P (5.0)	G (2.0)	P (5.0)	P (5.0)	P (5.0)
Acetonitrile	P (5.0)	I (5.0)	P (5.0)	P (5.0)	P (5.0)
PC	P (5.0)	P (5.0)	P (5.0)	P (5.0)	P (5.0)
GBL	P (5.0)	G (3.0)	P (5.0)	P (5.0)	P (5.0)

^[a] G, S, I and P are gel, sol, insoluble and precipitated states, respectively. For gels, the critical gelation concentrations (CGCs) at room temperature were shown in parentheses, for P and S, compounds **E2-R** and **E3-n** were precipitated and soluble respectively at the concentrations in parentheses; ^[b] PC and GBL indicated propylene carbonate and γ -Butyrolactone, respectively.

Thermodynamic stability of supramolecular gels formed by compound **E2-OC₆H₁₃** has been explored. T_{gel} was plotted against the gelator weight concentration (wt%) in *n*-octane, 1-octanol and GBL (**Figure 6-11**). Comparing with

compound **E2-n**, supramolecular gels formed by **E2-OC₆H₁₃** are more stable than compound **E2-n**.

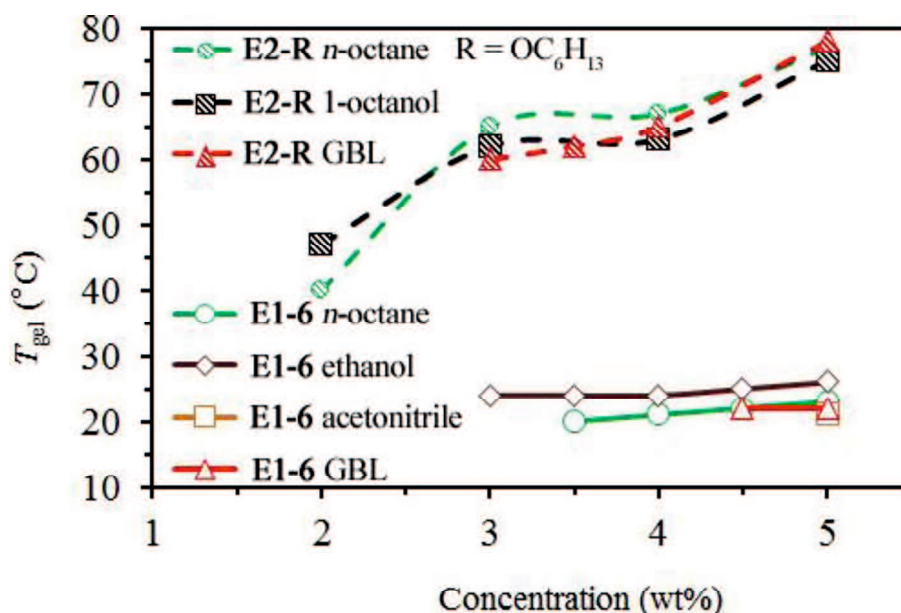


Figure 6-11. Plots of T_{gel} vs. concentration for **E1-6** and **E2-OC₆H₁₃**

6.4 Conclusions

4-[4-(perfluorohexyl)butoxy]phenyl 4-alkoxybenzoates as a new types of molecular structure were explored in liquid crystalline properties and gelation abilities. As the carbon number of terminal alkoxy group of the ester derivatives slightly increases, the gelation abilities are essentially changed. The ester derivatives with multiple aromatic cores show wider thermal range of mesophase than that with fewer aromatic cores. At the same time, the gel to sol transition temperature of ester derivatives with multiple aromatic cores in *n*-octane and GBL are higher than that with fewer aromatic cores. It means that aprotic low molecular weight gelators having multiple aromatic cores based on a semifluoroalkoxyl chains which show liquid crystalline properties and gel properties trend to display thermal stability of not only

liquid crystal properties but also gel properties. The core benzene groups, terminal substitution groups and perfluorohexyl groups play important roles in liquid crystalline properties and gelation abilities, which were proved again.

6.5 Reference

1. Demus, D. *Liquid Crystals* **1989**, 5 (1), 75.
2. Vorländer, D.; Apel, A. *Berichte der Deutschen Chemischen Gesellschaft (A and B Series)* **1932**, 65 (7), 1101.
3. (a) Okamoto, H.; Yamada, N.; Takenaka, S. *Journal of Fluorine Chemistry* **1998**, 91 (2), 125; (b) Takenaka, S. *Journal of the Chemical Society, Chemical Communications* **1992**, (23), 1748; (c) Okamoto, H.; Murai, H.; Takenaka, S. *Bulletin of the Chemical Society of Japan* **1997**, 70 (12), 3163; (d) Duan, M.; Okamoto, H.; Petrov, V. F.; Takenaka, S. *Bulletin of the Chemical Society of Japan* **1998**, 71 (11), 2735; (e) Yano, M.; Taketsugu, T.; Hori, K.; Okamoto, H.; Takenaka, S. *Chemistry—A European Journal* **2004**, 10 (16), 3991.
4. Pal, S. K.; Setia, S.; Avinash, B.; Kumar, S. *Liquid Crystals* **2013**, 40 (12), 1769.
5. Heinrich, B.; Guillon, D. *Molecular Crystals and Liquid Crystals* **1995**, 268 (1), 21.

Chapter 7 4-[2-(Perfluorohexyl)ethylthio]-3'-fluoro-4'-alkoxy-1,1'-biphenyl derivatives as low molecular weight gelators applied in quasi-solid-state dye-sensitized electrolytes

7.1 Introduction

Dye-sensitized solar cells (DSSCs) are considered as the most promising low-cost option for the high conversion of solar energy. So as a promising next-generation device and important solution to energy depletion and environmental pollution, DSSCs have rapidly become an important research orientation in electronic vehicles.¹

The electrolyte is one of the key materials that affect the photovoltaic performance of quasi-solid-state dye-sensitized solar cells.² Recently, Grätzel et al. reported that the liquid electrolyte based DSSC through the molecular engineering of porphyrin sensitizers has achieved the highest photoelectric conversion efficiency of 13%.³ Although the studies on DSSCs have made some progress, many undesirable properties, for example, volatility, shape flexibility and electrochemical stability, the problem of leaking and sealing, flammability issues faced by liquid electrolyte, which is crucial for the application and commercial production of DSSCs.⁴

However, in order to address the challenge, two major methods have been developed. One is that using a different class of solvents with high boiling points and low melting points (e.g. γ -butyrolactone, 3-methoxypropionitrile, propylenecarbonate and propionitrile), which has been employed. Especially, room temperature ionic liquids (RTILs) with negligible vapor pressure, low viscosity, high conductivity and wide electrochemical windows have been considered as viable replacements for

current organic liquid based electrolytes.⁵ Of the various RTILs studied, ionic liquids based *bis*(fluorosulfonyl)*imide* (FSI) and *bis*[(trifluoromethyl) sulfonyl]*imide* (TFSI) anion have gained significant attention for their relatively low viscosity and high conductivity.⁶

Another one is that solid and/or quasi-solid-state electrolytes have been developed to replace the conventional liquid electrolytes. To solidify liquid electrolytes, polymer, organic hole transport materials and inorganic semiconductors have been introduced into DSSCs electronic vehicles, which have attracted much attention for their good stability. Unfortunately, the solid and/or quasi-solid-state electrolytes based on those materials show lower performance than liquid electrolyte in ion diffusion.¹

Low molecular weight gelators (LMWGs) can efficiently gelatinize organic solvents with a small weight percent. Liquid electrolytes also can be solidified to form gel electrolytes by LMWGs. The gel electrolytes formed by LMWGs exhibit three dimensional nanofiber networks and generally possess higher ionic conductivity than other solid and/or quasi-solid-state electrolytes.⁷ At the same time, gel electrolytes show long-term electrochemical stability. Ionogels electrolytes formed by LMWGs and RTILs are exciting for academia and industry due to negligible vapor pressure, long-term electrochemical stability and high ionic conductivity.⁸ Some LMWGs such as 12-hydroxystearic acid,⁷ cyclohexanecarboxylic acid-[4-(3-octadecylureido)phenyl]amide,⁹ 1,3:2,4-di-*O*-benzylidene-D-sorbitol derivatives¹⁰ etc. have been developed and successfully applied in DSSCs.

than compound **T-2**. The most important thing for electrochemical applications is that both of compounds **T-1** and **T-2** gelatinize 1M [DEME][TFSI] in PC even at 0.4 wt% and 0.8 wt%, respectively.

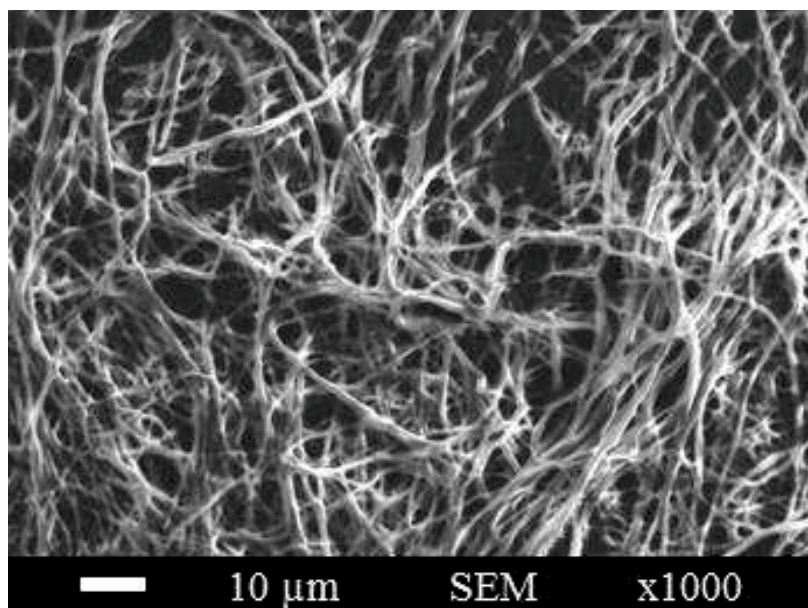
Table 7-1. Gelation properties of compounds **T-1** and **T-2** (wt%) at room temperature^{[a], [b]}

Solvents	Compound T-1 (wt%)	Compound T-2 (wt%)
<i>n</i> -Octane	G (5.0)	G (0.6)
Toluene	S (5.0)	G (5.0)
Ethanol	G (1.0)	G (0.7)
Acetonitrile	G (0.6)	G (1.0)
GBL	G (2.0)	G (1.0)
PC	G (0.4)	G (0.8)
1M [DEME][TFSI]/PC	G (0.4)	G (0.8)

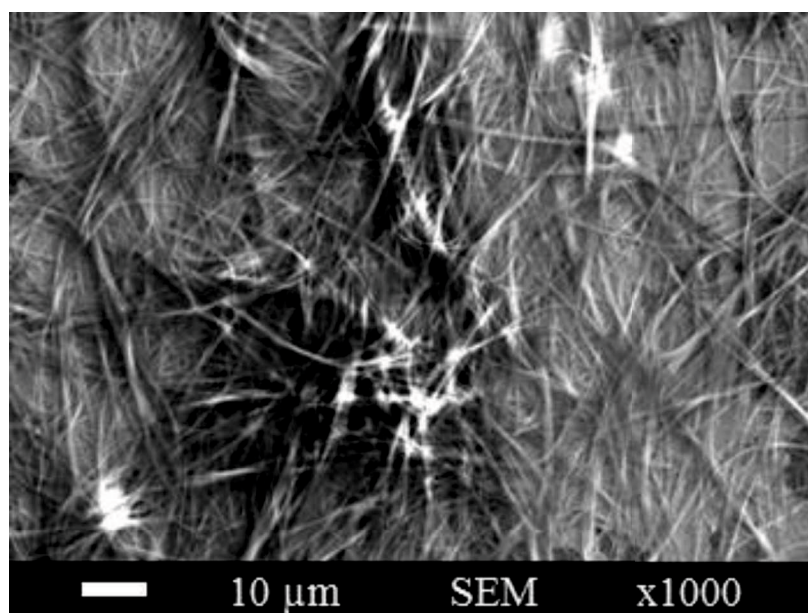
^[a] G: gel, S: soluble; for gels, the critical gelation concentrations at room temperature were shown in parentheses, for S, compound **T-1** was soluble at the concentrations in parentheses; ^[b] GBL, PC and [DEME][TFSI]/PC indicated γ -butyrolactone, propylene carbonate and *N,N*-diethyl-*N*-(2-methoxyethyl)-*N*-methylammonium bis(trifluoromethylsulphonyl)imide in propylene carbonate, respectively.

In order to gain visual insights into the aggregation mode, the fibrils of supramolecular gels formed with 1M [DEME][TFSI] at CGCs were explored using scanning electron microscopy (SEM) as shown in **Figure 7-2**. The SEM images mean

that three dimensional nanofiber networks have been formed by self-assembly of compounds **T-1** and **T-2**.



(a)



(b)

Figure 7-2. SEM images of xerogel system in 1M [DEME][TFSI]/PC formed by compound **T-1** shown in (a) and by compound **T-2** shown in (b) (scale bar = 10 μm)

The supramolecular gels formed by compounds **T-1** and **T-2** were thermoreversible. At the same time, the gel to sol transition temperature (T_{gel}) is also very important to gel electrolyte. Hence, T_{gel} plotted against the gelator weight concentration (wt%) in PC and 1M [DEME][TFSI] solution of PC were studied (Figure 7-3 and Figure 7-4).

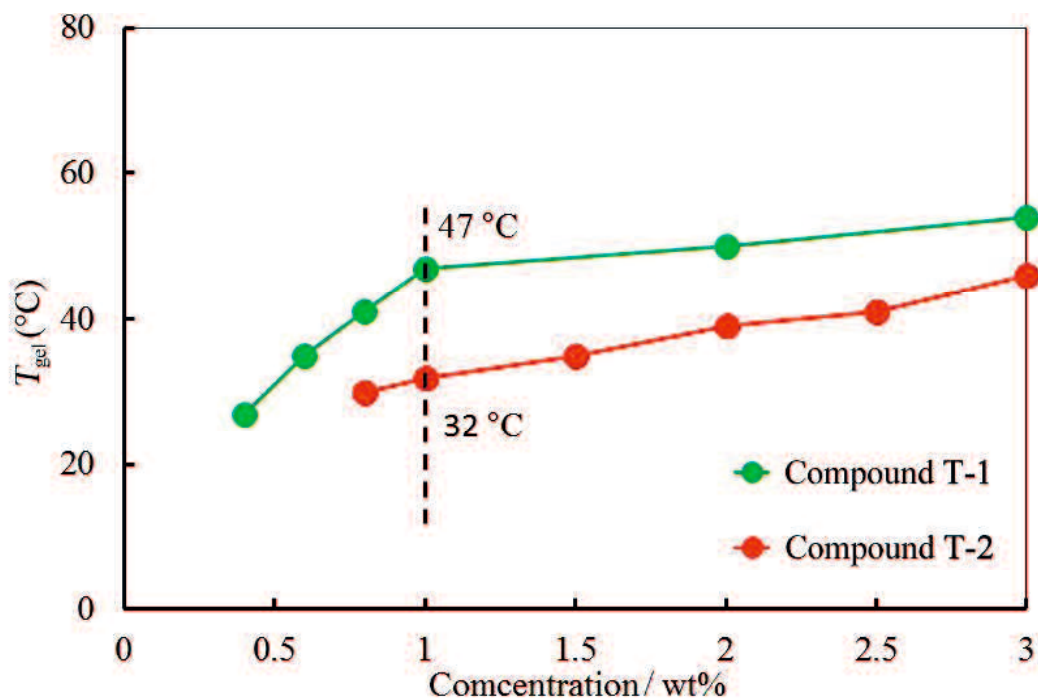


Figure 7-3. Plots of concentration for compounds **T-1** and **T-2** vs. T_{gel} in PC

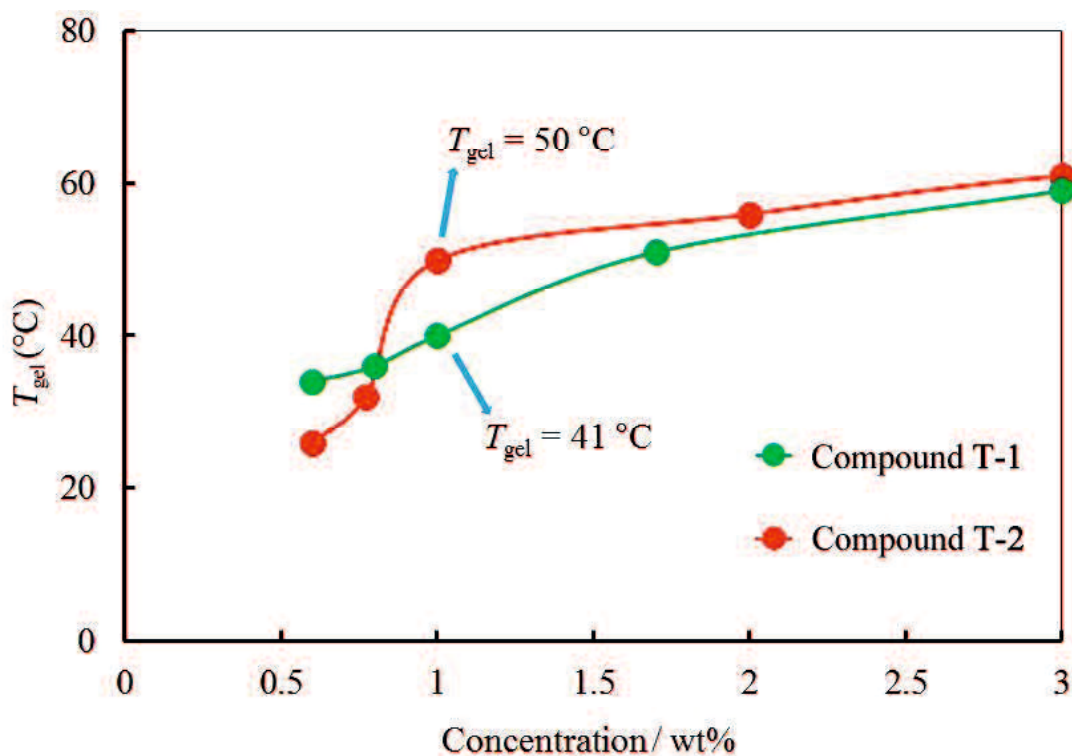


Figure 7-4. Plots of concentration for compounds **T-1** and **T-2** vs. T_{gel} in 1M [DEME][TFSI] solution of PC

Figure 7-3 shows that T_{gel} of supramolecular gel formed by compound **T-1** with PC is higher than that of compound **T-2** at the same weight concentration. For example, T_{gel} of supramolecular gel formed by compound **T-1** is 47 °C at 1 wt% while that by compound **T-2** is 32 °C. As the weight concentration decreases, T_{gel} of supramolecular gel formed by compound **T-1** slightly decreases at a concentration range from 3 to 1 wt% while sharply decreases at a concentration range from 1 to 0.6 wt%.

Figure 7-4 shows that T_{gel} of supramolecular gel formed by compound **T-2** in 1M [DEME][TFSI] solution of PC is 50 °C at 1 wt%, while that by compound **T-1** is 41 °C. At 1 wt%, T_{gel} of supramolecular gel formed by compound **T-2** has a sharp turning point. As the weight concentration decreases, T_{gel} of supramolecular gel

formed by compound **T-2** in 1M [DEME][TFSI] solution of PC slightly decreases at a concentration range from 3 to 1 wt% while sharply decreases at a concentration range from 1 to 0.5 wt% and even lower than that formed by compound **T-1** at the same concentration.

According to **Figure 7-3** and **Figure 7-4**, 1 M [DEME][TFSI] in propylene carbonate with 1 wt% 2-(perfluorohexyl)ethyl derivatives were selected and used as electrolytes for ensuing electrochemical experiment to investigate their electrochemical properties.

7.3 Electrochemical properties

Samples of electrolyte and gel electrolyte were prepared in Ar-filled glove box ($[\text{H}_2\text{O}] < 0.1$ ppm, 1AD-3KP, Miwa Mfg Co., Ltd.). These samples were contained in a flat conductivity cell (Hohsen Corp.) for liquids equipped with fixed platinum electrodes (15 mm ϕ) and separator (24 mm ϕ). Supor[®]200 (Pall Corporation) was used on a separator. The cell constant is periodically controlled by comparison with a 0.1M KCl aqueous solution.

In order to investigate the effect of gelator on ionic conductivity, the plots of $1000T^{-1}$ vs. ionic conductivity in 1M [DEME][TFSI]/PC and its gel electrolytes prepared with 1wt% compound **T-1** were shown in **Figure 7-5**.

It is well-known that increasing viscosity of electrolyte makes ionic conductivity decrease. To our surprise, gel electrolyte formed by compound **T-1** shows more effective ionic conductivity than 1M [DEME][TFSI]/PC electrolyte (**Figure 7-5**). The

ionic conductivity of gel electrolyte does not show turning point at the gel to sol transition temperature. In fact, temperature influences the values of the ionic conductivity of gel electrolyte, but does not change the variation tendency in gel state or solution state.

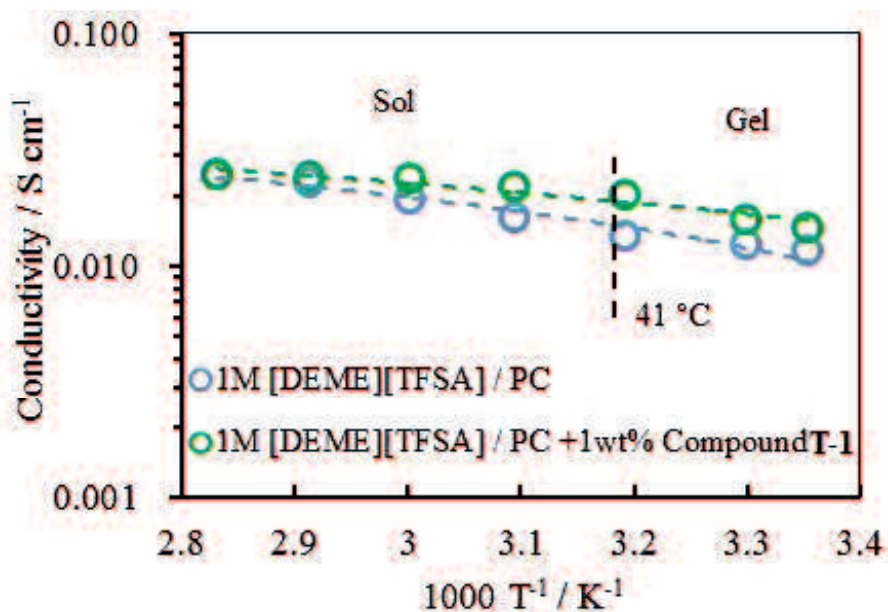


Figure 7-5. Plots of $1000T^{-1}$ vs. ionic conductivity in 1M [DEME][TFSA] / PC with or without 1 wt% compound **T-1**

In order to investigate the effect of terminal group on ionic conductivity, the plots of $1000T^{-1}$ vs. ionic conductivity in 1M [DEME][TFSA]/PC and its gel electrolytes prepared with 1wt% compound **T-2** were also investigated and showed in **Figure 7-6**. According to **Figure 7-6**, the ionic conductivity of gel electrolyte formed by compound **T-2** is lower than 1M [DEME][TFSA]/PC electrolyte. The ionic conductivity of gel electrolyte prepared by compound **T-2** also does not show turning point at the gel to sol transition temperature.

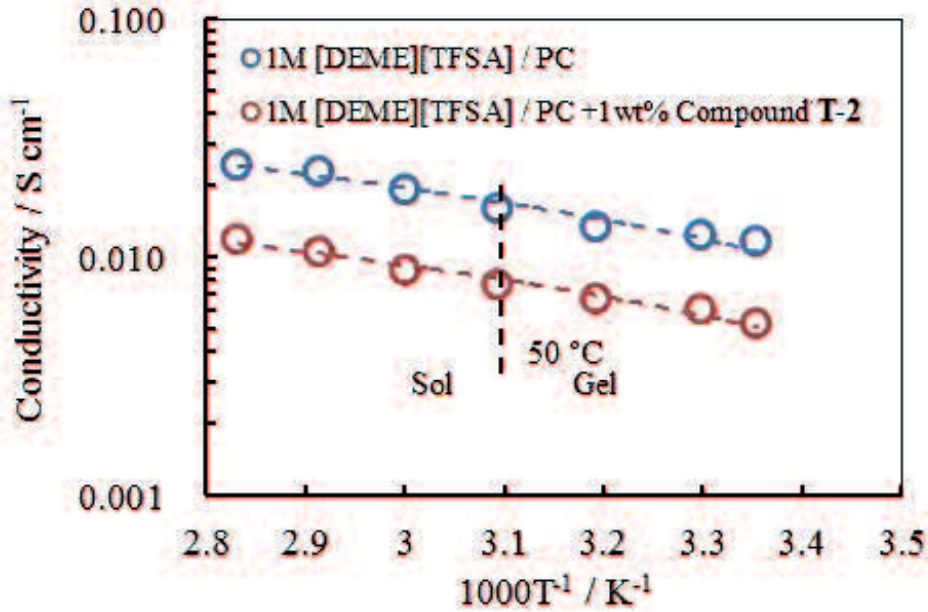


Figure 7-6. Plots of $1000T^{-1}$ vs. ionic conductivity in 1M [DEME][TFSA] / PC with or without 1 wt% compound T-2

Electrolyte activation energy (E_A) was studied by combining ionic conductivity. Activation energy can be calculated by Arrhenius equation. The temperature dependency shows an Arrhenius plot, as indicated by the Arrhenius equation below:

$$\sigma = \sigma_0 \exp(-E_A/RT) \quad [1]$$

$$\ln \sigma = -E_A/RT + \ln \sigma_0 \quad (R = k * N_A)$$

In the Arrhenius equation, σ is the ionic conductivity, E_A is the activation energy and k is Boltzmann's constant. That means a plot of $\ln \sigma$ vs. T^{-1} gives a straight line shown in **Figure 7-7**.

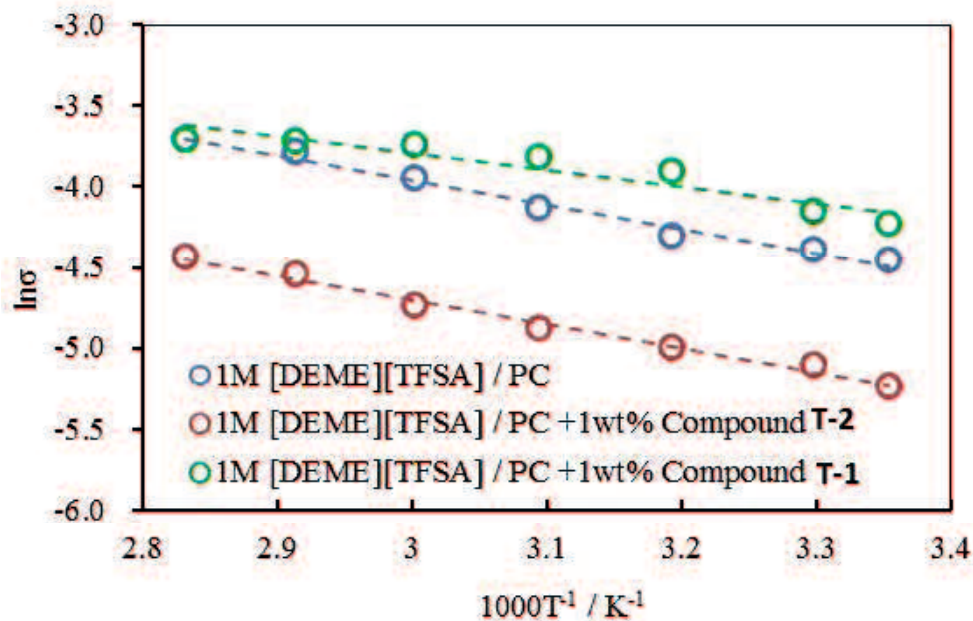


Figure 7-7. Arrhenius plots of $1000T^{-1}$ vs. $\ln \sigma$ in 1M [DEME][TFSA]/PC with or without 1 wt% gelator

According to **Figure 7-7**, E_A was calculated. The values are shown in **Table 7-2**. E_A of 1M [DEME][TFSA]/PC is between gel electrolyte formed with compound **T-1** and that formed with compound **T-2**. The value of gel electrolyte with compound **T-1** is just 70% of 1M [DEME][TFSA]/PC.

Table 7-2. The values of electrolyte activation

Electrolyte	E_A (kJ/mol)
1M [DEME][TFSA]/PC	12.38
1M [DEME][TFSA]/PC +1wt% Compound T-1	8.59
1M [DEME][TFSA]/PC +1wt% Compound T-2	12.61

7.4 Conclusions

As low molecular weight gelator compounds **T-1** and **T-2** having 2-(perfluorohexyl)ethylthiol group were synthesized. Their gelation properties and electrochemical properties were investigated.

The gelation properties of 2-(perfluorohexyl)ethylthiol derivatives with alkoxy group as terminal group are different from benzyl group. In polar solvents such as acetonitrile and PC, the gelation properties of compound **T-1** with terminal alkoxy group are better than that of compound **T-2** with benzyl group. While in nonpolar solvents, the gelation properties of compound **T-2** with terminal benzyl group are better than that of compound **T-1** with alkoxy group.

Ionic conductivity of compound **T-1** and compound **T-2** are increasing as temperature increases. The ionic conductivity of gel electrolyte with compound **T-1** shows more effective ionic conductivity than electrolyte. The value of electrolyte activation for gel electrolyte with compound **T-1** is just 70% of 1M [DEME][TFSI]/PC. The gel electrolyte with compound **T-1** will be explored in quasi-solid-state dye-sensitized solar cells in the future.

7.5 References

1. Tao, L.; Huo, Z.; Ding, Y.; Li, Y.; Dai, S.; Wang, L.; Zhu, J.; Pan, X.; Zhang, B.; Yao, J. *Journal of Materials Chemistry A* **2015**, *3* (5), 2344.
2. Li, B.; Wang, L.; Kang, B.; Wang, P.; Qiu, Y. *Solar Energy Materials and Solar Cells* **2006**, *90* (5), 549.
3. Mathew, S.; Yella, A.; Gao, P.; Humphry-Baker, R.; Curchod, B.; Ashari-Astani, N.; Tavernelli, I.; Rothlisberger, U. *Nature Chemistry* **2014**, *6*, 242.
4. Wang, G.; Zhang, L.; Zhang, J. *Chemical Society Reviews* **2012**, *41* (2), 797.
5. Girard, G.; Hilder, M.; Zhu, H.; Nucciarone, D.; Whitbread, K.; Zavorine, S.; Moser, M.; Forsyth, M.; MacFarlane, D.; Howlett, P. *Physical Chemistry Chemical Physics* **2015**, *17* (14), 8706.
6. Handa, N.; Sugimoto, T.; Yamagata, M.; Kikuta, M.; Kono, M.; Ishikawa, M. *Journal of Power Sources* **2008**, *185* (2), 1585.
7. Huo, Z.; Dai, S.; Zhang, C.; Kong, F.; Fang, X.; Guo, L.; Liu, W.; Hu, L.; Pan, X.; Wang, K. *The Journal of Physical Chemistry B* **2008**, *112* (41), 12927.
8. Gorlov, M.; Kloo, L. *Dalton Transactions* **2008**, (20), 2655.
9. Yu, Q.; Yu, C.; Guo, F.; Wang, J.; Jiao, S.; Gao, S.; Li, H.; Zhao, L. *Energy & Environmental Science* **2012**, *5* (3), 6151.
10. Mohmeyer, N.; Wang, P.; Schmidt, H.-W.; Zakeeruddin, S. M.; Grätzel, M. *Journal of Materials Chemistry* **2004**, *14* (12), 1905.
11. Schwendeman, I.; Gaupp, C. L.; Hancock, J. M.; Groenendaal, L.; Reynolds, J. R. *Advanced Functional Materials* **2003**, *13* (7), 541.

12. (a) Miura, M.; Iuchi, A.; Morita, Y.; Kasatani, K.; Okamoto, H. *ECS Transactions* **2013**, *50* (48), 89; (b) Yoshida, T.; Hirakawa, T.; Nakamura, T.; Yamada, Y.; Tatsuno, H.; Morita, Y.; Okamoto, H. *ECS Transactions* **2013**, *50* (48), 95.

Chapter 8 General conclusions

4-Alkoxy-4'-semifluoroalkoxybiphenyl derivatives, 4-[4-(perfluorohexyl)-butoxy]phenyl 4-alkoxybenzoates derivatives and 4-[2-(perfluorohexyl)ethylthio]-3'-fluoro-4'-alkoxy-1,1'-biphenyl derivatives based on semifluoroalkyl groups have been synthesized and studied.

Both of 4-alkoxy-4'-semifluoroalkoxybiphenyl derivatives and 4-[4-(perfluorohexyl)-butoxy]phenyl 4-alkoxybenzoates derivatives have liquid crystalline properties and gelation abilities. The liquid crystalline properties depending on the core group and terminal group were proved. Semifluoroalkyl groups play an important role in liquid crystalline properties and gelation abilities by hydrophobic or fluorophilic/solvophobic interactions.

4-Alkoxy-4'-semifluoroalkoxybiphenyl derivatives show effective phase selective abilities. Tested oils can be selectively gelatinized from basic aqueous-oil biphasic mixture, acidic aqueous-oil biphasic mixture and ocean water. Some special volatile organic compounds also can be gelatinized, such as acetic acid, caproic acid and benzaldehyde.

The gelation abilities of 4-[4-(perfluorohexyl)butoxy]phenyl-4-alkoxybenzoates derivatives are weaker than that of 4-alkoxy-4'-semifluoroalkoxybiphenyl derivatives. The supramolecular gels gelatinized by 4-[4-(perfluorohexyl)butoxy]phenyl 4-alkoxybenzoates derivatives are difficult to be judged by visual method.

Although 4-alkoxy-4'-semifluoroalkoxybiphenyl derivatives and 4-[4-(perfluorohexyl)butoxy]phenyl-4-alkoxybenzoates derivatives having mesogenic

properties and gelation abilities have been found, molecular self-assembly is still not clear. Liquid crystals and supramolecular gels are soft materials, and both of them can be easily deformed through self-assembly using non-covalent bonds. The packing in the self-assembled state may be different, because the environments of liquid crystals and supramolecular gels are different. In order to find the packing relations between liquid crystals and supramolecular gels and the relation between molecular fragments and material properties, 4-alkoxy-4'-semifluoroalkoxybiphenyl derivatives and 4-[4-(perfluorohexyl)butoxy]phenyl-4-alkoxybenzoates derivatives should be investigated by other analytical methods such as X-ray diffraction.

4-[2-(Perfluorohexyl)ethylthio]-3'-fluoro-4'-alkoxy-1,1'-biphenyl derivatives as low molecular weight gelators can gelatinize 1 M [DEME][TFSI]/PC electrolyte. The ionic conductivity of gel electrolyte formed by 4-[2-(perfluorohexyl)ethylthio]-3'-fluoro-4'-dodecyloxy-1,1'-biphenyl with a terminal dodecyloxy group is more effective than electrolyte's. The gel electrolyte will be explored in quasi-solid-state dye-sensitized solar cells in the future.

Acknowledgments

The research based on this dissertation was carried out at the Department of Materials Engineering, Faculty of Science and Engineering, Yamaguchi University, Ube, Japan.

I would like to take this opportunity to express my deepest thanks to my advisor, Associate Professor Hiroaki Okamoto, for continuous interest, valuable guidance and kind encouragement during three years of my doctor course.

I am very grateful to Dr. Qiang Xiao whose encourage me to do my best and to Ms. Yuki Morita for continuous help with experiment and daily life.

I wish to thank to Professor Kazuo Kasatani for his kind help. I would like to thank Professor Kenjiro Omimura, Professor Hiromori Tsutsumi, Research Assistant Kazuhiro Yamabuki for their help.

I also wish to thank to Dr. Tetsuko Inokuma and other members of Ube Rotary group for their kind help.

Special thanks are express to Dr. Lingfang Qiu, Dr. Tomohiro Yoshida, Mr. Masato Kiriki, Mr. Yuta Kaneshige and others Japanese friends who studied in this laboratory during past three years for their kind help.

Finally, I express my sincere thanks to my parents and other kind person for their supports and encouragement.